Stony Brook University

Preparation and characterization of stimuli-responsive star-shaped triblock copolymers for gene delivery

A Thesis Presented

by

Tianyuan Wu

to

The Graduate School

in Partial Fulfillment of the

Requirements

for the Degree of

Doctor of Philosophy

in

Chemistry

Stony Brook University

December 2015

Stony Brook University

The Graduate School

Tianyuan Wu

We, the thesis committee for the above candidate for the

Doctor of Philosophy degree, hereby recommend

Acceptance of this thesis.

Robert B. Grubbs
Associate Professor, Chemistry Department

Surita R. Bhatia
Associate Professor, Chemistry Department

Melanie Chiu
Assistant Professor, Chemistry Department

Jin Kim Montclare
Associate Professor, Chemical and Biomolecular Engineering Department
NYU Polytechnic School of Engineering

This thesis is accepted by the Graduate School

Charles Taber
Dean of the Graduate School

Abstract of the Thesis

Preparation and characterization of stimuli-responsive

star-shaped triblock copolymers

for gene delivery

by

Tianyuan Wu

Doctor of Philosophy

in

Chemistry

Stony Brook University

2015

Amphiphilic block copolymers with both a hydrophobic domain and a hydrophilic domain can thermodynamically self-assemble into ordered structures such as spherical micelles, worm-like micelles or vesicles in selective solvents which have great potential for biomedical applications such as drug/gene delivery. Stimuli-responsive amphiphilic block copolymers which can change morphology in response to internal or external stimulus have great potential to achieve controlled release of drugs or genes at specific sites. In this dissertation, two types of stimuli-responsive star-shaped triblock copolymers PEO-S(CK_n)-PLA and PEO-(PDEAm)-PLA were synthesized and studied.

Amphiphilic cationic star-shaped triblock copolymers with poly(ethylene oxide), poly(D,L-lactide), and poly(L-lysine arms) (PEO-S(CK_n)-PLA) were synthesized by a combination of ring opening polymerization (ROP) and arm coupling through a thiol-disulfide exchange reaction. The morphology of PEO-S(Boc)-PLA diblock copolymers, PEO-S(CK_n)-PLA triblock copolymers,

and PEO-S(CK_n)-PLA /GFP DNA complexes were characterized by dynamic light scattering (DLS) and small-angle X-ray scattering (SAXS). PEO-S(CK_n)-PLA could effectively condense DNA into nanosized complexes suitable for endocytotic cellular uptake and retard GFP DNA migration in agarose gel electrophoresis at N/P ratios (ratio of moles of the primary amine groups of cationic polymers to those of the phosphate groups of DNA)) greater than 1. *In vitro* gene transfection studies in the HeLa cell line showed that the amphiphilic structure could enhance gene transfection when compared to the corresponding polylysine. Addition of chloroquine could further enhance the gene transfection efficiency by interfering with the endocytosis process to enhance endosomal escape of the complexes. The cytotoxicity of PEO-S(CK_n)-PLA triblock copolymers was studied in HeLa cells by MTS assay. PEO2k-S(CK_{40})-PLA2k triblock copolymers showed almost no toxicity at all conditions examined while the corresponding polylysine PLL_{40} and branched PEI showed relatively low toxicity at low concentrations but high toxicity at high concentrations.

Table of Contents

List of Figures

List of Tables

List of Abbreviations

Boc	t-Butyloxycarbonyl
C or Cys	Cysteine
Cbz	Carboxybenzyl
DCC	*N, N'*-Dicyclohexylcarbodiimide
DLS	Dynamic light scattering
DMEM	Dulbecco's Modified Eagle's medium
DMF	*N, N*'-Dimethylformamide
EDC	1-(3-Dimethylaminopropyl)-3-ethylcarbodiimide
EPR	Enhanced permeation and retention
FBS	Fetal bovine serum
Fmoc	9-Fluorenylmethoxycarbonyl
GFP	Green fluorescence protein
GPC	Gel Permeation Chromatography
K or Lys	Lysine
LCST	Lower critical solution temperature
MEM	Minimum essential medium

MTS	3-(4,5-dimethylthiazol-2-yl)- 5-(3-carboxymethoxyphenyl)-2-(4-sulfophenyl)-2H-tetrazolium
MTT	3-(4,5-dimethylthiazol-2-yl)-2,5-diphenyltetrazolium bromide
MWCO	Molecular weight cutoff
NHS	N-hydroxysuccinimide
NMR	Nuclear magnetic resonance
PEO	Poly(ethylene oxide)
PLA	Poly(lactic acid)
RES	Reticuloendothelial system
ROP	Ring opening polymerization
SAXS	Small angle X-ray scattering
SPDP	*N*-Succinimidyl 3-(2-Pyridyldithio) Propionate
Trt	Triphenylmethyl

Acknowledgements

I would first thank my advisor, Prof. Robert B. Grubbs, for the opportunity to conduct my research in his group. I have greatly benefited from his motivation, encouragement and support. His guidance helped me in all the time of research and writing of this thesis. I would also thank my two co-advisors, Prof. Benjamin Chu and Prof. Benjamin Hsiao, for the stimulating discussions and valuable advices. Without their help, the work presented here could not have been done.

I would like to thank my former and current committee members, Prof. Frank W. Fowler, Prof. Surita Bhatia, Prof. Melanie Chiu and Prof. Jin Kim Montclare for their insightful comments for my thesis and valuable time for attending my meetings and defense.

I thank my collaborators, Prof. Michael Hadjiargyrou and his student Xia Zhao, for working with me in the bio-related research. Prof. Michael Hadjiargyrou provided me with all the necessary facilities and valuable advice for the gene delivery research. Xia Zhao helped me with the cell culture, gene transfection protocol and cytotoxicity test which were important for my research on gene delivery.

I am grateful to the following persons for the help for polymer characterizations: Dr. James Marecek for NMR training and troubleshooting, Dr. Linghui Wu (Prof. Sampson's group) for DLS, Dr. Yanjie Chu (Prof. Carrico's group) for agarose gel electrophoresis.

I would also thank all the previous and current group members for their kind help. My special thanks goes to Dr. Yu Cai, Chai Ngai, Menglan Jiang, Bingyin Jiang, Zhe Sun, Yimin Mao, Xiaowei Li, Ying Su, Xiao Wang, and Rui Yang.

Finally, I would like to thank my family. Without their love and support, I would not be able to finish my Ph.D. study. I owe the greatest thanks to my husband, Cheng Pan, for supporting me spiritually throughout my life.

Chapter 1 General Introduction

1.1 Nanomedicine

According to the definition given by the US National Nanotechnology Initiative: "Nanotechnology is concerned with materials and systems whose structures and components exhibit novel and significantly improved physical, chemical and biological properties, phenomena and processes due to their nanoscale size." [1] In general, nanotechnology is regarded as the study and manipulation of single atoms, molecules and other artificially-constructed matter in the size limits of 0.1-100 nm. Nanomedicine is an important application of nanotechnology to healthcare, which requires the combination of various disciplines such as biology, chemistry, physics, chemical and mechanical engineering, material science and clinical medicine[2]. Nanomedicine has changed the fundamental concepts of disease diagnosis, treatment and prevention because nanomedicine is similar in scale to biologic molecules and systems and provides control on the subcellular level [3]. Although nanomedicine seems to be a relatively recent field, the basic scientific research of nanomedicine such as lipid vesicles [4], controlled release polymeric nanoparticles[5], stealth polymeric nanoparticles[6], quantum dot bioconjugates[7, 8] and nanowire nanosensors[9] started several decades ago. Today, nanomedicine has become a large subject area including metallic (e.g., gold nanoparticles), atomic (e.g., fullerenes and carbon nanotubes), semiconductor (e.g., quantum dots),

organic (e.g., liposomes, polymeric nanoparticles, and dendrimers) and biological (e.g., engineered viral nanoparticles and nucleic acid based nanostructures) nanoparticles[10]. Some unique properties of these nanoparticles such as versatile modification possibilities, high surface to volume ratio, and well controlled size and shape make nanomedicine more attractive for a new generation of clinical applications when compared to macroscopic materials[11]. Several nanomedicines have been approved by the Food and Drug Administration (FDA) for use in humans or are in clinical trials or the proof-of-concept stage in research labs. (Table 1-1)

Table 1-1. Examples of nanomedicines in clinical use, summarized in 2010. Reproduced with permission from [3], Copyright Massachusetts Medical Society.

Nanomaterial	Trade Name	Application	Target	Adverse Effects	Manufacturer	Current Status
Metallic						
Iron oxide	Feridex	MRI contrast	Liver	Back pain, vasodilatation	Bayer Schering	FDA approved
	Resovist	MRI contrast	Liver	None	Bayer Schering	FDA approved
	Combidex	MRI contrast	Lymph nodes	None	Advanced Magnetics	In phase 3 clinical trials
	NanoTherm	Cancer therapy	Various forms	Acute urinary retention	MagForce	In phase 3 clinical trials
Gold	Verigene	In vitro diagnostics	Genetic	Not applicable	Nanosphere	FDA approved
	Aurimmune	Cancer therapy	Various forms	Fever	CytImmune Sciences	In phase 2 clinical trials
Nanoshells	Auroshell	Cancer therapy	Head and neck	Under investigation	Nanospectra Biosciences	In phase 1 clinical trials
Semiconductor						
Quantum dot	Qdots, EviTags, semiconductor nanocrystals	Fluorescent contrast, in vitro diagnostics	Tumors, cells, tissues, and molecular sensing structures	Not applicable	Life Technologies, eBioscience, Nanoco, CrystalPlex, Cytodiagnostics	Research use only
Organic						
Protein	Abraxane	Cancer therapy	Breast	Cytopenia	Abraxis Bioscience	FDA approved
Liposome	Doxil/Caelyx	Cancer therapy	Various forms	Hand–foot syndrome, stomatitis	Ortho Biotech	FDA approved
Polymer	Oncaspar	Cancer therapy	Acute lymphoblastic leukemia	Urticaria, rash	Rhône-Poulenc Rorer	FDA approved
	CALAA-01	Cancer therapy	Various forms	Mild renal toxicity	Calando	In phase 2 clinical trials
Dendrimer	VivaGel	Microbicide	Cervicovaginal	Abdominal pain, dysuria	Starpharma	In phase 2 clinical trials
Micelle	Genexol-PM	Cancer therapy	Various forms	Peripheral sensory neuropathy, neutropenia	Samyang	For phase 4 clinical trials

1.2 Stimulus-responsive polymeric nanocarriers

Engineered nanocarriers, especially polymeric nanocarriers, have drawn increased attention in the nanomedicine field for transportation of active compounds such as small-molecular drugs, imaging materials, peptides or genes. These polymeric nanocarriers can enhance the solubility, bioavailability and prolonged circulation times of encapsulated or conjugated active compounds and also can be easily tailored for specific targeting and selective release at desired sites of action [12, 13]. Stimuli-responsive polymeric nanocarriers are nanometer-sized active polymeric delivery vehicles containing functional groups or blocks that are sensitive to internal or external stimulus. Chemical, biochemical or physical stimulus can significantly change the morphology or structure of the polymeric nanocarriers and thereby trigger the release of active species at specific sites. Figure 1-1 shows a general scheme of a stimuli-responsive nanocarrier to delivery active compounds.

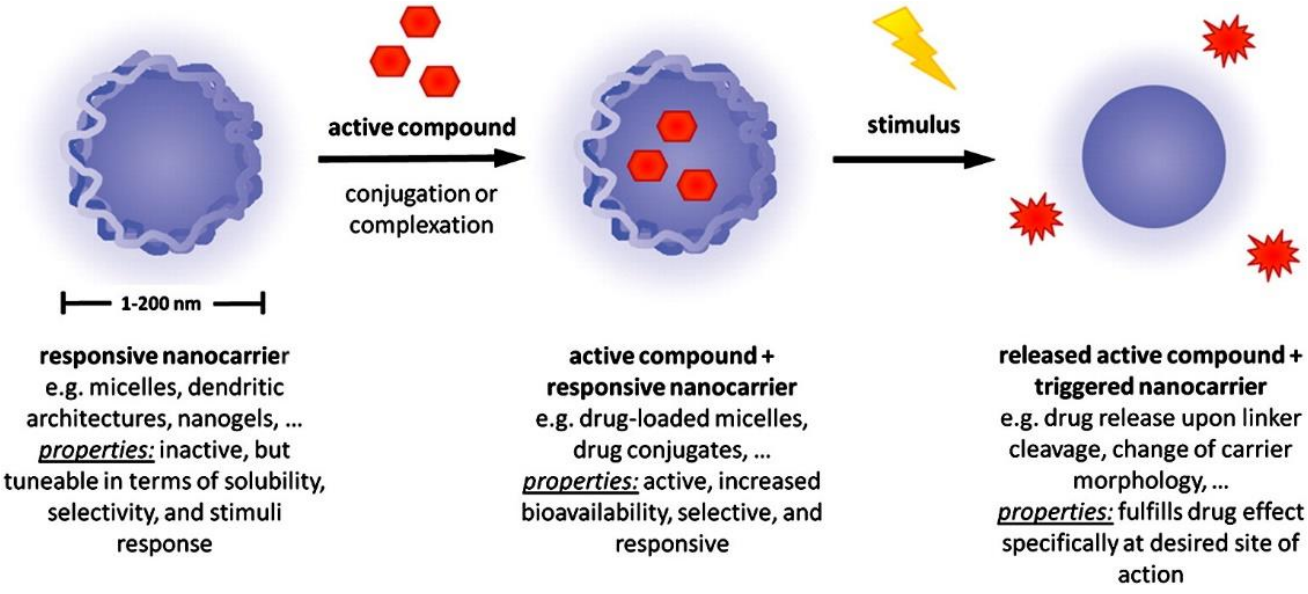

Figure 1-1 General scheme for delivery of an active compound from a stimuli-responsive nanocarrier. Reprinted from [13], with permission from Elsevier.

1.2.1 pH-sensitive polymeric nanocarriers

In biological system, there are various pH differences on both cellular and systemic levels in pathological states. Tumors and inflamed tissues are reported to be 0.5-1 pH units lower than ordinary cells and tissue[14]. This property can be utilized for the targeted stimuli-responsive delivery of drugs or genes to the diseased site. After the polymeric nanocarriers have undergone cellular uptake, they go through various well-defined pathological states with strongly different pH ranges. The endosomes (pH 6-6.8) as well as lysosomes (pH 4-5) have a typical reduced pH compared to the physiological pH of 7.2-7.4[15]. These pH differences provide a great localized trigger for the drug/gene release from polymeric nanocarriers[16].

The pH-sensitive polymeric nanocarriers can be constructed from polymers with ionizable functional groups such as amines or carboxylic acids. Polymeric nanocarriers with amine groups are fabricated at a pH above the pK_a of the amine groups. When the external pH decreases below the pK_a of the amine groups, the ionization will increase both the hydrophilicity and electrostatic repulsion of the polymer block and will lead to the destabilization to the polymeric nanocarriers and release of active compounds. Armes and coworkers reported a pH-sensitive polymeric nanocarrier formed at physiological pH by poly(2-(methacryloyloxy)ethylphosphorylcholine)-*co*-poly(2-(diisopropylamino)ethyl methacrylate) diblock copolymers (PMPC–PDPA)[17]. When below pH 6, the vesicles dissociate completely because of protonation of the tertiary amine groups on the PDPA block. The polymeric nanocarrier fabricated by PMPC-PDPA was applied as a gene delivery system [18]. The encapsulation and release of a DNA plasmid was achieved by tuning the solution pH. In mildly acidic aqueous solution (pH=6), the PMPC-*b*-PDPA

block copolymer and DNA plasmid were dissolved, while when the pH was increased to 7.5 the PMPC-*b*-PDPA polymeric nanocarrier were formed with DNA plasmid encapsulated. Poly(acrylic acid)-block-polystyrene-block-poly(4-vinylpyridine) (PAA_{26}-*b*-PS_{890}-*b*-$P4VP_{40}$) triblock copolymers were reported to form different aggregated morphologies ranging from vesicles, solid spherical aggregates, ellipsoidal aggregates, and back to vesicles with pH changes from 1 to 14[19]. The reason for the morphology changes was the difference in repulsive interactions inside the PAA or P4VP coronas at different pH conditions. Bae and coworkers reported the preparation of one pH-sensitive polymeric nanocarrier composed of poly(L-histidine)-*b*-poly(ethylene glycol) diblock copolymers (polyHis5K–*b*–PEG2K) which could release anticancer drugs at relatively acidic tumors[20]. An innovative pH-sensitive delivery system also reported by Bae's group [21] was formed by two block copolymers: poly(ethylene glycol)-*b*-poly(methyacryloyl sulfadimethoxine) (PEG-*b*-PSD), which was pH sensitive, and poly(ethylene glycol)-*b*-poly(l-lactic acid) (PEG-*b*-PLLA), which was conjugated to the TAT peptide (one group of cell permeable peptides containing a specific sequence such as H - Gly - Arg - Lys - Lys - Arg - Arg - Gln - Arg - Arg - Arg - OH). At neutral pH or physiological pH polyion complexes which formed between a positively charged TAT chain and a negative charged PSD block would be stable. At acidic pH/tumor pH, the complex would be destabilized and expose the TAT on the surface to penetrate the target tumor cells.

Another type of polymeric nanocarrier was constructed with a biocompatible nonresponsive polymer with pH-sensitive linkages between the active compound and polymer backbone. Ulbrich et al. synthesized one polymeric nanocarrier composed of N-(2-hydroxypropyl)methacrylamide (HPMA) conjugated with doxorubicin (DOX) via

hydrazone linkages [22]. The hydrazone linkage was cleaved upon the environment change from blood circulation and extracellular environment (pH 7.4) to intracellular compartment (pH~5-6) and enabled the pH triggered controlled release of DOX.

1.2.2 Redox sensitive polymeric nanocarriers

The intracellular and extracellular redox environments have a great difference: the redox environment inside cells is slightly reducing and outside cells is slightly oxidizing. Cysteine and glutathione are believed to be the main reducing agents that maintain both intracellular and extracellular redox equilibria[23]. For example, in humans, the reduced glutathione free thiol form is found at millimolar levels in the cellular fluids but only at micromolar levels in other body fluids [24]. The glutathione levels are found to be 7-10 fold higher in tumor cells than normal cells in vitro. These differences provide an opportunity for application of redox sensitive polymeric nanocarriers in programmed delivery of drugs and genes.

Polymeric nanocarriers with disulfide bonds can either encapsulate or conjugate with active genes and drugs outside the cell. Once the nanocarriers get into the cell, the disulfide bonds are reduced by the excess of reduced glutathione (GSH), therefore the drugs and genes present in the polymeric nanocarriers are released. Cavallaro and his coworkers [25] have reported a polymeric nanocarrier for gene delivery based on the highly water-soluble polymer α,β-poly(N-2-hydroxyethyl)-D,L-aspartamide (PHEA). Positively charged 3-trimethylammonium chloride groups were conjugated to the PHEA backbone to complex with negatively charged DNA and 3-(2-pyridyldithio)propionate groups were conjugated to the backbone to allow for formation of disulfide linkages between polymer chains to

stabilize the complexes in the extracellular environment. The fabricated PHEA-EDA-PDP-CPTA polymeric nanocarriers showed great stability in blood and selective DNA release under intracellular reductive environment. Kataoka's group [26] has synthesized PEG-SS-P[Asp(DET)] diblock copolymers which had one cationic segment based on poly(aspartamide) with a flanking diethylenetriamino group, P[Asp(DET)], conjugated to PEG through disulfide bonds. Nanocarriers fabricated from PEG-SS-P[Asp(DET)] exhibited stability with plasmid DNA and enhanced gene transfection efficiency and more rapid onset of gene expression than corresponding PEG-P[Asp(DET)] without disulfide bonds. Hubbell's group [27] has reported the synthesis and application of amphiphilic copolymer poly(ethylene glycol)-disulfide-poly(propylene sulfide) block copolymers (PEG-SS-PPS). Polymeric nanocarriers formed from PEG_{17}-SS-PPS_{30} could protect biomolecules outside cells but burst suddenly in the presence of cysteine or glutathione inside cells to release the encapsulated biomolecules, which could be useful in cytoplasmic delivery of biomolecular compounds. Wang's group [28] reported a polymeric nanocarrier for doxorubicin (DOX) delivery composed of the single disulfide bond-bridged block polymer of poly(ε-caprolactone) and poly(ethyl ethylene phosphate) (PCL-SS-PEEP). This PCL-SS-PEEP polymeric nanocarrier could achieve enhanced intracellular drug release and higher drug accumulation and retention in multidrug resistance (MDR) cancer cells. Another polymeric nanocarrier for DOX delivery based on poly(ethylene oxide)-b-poly(N-methacryloyl-N′-(t-butyloxycarbonyl)cystamine) (PEO-b-PMABC) diblock copolymers was reported by Gan's group [29]. In the cell experiment, PEO-b-PMABC nanocarriers encapsulating DOX were stable at physiological conditions and accomplished

faster drug release under reducing intracellular environment and higher anticancer efficacy compared to the non-redox-sensitive control.

1.2.3 Thermo-sensitive polymeric nanocarrier

At certain temperatures, thermo-sensitive polymers undergo phase-transitions and exhibit changes in conformation, solubility and other properties [30]. Depending on the different responses to heating, thermo-sensitive polymers can be divided into two kinds: polymers that become soluble upon heating have upper critical solution temperature (UCST); polymers which become insoluble upon heating have lower critical solution temperature (LCST). The thermo-sensitive LCST polymers are hydrophobic above the phase transition temperature while hydrophilic below the phase transition temperature. The thermo-sensitive LCST fragments can be used as either hydrophobic blocks or hydrophilic blocks upon morphology formation depending on temperature selection.

Developing thermo-sensitive polymeric nanocarriers for drug and gene delivery able to respond to small changes in temperature has recently attracted great research interest. In particular, poly(N-isopropylacrylamide) (PNIPAAm) with an LCST in water around 32 ℃ has been investigated as one component of temperature-sensitive polymeric nanocarriers [31, 32]. Discher, Yang and coworkers [31] synthesized narrowly distributed (PDI< 1.2) PEO-*b*-PNIPAAm block copolymers using reversible addition–fragmentation chain transfer (RAFT) polymerization. The PEO-*b*-PNIPAAm copolymers exhibited an LCST at 32 ℃. The block copolymers could form vesicles and incorporate either hydrophilic (e.g., DOX) or hydrophobic drugs above the LCST at 37 ℃, but were destabilized below the LCST at 25 ℃ to allow temperature-controlled quick release. The reported phase-transition

window was quite narrow which made the fabricated PEO-*b*-PNIPAAm nanocarriers quite attractive for temperature-triggered drug and gene delivery. Wei et al. [32] have reported the synthesis of a four-arm star block copolymer composed of a hydrophobic PMMA arm and an average of three hydrophilic PNIPAAm arms. Below the LCST of PNIPAAm (34 ℃), the star copolymers could self-assemble into thermo-sensitive polymeric nanocarriers with PMMA as the core and PNIPAAm as the shell. PMMA-PNIPAAm nanocarriers loaded with the anti-inflammation drug prednisone acetate showed thermo-responsive release behavior because of temperature-induced structural changes. At a temperature (25 ℃) below the PNIPAAm LCST, the PMMA-PNIPAAm nanocarriers released drug at a relatively low rate and retained 45 mol% of the initial drug loading after 240 h. At a temperature (40 ℃) above the PNIPAAm LCST, the PNIPAAm arm became hydrophobic and 90 mol% of the encapsulated drug was released after 240 h.

1.3 Passive targeting and active targeting

To design efficient polymeric nanocarriers, both passive targeting and active targeting can be utilized depending on the chemical and biological properties of target sites. Figure 1-2 illustrates the basic concept of passive targeting and active targeting.

Passive targeting is based on the enhanced permeation retention effect (EPR) which was first demonstrated by Maeda in the (styrene maleic acid) to neocarzinostatin (SMANCS) systems [33, 34]. The poorly formed vasculature around cancer cells and large gaps between the cells enhances permeation of large macromolecular drugs with sizes from 20 to 200 nm. Furthermore, tumor tissues lack effective lymphatic drainage due to the abnormal growth of the tumor which results in macromolecular drugs being trapped in the

vicinity of tumor tissue. This phenomenon has been referred to as the enhanced permeation retention (EPR) effect and has been found to be present not only in tumors but other diseases such as chronic inflammation and infection. The EPR effect offers opportunities for passive targeting simply by controlling the size of the macromolecular nanocarriers without involvement of targeting ligands. In addition to the EPR effect, the size of nanocarriers also influences the cellular uptake efficiency and pathway [35, 36].

Active targeting is to target diseased cells by introducing active targeting ligands such as large antibodies or small molecule ligands to the nanocarriers for cell surface receptors [37-40]. Reported successful examples of active targeting have usually had post assembly surface functionalization of nanocarriers with targeting ligands, including TAT peptide [37], hydrazide [38], adamantine-PEG and adamantine-PEG-human transferrin conjugates[39, 40].

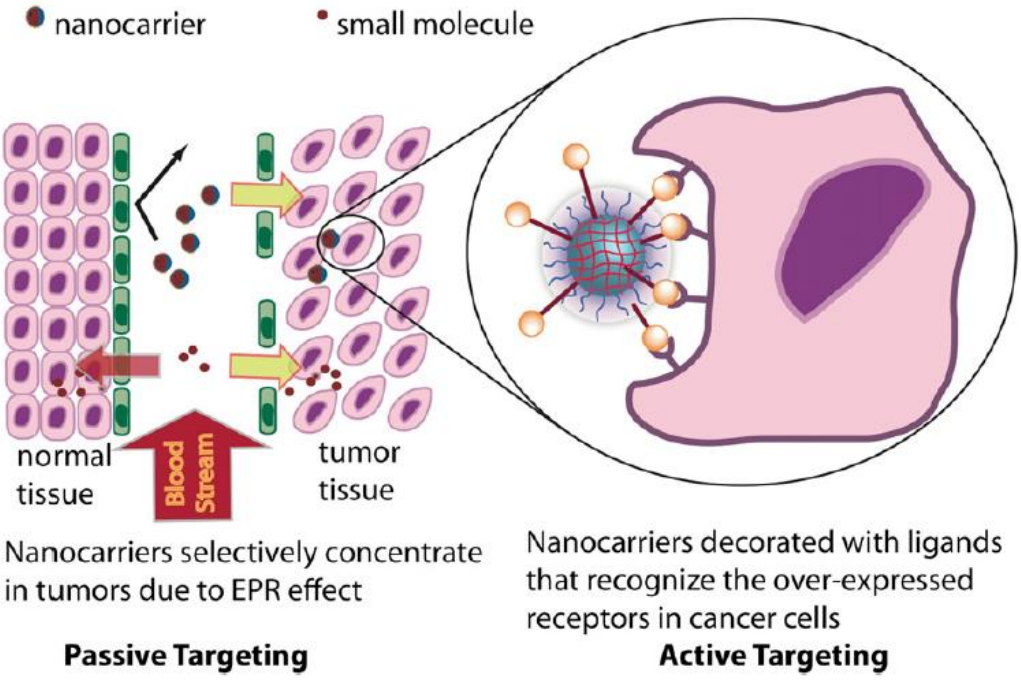

Figure 1-2 The concept of passive targeting and active targeting. Reprinted from [12], with permission from Elsevier.

1.4 Scope of the Thesis

This research was devoted to the preparation and characterization of stimuli-responsive star-shaped triblock copolymers, as well as their self-assembly in aqueous solution and biological application for drug and gene delivery.

Chapter 2 describes several key instruments and technologies for the analysis of star-shaped triblock copolymers and the complexes formed by the triblock copolymers and DNA plasmids. Dynamic light scattering (DLS) and small angle X-ray scattering (SAXS) were used to characterize the size of the nanoparticles formed by star-shaped triblock copolymers; agarose gel electrophoresis was applied to check the DNA condensation ability of the triblock copolymer; flow cytometry was used to quantitatively measure the transfection efficiency of the complexes formed by triblock copolymer and DNA plasmid; cytotoxicity assays were used to screen for cytotoxicity of the triblock copolymer.

Chapter 3 describes the synthesis of a redox-responsive triblock copolymer poly(ethylene oxide)/polylactide/polylysine (PEO-S(CK_n)-PLA) for gene delivery. A series of triblock copolymers with different block lengths has been synthesized.

Chapter 4 describes the application of triblock copolymer PEO-S(CK_n)-PLA in gene delivery. The complexes formed by PEO-S(CK_n)-PLA and green fluorescent protein (GFP) DNA plasmid were examined by DLS and agarose gel electrophoresis to study the DNA condensation ability, and further applied to HeLa cells line for gene transfection *in vitro*. The cytotoxicity of the triblock copolymer PEO-S(CK_n)-PLA was tested and compared to the corresponding polylysine and branched polyethylenimine (bPEI).

Chapter 5 contains conclusions and suggestions for future work.

References (Chapter 1)

1. Committee on Technology, N.S.a.T.C., *National nanotechnology initiative: Leading to the next industrial revolution*. 2000.

2. Farokhzad, O.C. and R. Langer, *Nanomedicine: Developing smarter therapeutic and diagnostic modalities.* Advanced Drug Delivery Reviews, 2006. **58**(14): p. 1456-1459.

3. Kim, B.Y.S., J.T. Rutka, and W.C.W. Chan, *Current concepts: Nanomedicine.* New England Journal of Medicine, 2010. **363**(25): p. 2434-2443.

4. Bangham, A.D., M.M. Standish, and J.C. Watkins, *Diffusion of univalent ions across the lamellae of swollen phospholipids.* Journal of Molecular Biology, 1965. **13**(1): p. 238-IN27.

5. Langer, R. and J. Folkman, *Polymers for the sustained release of proteins and other macromolecules.* Nature, 1976. **263**(5580): p. 797-800.

6. Gref, R., et al., *Biodegradable long-circulating polymeric nanospheres.* Science, 1994. **263**(5153): p. 1600-1603.

7. Bruchez, M., et al., *Semiconductor nanocrystals as fluorescent biological labels.* Science, 1998. **281**(5385): p. 2013-2016.

8. Chan, W.C.W. and S.M. Nie, *Quantum dot bioconjugates for ultrasensitive nonisotopic detection.* Science, 1998. **281**(5385): p. 2016-2018.

9. Cui, Y., et al., *Nanowire nanosensors for highly sensitive and selective detection of biological and chemical species.* Science, 2001. **293**(5533): p. 1289-1292.

10. Ferrari, M., *Cancer nanotechnology: Opportunities and challenges.* Nat Rev Cancer, 2005. **5**(3): p. 161-171.

11. Doane, T.L. and C. Burda, *The unique role of nanoparticles in nanomedicine: Imaging, drug delivery and therapy.* Chemical Society Reviews, 2012. **41**(7): p. 2885-2911.

12. Chacko, R.T., et al., *Polymer nanogels: A versatile nanoscopic drug delivery platform.* Advanced Drug Delivery Reviews, 2012. **64**(9): p. 836-851.

13. Fleige, E., M.A. Quadir, and R. Haag, *Stimuli-responsive polymeric nanocarriers for the controlled transport of active compounds: Concepts and applications.* Advanced Drug Delivery Reviews, 2012. **64**(9): p. 866-884.

14. Vaupel, P., F. Kallinowski, and P. Okunieff, *Blood-flow, oxygen and nutrient supply, and metabolic microenvironment of human-tumors - a review.* Cancer Research, 1989. **49**(23): p. 6449-6465.

15. Mukherjee, S., R.N. Ghosh, and F.R. Maxfield, *Endocytosis.* Physiological Reviews, 1997. **77**(3): p. 759-803.

16. Otto, K.R.W.a.S., *Reversible covalent chemistry in drug delivery.* Current Drug Discovery Technologies, 2005. **2**(3): p. 123-160.

17. Du, J.Z., et al., *Ph-sensitive vesicles based on a biocompatible zwitterionic diblock copolymer.* Journal of the American Chemical Society, 2005. **127**(51): p. 17982-17983.

18. Lomas, H., et al., *Biomimetic ph sensitive polymersomes for efficient DNA encapsulation and delivery.* Advanced Materials, 2007. **19**(23): p. 4238-+.

19. Liu, F.T. and A. Eisenberg, *Preparation and ph triggered inversion of vesicles from poly(acrylic acid)-block-polystyrene-block-poly(4-vinyl pyridine).* Journal of the American Chemical Society, 2003. **125**(49): p. 15059-15064.

20. Lee, E.S., et al., *Poly(l-histidine)-peg block copolymer micelles and ph-induced destabilization.* Journal of Controlled Release, 2003. **90**(3): p. 363-374.

21. Sethuraman, V.A. and Y.H. Bae, *Tat peptide-based micelle system for potential active targeting of anti-cancer agents to acidic solid tumors.* Journal of Controlled Release, 2007. **118**(2): p. 216-224.

22. Ulbrich, K., et al., *Antibody-targeted polymer-doxorubicin conjugates with ph-controlled activation.* Journal of Drug Targeting, 2004. **12**(8): p. 477-489.

23. Onaca, O., et al., *Stimuli-responsive polymersomes as nanocarriers for drug and gene delivery.* Macromolecular Bioscience, 2009. **9**(2): p. 129-139.

24. Saito, G., J.A. Swanson, and K.D. Lee, *Drug delivery strategy utilizing conjugation via reversible disulfide linkages: Role and site of cellular reducing activities.* Advanced Drug Delivery Reviews, 2003. **55**(2): p. 199-215.

25. Cavallaro, G., et al., *Reversibly stable thiopolyplexes for intracellular delivery of genes.* Journal of Controlled Release, 2006. **115**(3): p. 322-334.

26. Takae, S., et al., *Peg-detachable polyplex micelles based on disulfide-linked block catiomers as bioresponsive nonviral gene vectors.* Journal of the American Chemical Society, 2008. **130**(18): p. 6001-6009.

27. Cerritelli, S., D. Velluto, and J.A. Hubbell, *Peg-ss-pps: Reduction-sensitive disulfide block copolymer vesicles for intracellular drug delivery.* Biomacromolecules, 2007. **8**(6): p. 1966-1972.

28. Wang, Y.C., et al., *Redox-responsive nanoparticles from the single disulfide bond-bridged block copolymer as drug carriers for overcoming multidrug resistance in cancer cells.* Bioconjugate Chemistry, 2011. **22**(10): p. 1939-1945.

29. Sun, P.J., D.H. Zhou, and Z.H. Gan, *Novel reduction-sensitive micelles for triggered intracellular drug release.* Journal of Controlled Release, 2011. **155**(1): p. 96-103.

30. Schmaljohann, D., *Thermo- and ph-responsive polymers in drug delivery.* Advanced Drug Delivery Reviews, 2006. **58**(15): p. 1655-1670.

31. Qin, S.H., et al., *Temperature-controlled assembly and release from polymer vesicles of poly(ethylene oxide)-block-poly(n-isopropylacrylamide).* Advanced Materials, 2006. **18**(21): p. 2905-+.

32. Wei, H., et al., *Self-assembled, thermosensitive micelles of a star block copolymer based on pmma and pnipaam for controlled drug delivery.* Biomaterials, 2007. **28**(1): p. 99-107.

33. Ohtsuka, N., et al., *Anticancer effects of arterial administration of the anticancer agent smancs with lipiodol on metastatic lymph-nodes.* Cancer, 1987. **59**(9): p. 1560-1565.

34. H. Maeda, Y.M., *Tumouritropic and lymphotropic principles of macromolecular drugs.* Crit. Rev. Ther. Drug Carrier Syst, 1989. **6**: p. 193-210.

35. Godbey, W.T., K.K. Wu, and A.G. Mikos, *Size matters: Molecular weight affects the efficiency of poly(ethylenimine) as a gene delivery vehicle.* Journal of Biomedical Materials Research, 1999. **45**(3): p. 268-275.

36. Rejman, J., et al., *Size-dependent internalization of particles via the pathways of clathrin-and caveolae-mediated endocytosis.* Biochemical Journal, 2004. **377**: p. 159-169.

37. Roy, R., D.J. Jerry, and S. Thayumanavan, *Virus-inspired approach to nonviral gene delivery vehicles.* Biomacromolecules, 2009. **10**(8): p. 2189-2193.

38. Hayashi, H., et al., *Ph-sensitive nanogel possessing reactive peg tethered chains on the surface.* Macromolecules, 2004. **37**(14): p. 5389-5396.

39. Davis, M.E., et al., *Evidence of rnai in humans from systemically administered sirna via targeted nanoparticles.* Nature, 2010. **464**(7291): p. 1067-U140.

40. Heidel, J.D., et al., *Administration in non-human primates of escalating intravenous doses of targeted nanoparticles containing ribonucleotide reductase subunit m2 sirna.* Proceedings of the National Academy of Sciences of the United States of America, 2007. **104**(14): p. 5715-5721.

Chapter 2 Analytical Instrumentation

2.1 Dynamic light scattering (DLS)

Dynamic light scattering (DLS) is an important technique to measure size and size distribution of polymer or biomolecule dispersions because this method can quickly generate results without changing or destroying the samples. DLS based on the time-dependent scattered intensity became practical after the invention of the monochromatic and coherent laser about five decades ago [1-4]. Figure 2-1 illustrates the main components of a typical DLS system. The laser light is shot through a polarizer to define the polarization of the incident beam and impinges on the sample cell. The scattered light (Rayleigh scattering) then goes through an analyzer to select a given polarization and a detector to measure the intensity of the scattered light. The position of the detector defines the scattering angle θ. The intensity of scattered light is input to an autocorrelator to compare the scattered light intensity at successive time intervals to monitor the time fluctuations in the intensity of light scattered. The autocorrelation of the scattered intensity could be further analyzed by software based on theoretical relationships.

In DLS, the intensity-intensity time correlation function $G^{(2)}(t)$ in the self-beating mode is measured and the normalized distribution function of the characteristic line width $G(\Gamma)$ is obtained by using Laplace inversion [5, 6]. The line width Γ could be expressed as

$$\frac{\Gamma}{q^2} = D_t(1 + k_d C)[1 + f\left(R_g q\right)^2] \quad (2\text{-}1)$$

where D_t is the translational diffusion coefficient, C is the solution concentration and q is the wave vector defined as

$$q = \frac{4\pi n}{\lambda} \sin(\frac{\theta}{2}) \quad (2\text{-}2)$$

where λ is the incident laser wavelength, n is the refractive index of the sample and θ is the scattering angle.

When $C \rightarrow 0$ and $q \rightarrow 0$, Γ/q^2 is approximately equal to D_t. The hydrodynamic radius R_h could be obtained by using the Stokes-Einstein equation

$$D_t = \frac{k_B T}{6\pi\eta R_h} \quad (2\text{-}3)$$

where k_B, T and η are the Boltzmann constant, the absolute temperature and the solvent viscosity, respectively.

The application of DLS to measure sizes of polymeric nanoparticles in liquid dispersion depends on the validity of the Stokes-Einstein relation for spherical particles and its analogs for non-spherical particles. It requires the dispersion to be very dilute to eliminate the correlations between the polymeric nanoparticles. Also because polymeric nanoparticle dispersions are particles with a distribution of sizes and shapes, the measurement of the hydrodynamic radius needs different mathematical analysis methods. A program called "CONTIN" has been developed by Provencher [7], which finds the smoothest simulation curve consistent with the data and noise in it and gives estimates for the widths and peaks of unimodal distribution, even bimodal distribution with some limitations.

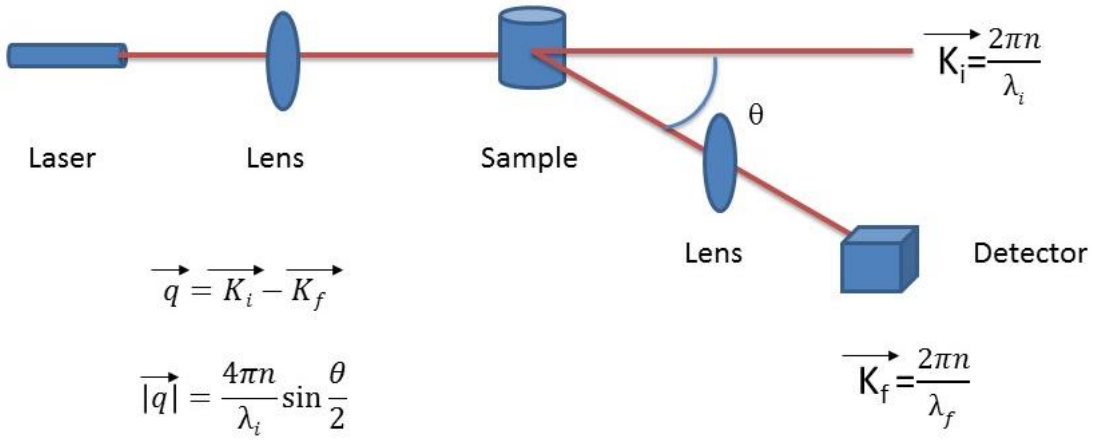

Figure 2- 1 A schematic representation of the dynamic light-scattering experiment.

The commercial DLS instrument (Brookhaven Instruments Corp. 90 Nanosizer) was used to measure the size of diblock copolymer PEO-S-PLA and triblock copolymer PEO-S(CK_n)-PLA and the complexes formed by triblock copolymer PEO-S(CK_n)-PLA and GFP DNA plasmid.

2.2 Small angle X-ray scattering (SAXS)

Small angle X-ray scattering (SAXS) is one type of small-angle scattering (SAS) technique that can be used to analyze the microscale or nanoscale structure of various systems such as metal alloys, nanoparticles, biological macromolecules in solution, emulsions, porous materials, and synthetic polymers in solution or in bulk [6, 8-13]. In a scattering experiment with a polymer solution, X-rays with wavelength λ typically around 0.15 nm are scattered by the polymer and the scattered intensity I(Q) is recorded as a

function of wavevector transfer Q (Q=4πsinθ/λ, where 2θ is the angle between the incident and scattered radiation). Figure 2-2 illustrates the main components of the SAXS experiment.

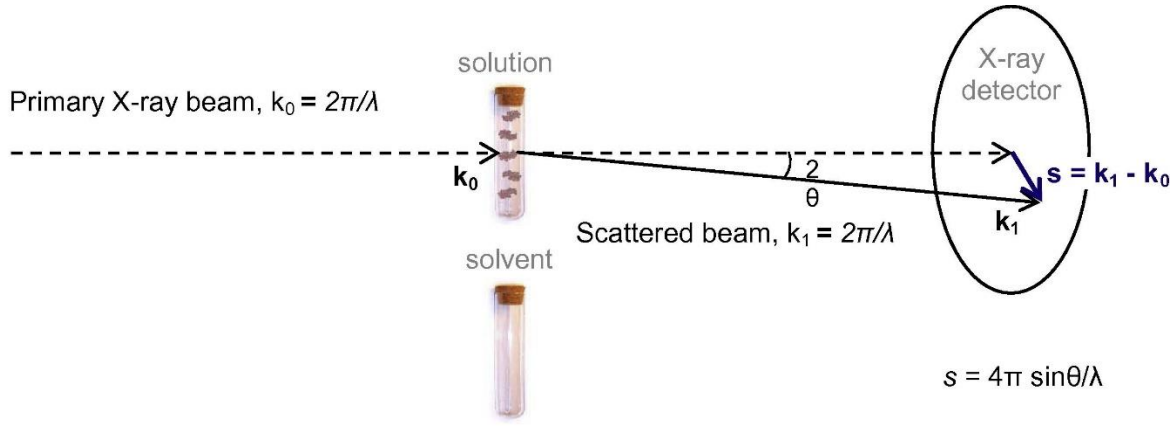

Figure 2- 2 Schematic representation of a SAXS experiment. Reprinted from [13] with permission from Elsevier.

In SAXS, the size of micelles formed in polymer solution can be estimated by the radius of gyration R_g, which can be extracted using the Guinier Approximation

$$I(Q) \propto \exp(-R_g^2 Q^2/3) \quad (2\text{-}4)$$

$$\mathrm{Ln}I(Q) \sim -R_g^2 Q^2/3 \quad (2\text{-}5)$$

in the low-q regime ($R_g Q \leq 1$) of an SAXS profile [6].

2.3 Agarose gel electrophoresis

Agarose gel electrophoresis is one type of gel electrophoresis used to separate DNA or proteins in a matrix of agarose which has been widely used in biochemistry, molecular biology, microbial genetics and clinical chemistry [14]. Agarose, a polysaccharide consisting of 1,3-linked β-D-galactopyranose and 1,4-linked 3,6-anhydro-α-L-galactopyranose, can be dissolved in a suitable electrophoresis buffer at a concentration of 0.7-2% w/v to form an agarose gel which has a three-dimensional matrix with channels and pores for biomolecules to pass through. The pore size of the agarose gel may vary with different concentrations and the pore size of the commonly used 1% gel is roughly between 100 nm to 500 nm [15, 16].

When DNA is separated by agarose gel electrophoresis, the negative charge of its phosphate backbone moves the DNA towards the positively charged anode. The migration of DNA in agarose gel electrophoresis is affected by several factors such as size of the DNA, conformation of DNA, gel concentration, voltage, the ionic strength of the buffer and the concentration of the intercalating dye if used. In a specific agarose gel electrophoresis experiment, factors other than size and conformation of DNA will be adjusted to ideal values to make sure that DNA components can be separated by size and conformation [17]. In general, the size of DNA affects DNA migration in such a way that smaller DNA with a lower number of base pairs (bp) travels faster in the agarose gel than larger DNA with a higher number of base pairs (bp). The effect of DNA conformation on DNA migration is reflected by the fact that supercoiled DNA usually migrates faster than relaxed DNA because the supercoiled DNA is tightly coiled and more compact, thus travelling faster in the agarose gel.

For standard agarose gel electrophoresis, a general procedure includes the casting of gel, loading of samples, electrophoresis, staining and visualization. As described in the previous paragraph, the agarose gel can be cast by dissolving agarose in a suitable electrophoresis buffer at an appropriate concentration. A comb is usually placed to create sample loading wells before the gel is completely set. After the gel has set, DNA samples with loading buffer are added to the wells by pipette. Then the agarose gel slab is placed in an electrophoresis tank submerged in buffer and the electrophoresis starts once the voltage is applied. The visualization of DNA can be achieved either by UV staining (e.g., ethidium bromide) or non UV staining (e.g., crystal violet).

2.4 Flow Cytometry

Flow cytometry is a powerful tool to measure and distinguish cells with different physical properties.[18-21] Flow cytometry has several advantages such as measuring multiple parameters simultaneously, high-speed analysis of 100-1000 cells per second and fluorescent based cell sorting [18]. In a typical flow cytometry test, the single cell suspension is passed through the laser intercept in such a way that multiple laser light signals are measured and recorded for each cell. The laser light signals could be divided into two categories: scattered laser light signals and fluorescent signals. Forward-scattered light (FSC) and side-scattered light (SSC) signals are usually used to count the total number of tested cells. The fluorescent light (FL) signals could distinguish tested cells with different fluorescent properties. Through combination of FSC, SSC and FL signals, the percentage of specific fluorescent cells within the tested cells could be estimated.

2.5 Cytotoxicity Assay

The cytotoxicity of compounds limits the potential pharmaceutical applications and needs to be measured prior to any further clinical investigations. Cytotoxicity can be measured by several methods such as assessing cell membrane integrity (e.g., LDH assay, ATP assay), reducing potential (e.g., MTT assay, MTS assay, XTT assay and WST-1 assay) and protease activity (e.g., GF-AFC assay)[22] .

The MTT (3-(4,5-dimethylthiazol-2-yl)-2,5-diphenyltetrazolium bromide) tetrazolium reduction assay was the first homogeneous colorimetric assay developed [23-25]. Yellow MTT can be reduced by viable cells with active metabolism to purple formazan with an absorbance maximum near 570 nm. Because the formazan of MTT is insoluble in culture media, selected solvents such as DMF need to be used to dissolve the formazan form of MTT and the absorbance of resulted solution is measured.

The MTS 3-(4,5-dimethylthiazol-2-yl)-5-(3-carboxymethoxyphenyl)-2-(4-sulfophenyl)-2H-tetrazolium) reduction assay also been used for cytotoxicity tests[26-29]. Commercial MTS assays contain phenazine methyl sulfate (PMS) or phenazine ethyl sulfate (PES) to enhance the cell penetration ability and stability of MTS. The formazan form of MTS is water soluble with an absorbance maximum around 490 nm and can be directly measured without any additional solvents by a plate-reader.

References (Chapter 2)

1. Chu, B., *Laser light scattering of polymer solutions.* Applied Optics, 1997. **36**(30): p. 7650-7656.

2. Pecora, R., *Dynamic light scattering measurement of nanometer particles in liquids.* Journal of Nanoparticle Research, 2000. **2**(2): p. 123-131.

3. Bruce J. Berne, R.P., *Dynamic light scattering: With applications to chemistry, biology and physics.* Courier Dover Publicatios (2000), 2000.

4. Chu, B., *Dynamic light scattering.* Soft Matter Characterization, 2008: p. 335-372.

5. Liang, D.H., et al., *In vitro non-viral gene delivery with nanofibrous scaffolds.* Nucleic Acids Research, 2005. **33**(19): p. 8.

6. Ozcan, Y., et al., *Micellization behavior of tertiary amine-methacrylate-based block copolymers characterized by small-angle x-ray scattering and dynamic light scattering.* Materials Chemistry and Physics, 2013. **138**(2-3): p. 559-564.

7. Provencher, S.W., *Contin: A general purpose constrained regularization program for inverting noisy linear algebraic and integral equations.* Computer Physics Communications 1982. **27**: p. 229-242.

8. Svergun, D.I. and M.H.J. Koch, *Small-angle scattering studies of biological macromolecules in solution.* Reports on Progress in Physics, 2003. **66**(10): p. 1735-1782.

9. Pople, J.A., et al., *Ordered phases in aqueous solutions of diblock oxyethylene/oxybutylene copolymers investigated by simultaneous small-angle x-ray scattering and rheology.* Macromolecules, 1997. **30**(19): p. 5721-5728.

10. Pedersen, J.S., et al., *A small-angle neutron and x-ray contrast variation scattering study of the structure of block copolymer micelles: Corona shape and excluded volume interactions.* Macromolecules, 2003. **36**(2): p. 416-433.

11. Jeng, U.S., et al., *Study of aggregates of fullerene-based ionomers in aqueous solutions using small angle neutron and x-ray scattering.* Journal of Physical Chemistry B, 1999. **103**(7): p. 1059-1063.

12. Jeng, U., et al., *Study on aqueous mixtures of fullerene-based star lonomers and sodium dodecyl sulfate using small angle scattering with contrast variation.* Journal of Physical Chemistry A, 2002. **106**(51): p. 12209-12213.

13. Kikhney, A.G. and D.I. Svergun, *A practical guide to small angle x-ray scattering (saxs) of flexible and intrinsically disordered proteins.* Febs Letters, 2015. **589**(19): p. 2570-2577.

14. Serwer, P., *Agarose gels - properties and use for electrophoresis.* Electrophoresis, 1983. **4**(6): p. 375-382.

15. Zimm, B.H. and S.D. Levene, *Problems and prospects in the theory of gel-electrophoresis of DNA.* Quarterly Reviews of Biophysics, 1992. **25**(2): p. 171-204.

16. Viovy, J.L., *Electrophoresis of DNA and other polyelectrolytes: Physical mechanisms.* Reviews of Modern Physics, 2000. **72**(3): p. 813-872.

17. Sinden, R.R., *DNA structure and function*. 1994: Gulf Professional Publishing. 398.

18. Davey, H.M. and D.B. Kell, *Flow cytometry and cell sorting of heterogeneous microbial populations: The importance of single-cell analyses.* Microbiological Reviews, 1996. **60**(4): p. 641-&.

19. Jennings, C.D. and K.A. Foon, *Recent advances in flow cytometry: Application to the diagnosis of hematologic malignancy.* Blood, 1997. **90**(8): p. 2863-2892.

20. Doan, H., G.M. Chinn, and R.R. Jahan-Tigh, *Flow cytometry ii: Mass and imaging cytometry.* Journal of Investigative Dermatology, 2015. **135**(9): p. 1-4.

21. Pedreira, C.E., et al., *Overview of clinical flow cytometry data analysis: Recent advances and future challenges.* Trends in Biotechnology, 2013. **31**(7): p. 415-425.

22. Terry L Riss, R.A.M., Andrew L Niles, Helene A Benink, Tracy J Worzella, and Lisa Minor, *Cell viability assays*, in *Assay guidance manual*, C.N. Sittampalam GS, Nelson H, et al, Editor. 2013.

23. Mosmann, T., *Rapid colorimetric assay for cellular growth and survival - application to proliferation and cyto-toxicity assays.* Journal of Immunological Methods, 1983. **65**(1-2): p. 55-63.

24. Berridge, M.V. and A.S. Tan, *Characterization of the cellular reduction of 3-(4,5-dimethylthiazol-2-yl)-2,5-diphenyltetrazolium bromide (mtt) - subcellular-localization, substrate dependence, and involvement of mitochondrial electron-transport in mtt reduction.* Archives of Biochemistry and Biophysics, 1993. **303**(2): p. 474-482.

25. Marshall, N.J., C.J. Goodwin, and S.J. Holt, *A critical-assessment of the use of microculture tetrazolium assays to measure cell-growth and function.* Growth Regulation, 1995. **5**(2): p. 69-84.

26. Cory, A.H., et al., *Use of an aqueous soluble tetrazolium formazan assay for cell-growth assays in culture.* Cancer Communications, 1991. **3**(7): p. 207-212.

27. Yang, Y., et al., *Synthesis of amine-functionalized diene-based polymers as novel gene delivery vectors.* Macromolecules, 2006. **39**(25): p. 8625-8631.

28. Arote, R., et al., *A biodegradable poly(ester amine) based on polycaprolactone and polyethylenimine as a gene carrier.* Biomaterials, 2007. **28**(4): p. 735-744.

29. Yogesh Patil, J.P., , , *Polymeric nanoparticles for sirna delivery and gene silencing.* International Journal of Pharmaceutics, 2009. **367**(1-2): p. 195-203.

Chapter 3 Synthesis of redox-responsive amphiphilic PEO-S(CK_n)-PLA triblock copolymers for gene delivery

3.1 Introduction

3.1.1 Amphiphilic block copolymers

Block copolymers containing multiple polymer blocks formed by different monomer species can exhibit unique properties comparing to the homopolymers. Amphiphilic block copolymers with hydrophobic blocks and hydrophilic blocks can self-assemble into various structures such as spherical micelles, cylindrical micelles or vesicles (Figure 3-1) in selective solvents due to the minimization of Gibbs free energy [1-4].

The different morphologies are determined by the inherent molecular curvature which can be estimated by a dimensionless packing parameter p

$$\mathrm{p} = \frac{v}{a_o l_c} \qquad (3\text{-}1)$$

where v is the volume of the hydrophobic chains, a_o is the optimal area of the head group, and l_c is the length of the hydrophobic tail. As a general rule, amphiphilic polymers with $p \leq 1/3$ favor spherical micelles, with $1/3 \leq p \leq 1/2$ favor cylindrical micelles and with $½ \leq p \leq 1$ favor enclosed membrane structures such as vesicles [5]. However, these three factors, v, a_o, and l_c are not well-established for all given polymers. Another simple factor used to estimate the morphology is the hydrophilic mass fraction f_{philic}. In general, amphiphilic polymers with $f_{philic} > 50\%$ favor spherical micelles, with $40\% < f_{philic} < 50\%$ favor cylindrical micelles and with $f_{philic} < 40\%$ favor enclosed membranes structures [6].

Amphiphilic block copolymer micelles and vesicles have great potential for biomedical applications such as drug or gene delivery for the following reasons [7]: first, drugs and nucleic acids can be encapsulated or conjugated inside the core of block copolymer micelles or vesicles and transported at relatively high concentration. Second, hydrophilic blocks, usually poly(ethylene oxide) PEO, can hydrogen-bond to surrounding water molecules to make a shell to protect the micelles or vesicles core. Third, the sizes and morphologies of the micelles and vesicles can be easily controlled by modifying the chemical composition, molecular weight and block length ratio of the constituent polymers.

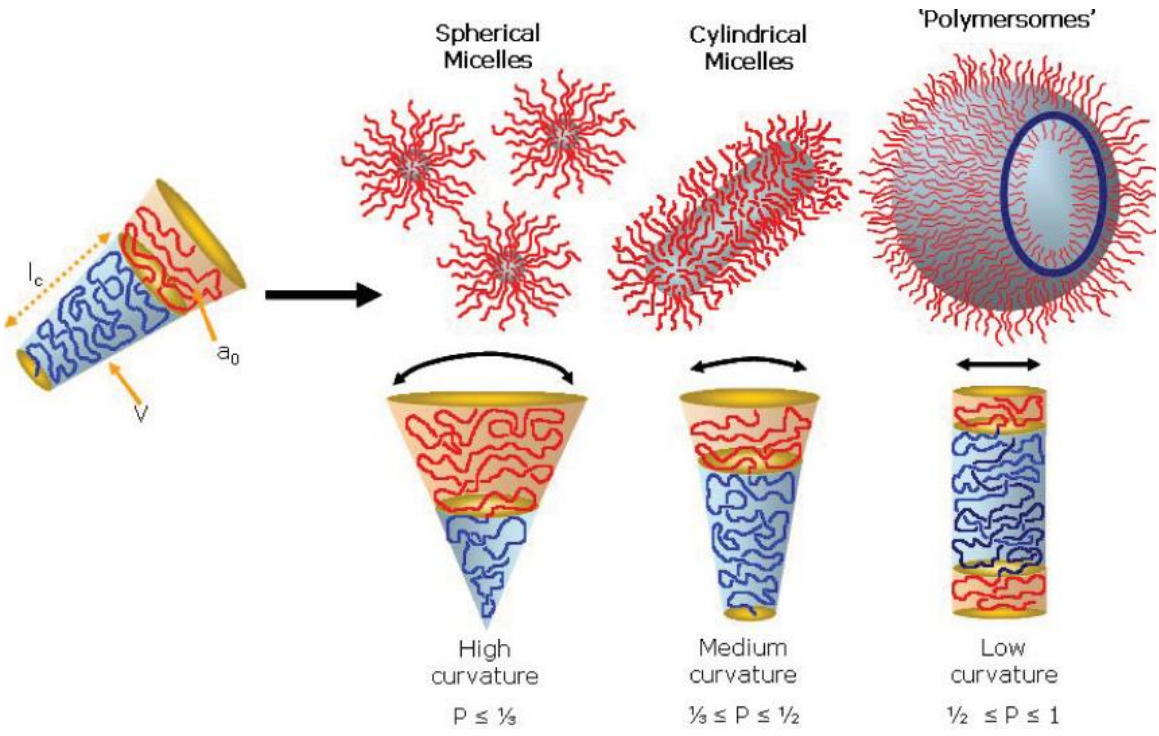

Figure 3- 1 Schematic of spherical micelles, worm-like micelles and vesicles. Reprinted from [3], with permission of John Wiley and Sons.

3.1.2 Gene Delivery

Gene delivery is the transport of foreign genetic materials (DNA, RNA, and other nucleic acids) to cells for gene expression modifications [8]. Gene vectors based on different type of materials have been studied and applied for gene delivery. Viral vectors based on retroviruses have the natural ability to transfect cells and achieve high gene transfection efficiency. However, the cytotoxicity and immunogenic response of viral vectors became a huge obstacle for clinical applications [8]. There was a clinical gene therapy trial involving retroviral vectors which was stopped after the observation of serious adverse events in two patients who developed a monoclonal lymphoproliferative disease during the treatment [9]. Nonviral vectors based on cationic lipids or polymers provide a

promising alternative approach for gene delivery. Both natural cationic polymers [10] (e.g., chitosan) and synthetic cationic polymers (e.g. PLL, PEI and PAMAM) [8, 11-13] have been studied as possible non-viral vectors for gene delivery. Natural cationic polymers have advantages as being biodegradable, non-toxic and biocompatible but little control over structure and homogeneity is possible [10]. Structure and homogeneity of synthetic cationic polymers can be controlled but these polymers may be non-biodegradable, toxic and non-biocompatible. Figure 3-2 shows structures of the most widely studied commercially available synthetic cationic polymers used for gene delivery: polylysine, polyethylenimine (PEI) and polyamidoamine (PAMAM). With an abundance of primary amine groups, these cationic polymers can complex with negatively charged DNA by electrostatic interactions and transport DNA. However, the free cationic groups also interact with the cell membranes and extracellular matrix proteins which can lead to cytotoxicity [14, 15]. The relatively low efficiency and cytotoxicity of synthetic cationic polymer gene vectors still needs to be improved for clinical applications of gene delivery.

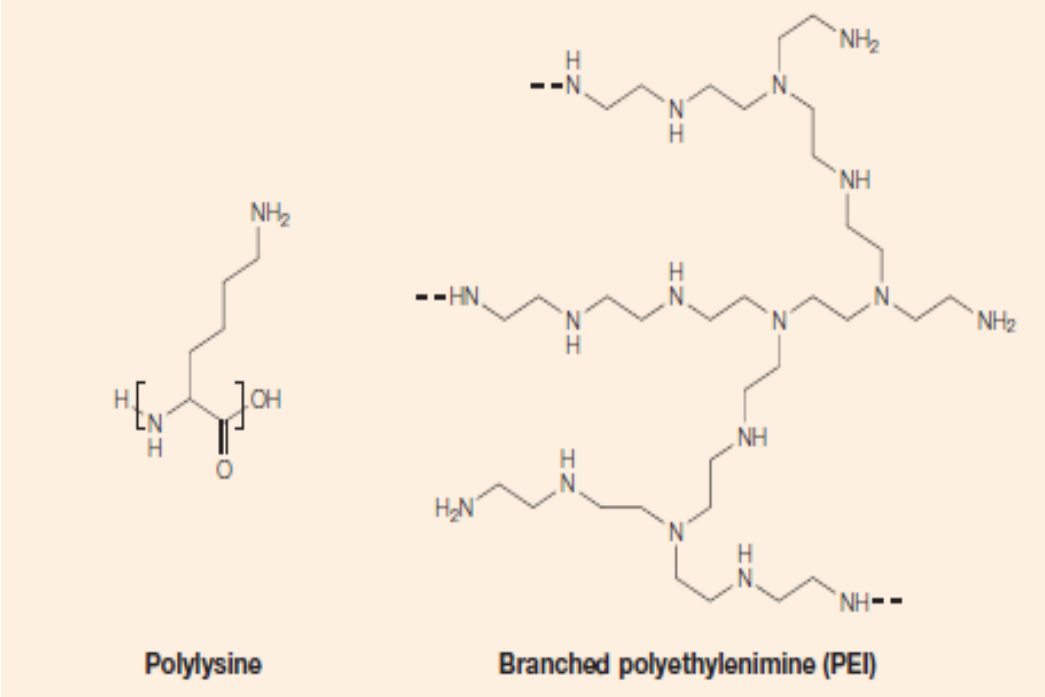

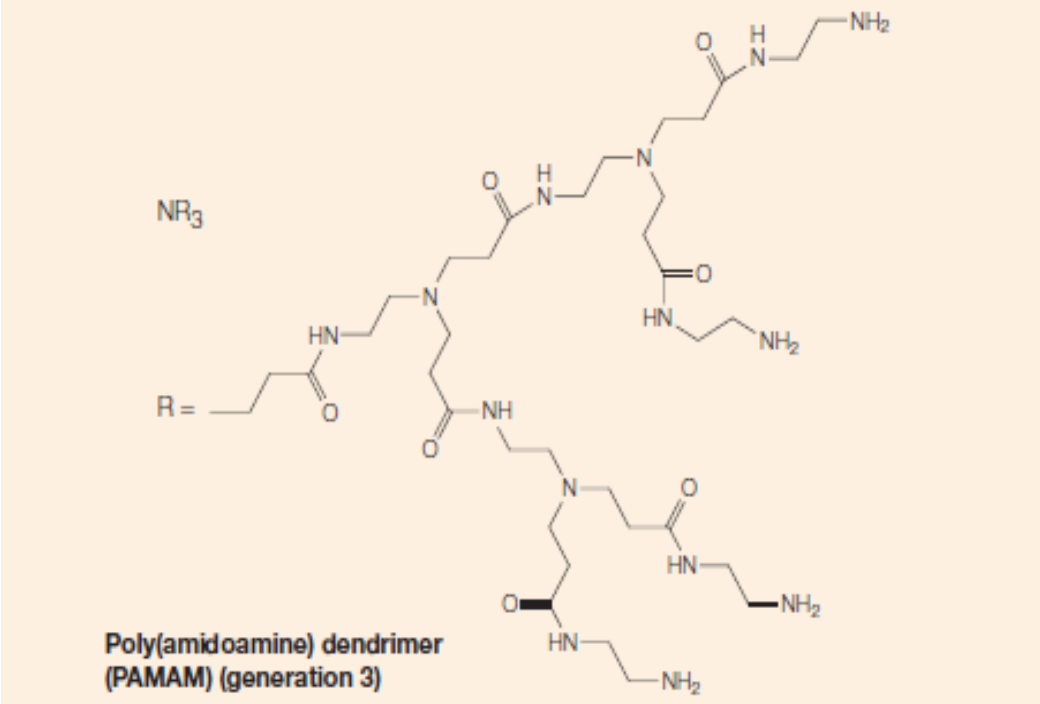

Figure 3- 2 Structures of commercially available synthetic cationic polymers PLL, PEI and PAMAM for gene delivery. Reprinted from [11] by permission from Macmillan Publishers Ltd.

3.1.3 Motivation and design of star-shaped triblock copolymer PEO-S(CK_n)-PLA

To develop a new type of synthetic polymer gene delivery vector with enhanced gene transfection efficiency and reduced cytotoxicity, an amphiphilic copolymer structure can be introduced into the cationic polymer gene delivery system and the hydrophilic blocks and hydrophobic blocks can stabilize the formed polymer/DNA complexes in both aqueous and hydrophobic environments. The designed cationic copolymer contain three arms: (1) a hydrophilic arm which can protect the DNA in aqueous solutions; (2) a biodegradable hydrophobic arm which can stabilize the polymer/DNA complex in hydrophobic environments; and (3) a cleavable positively charged arm which can complex with the DNA and release it inside the cells with excess of reduced glutathione (GSH).. Figure 3-3 illustrates the basic structure of the tri-arm star triblock copolymer with cleavable cationic segment.

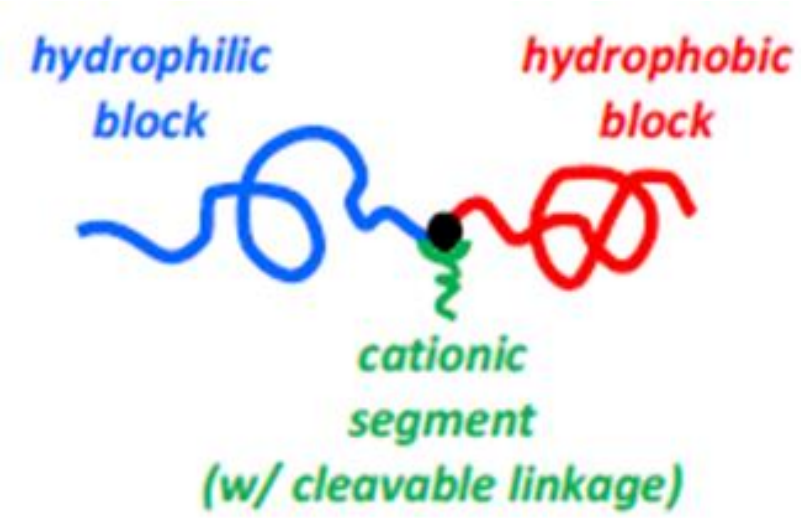

Figure 3- 3 Structure of the amphiphilic tri-arm star triblock copolymer.

Hydrophilic and biocompatible poly(ethylene oxide) PEO, also known as poly(ethylene glycol) PEG, has been widely used in biomedical applications because of its ability to hinder uptake of PEO-modified particles by the reticulo-endothelial system (RES) [16], thus elongating the blood circulation time of the particles. Therefore PEO has often been used as the hydrophiphilic block in amphiphilic copolymers to reduce interactions of polymer assemblies with serum proteins and to increase the stability of assemblies [17, 18]. PEOs at different molecular weights with various terminal functional groups are commercial available. In this thesis, amine terminated PEO with molecular weight 2 kg/mol or 5 kg/mol was used as the starting material.

Poly(lactic acid) (PLA) is a relatively hydrophobic, hydrolytic biodegradable and biocompatible polyester which has been widely studied for biomedical applications [19]. Because PLA homopolymer is too brittle and hydrophobic for biomedical applications, copolymers with PLA as the hydrophobic block are usually used as efficient drug/gene delivery vectors [3, 20, 21] or porous scaffold materials [22]. The PLA block can be synthesized by hydroxyl group initiated ring opening polymerization (ROP) of lactide monomer by various catalysts such as tin octoate $Sn(Oct)_2$ [23-25], thiourea-based bifunctional organocatalysts [26-28] (e.g. 1,5,7-Triazabicyclo[4.4.0]dec-5-ene (TBD), N-methyl-TBD (MTBD), and 1,8-diazabicyclo[5.4.0]-undec-7-ene (DBU)) and others [29]. The living nature of the ring opening polymerization of lactide provides a method to synthesize well-defined PLA blocks with narrow molecular weight distributions. The molecular weight of the PLA block can be easily controlled by the ratio of monomer and initiator in the ring opening polymerization.

Amine-functionalized polymers including polyethylenimine (PEI) and its derivatives [30-32], polylysine and its derivatives [33-35] and polyamidoamine (PAMAM) dendrimers [36-38] are among the most widely applied cationic polymers in gene delivery systems. Polylysine is a biodegradable poly(amino acid) with pendent amine groups that can ionically interact with the negatively charged DNA backbone [33, 34]. Polylysine can be easily synthesized from monomer Z-lysine-*N*-carboxyanhydride and act as the cationic block in synthetic cationic copolymer system [39, 40].

Introduction of degradable linkages such as hydrolytically degradable ester, phosphazene, or carbonate groups or bioreducible disulfide bonds into polymer backbones or side chains has been adopted as a strategy for reducing toxicity and improving biodegradability of cationic polymer gene vectors [41-44]. Among these degradable linkages, disulfide bonds show great stability during storage, during systemic circulation, and in extracellular environments, however, they are easily and quickly cleaved though a thiol-disulfide exchange reaction with glutathione inside the cell [41].

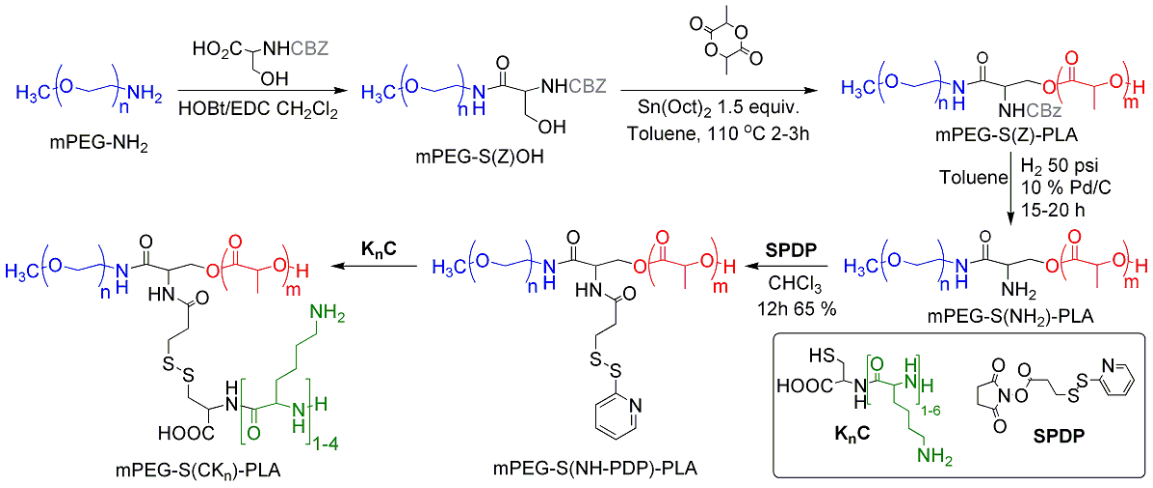

Figure 3- 4 Synthesis of amphiphilic tri-arm star copolymer for DNA delivery

The synthetic route to amphiphilic tri-arm star copolymers for DNA delivery is illustrated in Figure 3.4. The designed route to synthesize the tri-arm star triblock PEO-S(CK_n)-PLA polymers started with the coupling of benzyloxycarbonyl (CBZ)-protected serine with amine-terminated PEO to afford the hydroxyl-terminated polymer mPEO-S(Z)-OH [45]. Then the mPEO-S(Z)-OH could be used to initiate the ring opening polymerization (ROP) of lactide with an activating agent tin octoate to form the diblock copolymer mPEO-S(Z)-PL $Sn(Oct)_2$ [23-25]. After lactide polymerization, the CBZ group was removed by either reaction with HBr/acetic acid [46] or hydrogenolysis by H_2 with Pd/C [47] at room temperature to afford mPEO-S(NH_2)-PLA. The amine group in mPEO-S(NH_2)-PLA reacted with *N*-succimidyl-3-(2-pyridyldithio)propionate (SPDP) to form active disulfide intermediate mPEO-S(NH-PDP)-PLA [48-50]. Then the active mPEO-S(NH-PDP)-PLA diblock copolymer was reacted with lysine oligomers with a cysteine residue at the C-terminus (HS-CK_n) to form the PEO-S(CK_n)-PLA star copolymers .

3.2 Experimental

Materials

Methoxy poly(ethylene glycol) amines (PEO2k-amine M_n = 2170 g/mol, 98.8% and PEO5k-amine M_n = 5187 g/mol, 99.0%) were purchased from JenKem Technology (Beijing, China). 3,6-Dimethyl-1,4-dioxane-2,5-dione (*D,L*-lactide) and 1,8-diazabicyclo[5,4,0]undec-7-ene (DBU) (98%) were purchased from Sigma-Aldrich. Carbobenzoxyl-*D,L*-serine (*N*-Cbz-*D,L*-serine) was purchased from TCI. Triethylamine (TEA) (99%) was purchased from J. T. Baker. Trifluoroacetic acid (TFA) (99.5+ %), *N*-

carbobenzoxyl-*L*-lysine (*N*-Cbz-*L*-lysine), 2-mercaptopyridine (98%) and dithiothreitol (DTT) (98%) were purchased from Alfa Aesar. 1-(3-Dimethylaminopropyl)-3-ethylcarbodiimide hydrochloride (EDC•HCl) was purchased from Acros Organics. Hydroxybenzotriazole monohydrate (HOBt•H_2O) was purchased from Advanced ChemTech (Louisville, KY). *N*-(*tert*-Butoxycarbonyl)-*L*-serine (Boc-Ser-OH) (99%), Fmoc-*O*-*tert*-butyl-*L*-serine **(**Fmoc-Ser-OH) (99.5%) and *S*-trityl-*L*-cysteinamide hydrochloride (NH_2-Cys(Trt)-H) (97%) were purchased from Aapptec (Louisville, KY).

PEO2k-amine and PEO5k-amine were lyophilized from benzene before use. *D, L*-lactide was recrystallized from THF and then sublimed under vacuum. The purified lactide was stored in a N_2-filled dry box. Tin octoate was dissolved in toluene (~9 mg/mL) and stored over 4 Å molecular sieves. DBU was distilled from CaH_2, dissolved in THF (20 mg/mL), and stored over 4 Å molecular sieves under N_2. TEA was passed through a short basic alumina column before use. NH_2-Cys(Trt)-H was recrystallized from $CHCl_3$/MeOH (1:1 v/v). Other reagents were used as received.

Instrumentation

Polymer average molecular weights (M_w and M_n) and molecular weight distributions ($Đ$) were estimated by gel permeation chromatography (GPC) with tetrahydrofuran (THF) as eluent at 40 ℃ at a flow rate of 1.0 mL/min on a set of two PLgel 5μm Mixed-D columns and a PL-ELS 1000 evaporative light scattering detector (Polymer Laboratories). Data were analyzed with Cirrus GPC software (Polymer Laboratories) based upon polystyrene standards (EasiCal PS-2, Polymer Laboratories). Block copolymer compositions were

estimated by NMR spectroscopy (Varian 300Hz, $CDCl_3$). Dynamic light scattering (DLS) experiments were carried out with a BIC 90 plus Particle Size Analyzer (Brookhaven Instruments Corp.) at a wavelength of 659.0 nm and a constant angle of 90 º. Small angle X-ray scattering (SAXS) experiments were performed on Beamline X9 in the National Synchrotron Light Source (NSLS).

3.2.1 Synthesis of macroinitiator mPEO-(Boc)-OH

Macroinitiator mPEO-(Boc)-OH was synthesized by the coupling of amine-terminated PEO and Boc-protected serine[45]. PEO2k-amine (1.01 g, 0.465 mmol), Boc-Ser-OH (145 mg, 0.706 mmol), HOBt•H_2O (74 mg, 0.484 mmol) and EDC•HCl (93 mg, 0.485 mmol) were dissolved in CH_2Cl_2 (40 mL) and the resulting solution was cooled to 4 ℃ in an ice bath. Triethylamine (92 mg, 0.909 mmol) was dissolved in 5 ml CH_2Cl_2 and added to the above solution by syringe. The resulting solution was stirred at 4 ℃ for 2 h and then allowed to warm up to 25 ℃ slowly. After 20 h, the reaction mixture was washed with aqueous sodium bicarbonate (5%, 5 mL) once and then brine (5 mL) once. The organic fraction was dried over $MgSO_4$, filtered and concentrated by rotary evaporation and vacuum to afford a white solid (965 mg, 88%) after lyophilization from benzene, as confirmed by ^{1}H NMR.

^{1}H NMR (300 MHz, $CDCl_3$): δ 4.0-3.4 (br, t, 4H per $–OCH_2CH_2$- repeat unit), 3.4 (s, 3H, CH_3O-), 1.4 ppm (s, 9H, Boc protecting group).

3.2.2 Synthesis of diblock copolymer PEO-S(Boc)-PLA

Lactide polymerization with Sn(Oct)$_2$.[23, 25] In a typical procedure for synthesis of PEO-S(Boc)-PLA, PEO5k-S(Boc)-OH (128.1 mg, 0.024 mmol) and *D,L*-lactide (156.5 mg, 1.08 mmol, 45 equiv) were dissolved in dry toluene (5 mL) in a Schlenk tube inside a N_2-filled dry box. Sn(Oct)$_2$ solution in toluene (1.8 mL, 23.4 mM in toluene, 1.5 equivalent relative to macroinitiator-OH chain ends) was added to the solution by syringe. The sealed Schlenk tube was taken out of the dry box and the solution was stirred at 110 ℃. The polymerization was allowed to run for 2 h, after which the reaction mixture was removed from heat and HCl in MeOH (0.25 mL, 0.1 M in MeOH, 10 mol equiv of HCl per macroinitiator-OH chain ends) was added. The reaction mixture was evaporated to dryness, redissolved in THF and precipitated twice into hexanes/EtOAc (19:1 v/v) to afford a white solid (196 mg, ~70%), as confirmed by ^{1}H NMR (Figure A2) and GPC (M_n 5.7 kDa, DPI 1.15).

^{1}H NMR (300 MHz, $CDCl_3$): δ 5.2-5.0 (br, q, 1H per lactide repeat unit), 4.0-3.4 (br, t, 4H per –OCH_2CH_2- repeat unit), 3.4(s, 3H, CH_3O-), 1.8-1.6 (br, d, 3H per lactide repeat unit), 1.4 ppm (s, 9H, Boc protecting group).

Lactide polymerization with DBU [27, 28] In a typical procedure for synthesis of PEO2k-S(Boc)-PLA, PEO2k-S(Boc)-OH macroinitiator (127.9 mg, 0.054 mmol) and *D,L*-lactide (116.6 mg, 0.81 mmol) were dissolved in 5 mL THF in a Schlenk tube inside a N_2-filled dry box. DBU solution in THF (0.06 mL, 0.13 M in THF, 1 mol% relative to monomer) was added to the polymerization solution by syringe. The sealed Schlenk tube

was taken out of the dry box, and the solution was stirred at 25 ℃ for 2 h, at which point, benzoic acid (66.0 mg, 0.54 mmol) was added. The polymerization solution was concentrated and precipitated into diethyl ether. The white precipitate was redissolved in a minimal amount of THF and precipitated twice into hexanes/EtOAc (19:1 v/v) to afford a white solid (172 mg, ~70%), as confirmed ^{1}H NMR and GPC (M_n 4.5 kDa, DPI 1.06).

^{1}H NMR (300 MHz, $CDCl_3$): δ 5.2-5.0 (br, q, 1H per lactide repeat unit), 4.0-3.4 (br, t, 4H per –OCH_2CH_2- repeat unit), 3.4 (s, 3H, CH_3O-), 1.8-1.6 (br, d, 3H per lactide repeat unit), 1.4 ppm (s, 9H, Boc protecting group).

3.2.3 Synthesis of triblock copolymer PEO-S(CK_n)-PLA

Synthesis of PEO-S(NH_2)-PLA. In a typical procedure, PEO2k-S(Boc)-PLA2k (200 mg, 0.045 mmol) was dissolved in CH_2Cl_2 (2 mL). TFA (2 mL) was added, and the solution was stirred for 50 min. The solvents were removed by rotary evaporation. The residue was redissolved in THF and precipitated into isopropyl alcohol/Et_3N (19:1 v/v). The suspension was centrifuged at 6000 rpm for 15 min and the supernatant was discarded. The precipitation and centrifugation processes were repeated twice, which afforded a white solid (150 mg, 75%), as confirmed by ^{1}H NMR.

^{1}H NMR (300 MHz, $CDCl_3$): δ 5.2-5.0 (br, q, 1H per lactide repeat unit), 4.0-3.4 (br, t, 4H per –OCH_2CH_2- repeat unit), 3.4(s, 3H, CH_3O-), 1.8-1.6 ppm (br, d, 3H per lactide repeat unit).

Synthesis of PEO-S(PDP)-PLA. In a typical procedure, PEO2k-S(NH_2)-PLA2k (120 mg, 0.028 mmol) was dissolved in $CHCl_3$ (4 mL). SPDP (21.9 mg, 0.070 mmol) was added and the solution was stirred at 30 ℃ for 1.5 h under air. A second portion of SPDP (21.9 mg, 0.070 mmol) was added and the solution was stirred for another 1.5 h. The solvent was removed by rotary evaporation. The crude product mixture was separated by silica gel chromatography using $CHCl_3$/MeOH (40:1 followed by 10:1) as eluents. The product PEO-S(PDP)-PLA was eluted out in the 10:1 mixture (R_f 0.7, yield: 60%~90%). The degree of conjugation of PDP was quantified by measuring UV absorption (at 372 nm) of 2-mercaptopyridine cleaved from purified copolymers [51]. Briefly, a known amount of polymer (~2 mg) was dissolved in DMF (2 mL). DTT solution (20 mg/mL in DMF, 20 μL) was added, and the UV absorption of the solution was recorded every 2 minutes until it became constant (within 10 minutes). The conversions, back-calculated from the amount of 2-mercaptopyridine present in the sample solutions after cleavage for UV measurements, were usually around 90% for PEO2k and 60% for PEO5k.

^{1}H NMR (300 MHz, $CDCl_3$): δ 8.6 (d, 1H, m-C_5NH_4-), 7.6-7.4(d, 1H, o- C_5NH_4- ; dd, 1H, p-C_5NH_4-), 7.0(d, 1H, m- C_5NH_4-), 5.2-5.0 (br, q, 1H per lactide repeat unit), 4.0-3.4 (br, t, 4H per –OCH_2CH_2- repeat unit), 3.4(s, 3H, CH_3O-), 3.2 (t, 2H, -S-CH_2), 2.8(t, 2H, CH_2-CO-), 1.8-1.6 ppm (br, d, 3H per lactide repeat unit).

Synthesis of PEO-S(CK_n)-PLA. In a typical procedure, PEO2k-S(PDP)-PLA2k (100 mg, 0.022 mmol) was dissolved in DMF (5 mL). (For longer CK_n chains (n>30), mixtures of DMF/H_2O (2:1) were used as cosolvents due to low solubility in DMF). CK_n oligomer (116 mg, 0.022 mmol) was added, and the solution immediately turned yellow. The solution was stirred for 20 min before it was dialyzed (MWCO=3500 Da) against Nanopure

water. The extent of conjugated of CK_n was quantified by measuring UV absorption (at 372 nm) of 2-mercaptopyridine present in crude product mixtures. A known amount of crude product mixture (~3 mg) was dissolved in DMF (2 mL), and the UV absorption of the solution was recorded. The conversions, back-calculated from the amount of 2-mercaptopyridine present in the sample solutions for UV measurements, were usually greater than 90% for PEO2k and 60% for PEO5k.

^{1}H NMR (300 MHz, $CDCl_3$):): δ 5.2-5.0 (br, q, 1H per lactide repeat unit), 4.8-4.6 (br, s,1H, NH-CO-),CH4.0-3.4 (br, t, 4H per $–OCH_2CH_2$- repeat unit), 3.4 (s, 3H, CH_3O-), 3.4-3.2 (t, 2H, CH_2-NH), 1.8-1.4 ppm (br, d, 3H per lactide repeat unit; 6H per Lys side chain)

3.2.4 Synthesis of key compounds

Preparation of 2-carboxyethyl 2-pyridyl disulfide (PDP)[51, 52]

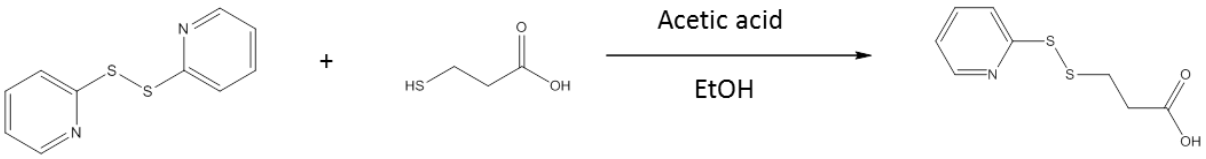

Figure 3- 5 Synthesis of 3-(2-pyridyldithio)propanoic acid (PDP)

2,2-Dipyridyldisulfide (DPDS) (2.5 g, 11.3 mmol) was dissolved in ethanol (20 mL) and 3-mercaptopropanoic acid (0.6 g, 5.65 mmol) in acetic acid (0.7 mL) was slowly added over a period of 10-15 minutes. The resulting yellow solution was left to stir at room

temperature for 2 h. The reaction mixture was evaporated and dried under vacuum to afford a pale yellow oil. The crude oil was then dissolved in dichloromethane/ethanol (3:2 v/v) and eluted through an Al_2O_3 column (2cm x 24cm). The column was washed with dichloromethane/ethanol (3:2 v/v) until all of the yellow color (2,2-dipyridyldisulfide and 2-mercaptopyridine) had been removed. The PDP product was then eluted with CH_2Cl_2/EtOH/HOAc (60:40:4) and dried under vacuum, to afford a white solid (808.6 mg, 65% yield).

^{1}H NMR (300MHz; DMSO-d_6): δ 8.4(dt, 1H), 7.8(dt, 2H), 7.2(m, 1H), 2.9 (t, 2H, J=7Hz), 2.2 (t, 2H, J=7Hz)

Preparation of N-succinimidyl 3-(2-pyridyldithio)propionate (SPDP) [51, 52]

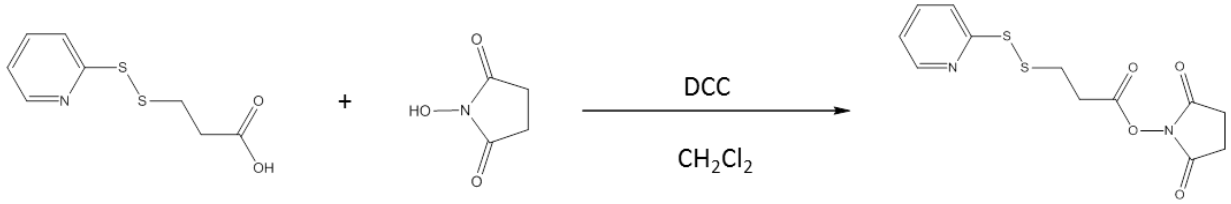

Figure 3- 6 Synthesis of *N*-succinimidyl 3-(2-pyridyldithio)propionate by DCC coupling

PDP (808.6 mg, 3.73 mmol) and NHS (519.0 mg, 4.51 mmol) were dissolved in dichloromethane (10 mL) and the resulting mixture was stirred in an ice bath for 5 to 10 minutes. Then DCC (838.1 mg, 4.06 mmol) in dichloromethane (4 mL) was added dropwise to the reaction solution and the reaction solution was left to stir in the ice bath for 3.5 h. After the reaction $MgSO_4$ was added and the resulting mixture was stirred at room temperature for a few minutes, cooled in an ice bath for a few minutes, then filtered to remove the urea. The filtrate was concentrated and dried in a vacuum oven to afford a

yellowish oil, which was then dissolved in ethanol (5-10 mL) (with some heating if needed, about 40°C) and left in the freezer(~ -20°C) for about a day until a solid white precipitate (fluffy white balls) formed on the bottom of the vial. The solid was dried and then dissolved with dichloromethane (~1 mL) and poured into isopropanol (~19 mL) and left in the freezer for about a day until rod like crystals formed. This process was repeated twice, and afforded the final product (236 mg, 20% yield).

^{1}H NMR (300MHz, $CDCl_3$): δ 8.5(dt, 1H), 7.6 (dt, 2H), 7.1(m, 1H), 3.1(m, 4H), 2.8 (s, 4H).

Preparation of CK_n oligomer by peptide synthesis

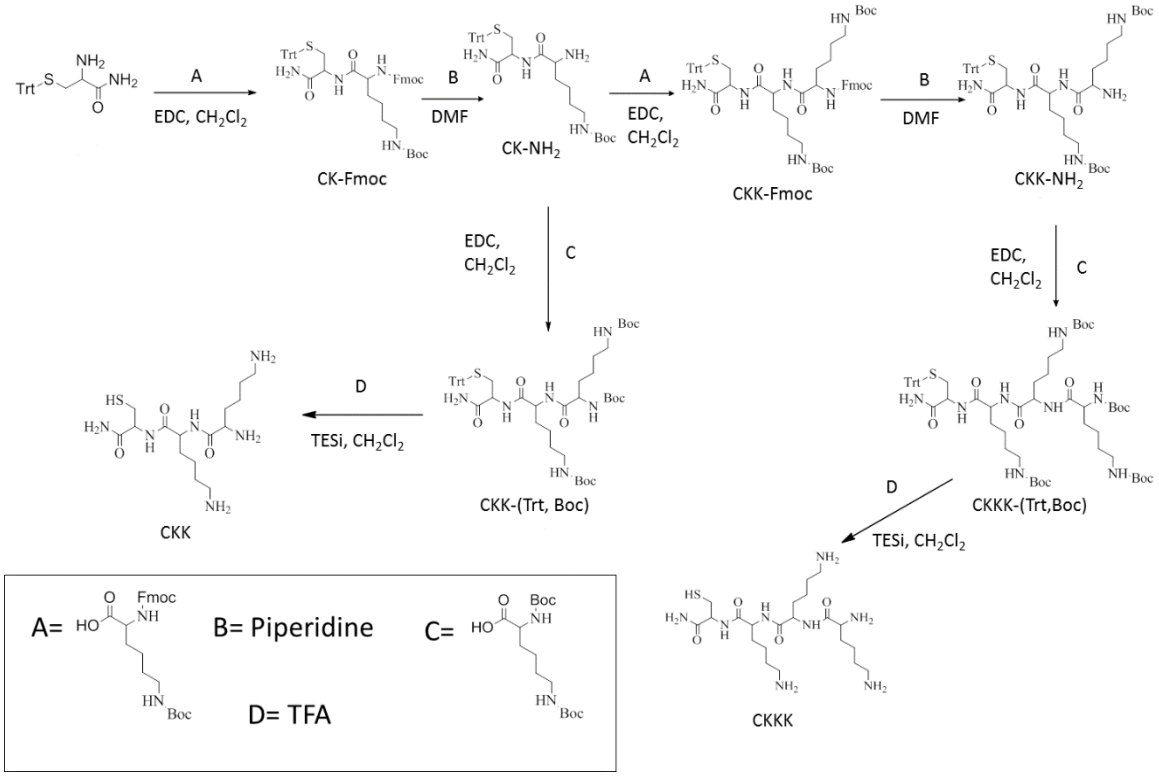

Figure 3- 7 Synthetic route for CKn oligomers (CK, CKK and CKKK) by peptide synthesis.

CK_n oligomers with with one to six lysine repeat units could be synthesized by sequential peptide synthesis. Figure 3.7 illustrates the synthetic routes to CK, CKK and CKKK utilizing the different protecting groups and their deprotection conditions.

For a typical synthesis procedure for CK-Fmoc, H-Cys(Trt)-NH_2 (3.89 g, 10.7 mmol), Fmoc-Lys(Boc)-OH (5.53 g, 11.8 mmol), HOBt•H_2O (1.73 g, 11.3 mmol) and EDC (2.16 g, 11.3 mmol) were dissolved in CH_2Cl_2 (180 mL). The solution was stirred in an ice bath for 15-20 mins. Triethylamine (1.09 g, 10.7 mmol) was then added to chilled solution by syringe. The resulting solution was stirred at 4 ℃ for 2h and then allowed to warm up to 25 ℃ slowly. After 20 h, the dark orange mixture was washed with brine (~150 mL) and deionized water (~150 mL). The organic fraction was dried with $MgSO_4$ and filtered, concentrated by rotary evaporation to afford, an orange solid. That was purified by flash chromatography (SiO_2, 25:1 $CHCl_3$/MeOH). The product was concentrated and dried under vacuum to afford a light orange solid (7.69 g, 86%). Product formation was tracked via TLC aided by UV and ninhydrin stain.

For a typical procedure to remove Fmoc protecting groups, CK-Fmoc (4.12g, 5.07mmol) and piperidine (10 mL) were dissolved in DMF (30 mL) and stirred for 3 hours at room temperature in air. The reaction mixture was evaporated to dryness, redissolved with 1 ml CH_2Cl_2 and precipitated into 50 ml hexane twice , dried and purified by flash chromatography (SiO_2, 20:1 $CHCl_3$/MeOH) until all byproduct had been eluted off (3 spots with R_f greater than 0.40, and was not stainable with ninhydrin with 10:1 $CHCl_3$/MeOH). Then, the deprotected product CK-NH_2 was washed out by $CHCl_3$/MeOH/Et_3N (20:1:0.5) (TLC: R_f = 0.18 in 10:1 $CHCl_3$/MeOH, light brown with ninhydrin staining). The solution

was concentrated by rotary evaporation and dried under vacuum to afford a white solid CK-NH_2 (2.47g, yield 82%).

For a typical procedure to synthesize CKK-(Trt, Boc), CK-NH_2 (1.445 g, 1.933 mmol), Boc-Lys(Boc)-OH (0.7735 g, 2.126 mmol), HOBt•H_2O (0.3109 g, 2.0297 mmol) and EDC (0.3892 g, 2.0297 mmol) were dissolved in CH_2Cl_2 (60 mL). The solution was stirred in an ice bath for 15-20 mins. Triethylamine (0.1956 g, 1.933 mmol) was then added to the chilled solution by syringe. The resulting solution was stirred at 4 ℃ for 2 h and then allowed to warm up to 25 ℃ slowly. After 20 h, the reaction mixture was washed with brine (~50 mL) and deionized water (~50 mL). The organic layer of dichloromethane was dried with $MgSO_4$ and filtered, concentrated by rotary evaporation and dried under vacuum to afford a slight yellow/white solid CKK-(Trt, Boc) (1.24 g, 59%). Product formation was tracked via TLC aided by UV and ninhydrin stain.

For a typical procedure to remove Trt and Boc protecting groups, CKK-(Trt, Boc) (253.2 mg, 0.2712 mmol) was dissolved in CH_2Cl_2 (20 mL) and TFA (20 mL). After the addition of triethylsilane (TESi) (159.3 mg, 1.356 mmol) in CH_2Cl_2 (5 mL), the bright yellow mixture solution became clear and colorless and was further stirred for 1 h at room temperature in air, then concentrated by rotary evaporation and dried under vacuum. The crude product was redissolved in 1 mL methanol and precipitated into 18 mL chloroform twice to afford a clear solid CKK (98.6 mg, 96%).

^{1}H NMR (300MHz, CD_3OD): 4.48(q, 1H), 4.39(q, 1H), 3.95 (t, 1H), 2.80(m, 6H, 2H per amino acid side chain), 1.97-1.35 (m, 12H, 6H per Lys side chain)

CK_n oligomers with three to six repeat units could be synthesized by similar procedures, with additional lysine chain propagation steps achieved by repeating the addition of Fmoc-Lys(Boc)-OH and deprotection of the Fmoc group. Addition of the terminal lysine unit was followed by deprotection of all the Trt and Boc groups. However, with the increase of the repeat unit number, the reaction system became very complicated and purification became difficult.

Preparation of CK_n oligomer by ring opening polymerization

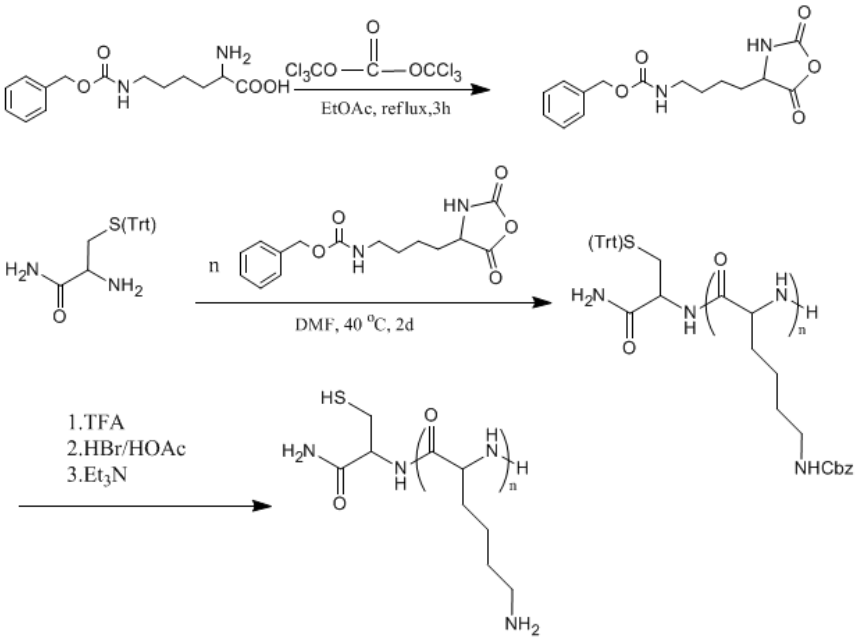

Figure 3- 8 Synthetic route for CK_n oligomers (n > 10) by ring opening polymerization.

Preparation of Cysteine-capped poly(Z)lysine (Cys(Trt)-poly(Z)lysine) NH_2-Cys(Trt)-H (10 mg, 0.028 mmol) was dissolved in dry DMF (10 mL) in a N_2-filled dry box. Z-Lysine-N-carboxyanhydride (345 mg, 1.13 mmol) was added to the solution. The

solution was taken out of the dry box and stirred under active N_2 flow at 40 ℃ for 2-4 days. The DMF solution was concentrated and precipitated twice into diethyl ether to afford Cys(Trt)-poly(Z)lysine as a white solid (280 mg, ~90%), as confirmed by ^{1}H NMR.

^{1}H NMR (300 MHz, DMSO-d^6): δ 7.4-7.0 (br, m, ArH), 5.0 (s, 2H, -CH_2-Ar), 4.2 (s, 1H, NH-CH_2-Ar), 3.8 (s, 1H, NH-CO-), 3.0 (t, 2H, CH_2-NH), 1.9-1.2 ppm (br, m, 6H per Lys side chain).

Preparation of Cys-Lys$_n$ (CK$_n$) Cys(Trt)-poly(Z)lysine (200 mg, 0.018 mmol) was dissolved in TFA (3 mL) and stirred for 20 min. The solution was chilled to 4 ℃ and HBr/HOAc (5 mL) was added under N_2 flow, which made the reaction vial fume immediately. The solution was allowed to warm up to room temperature slowly and stirred for another 45 min. The solution was added to isopropyl alcohol and the resulting suspension was centrifuged at 5500 rpm for 15 min. The supernatant was discarded and the solid was washed with isopropyl alcohol (20 mL×3) and dried under dynamic vacuum to afforded polymer (78 mg, yield ~ 80%), as confirmed by ^{1}H NMR.

^{1}H NMR (300 MHz, DMSO-d^6): (4.2 (s, 1H, NH-CH_2-Ar), 3.8 (s, 1H, NH-CO-), 3.0 (t, 2H, CH_2-NH), 1.9-1.2 ppm (br, m, 6H per Lys side chain).

3.3 Results and Discussion

3.3.1 Synthesis of macroinitiator mPEO-S(Boc)-OH

Boc-protected serine was adopted for the synthesis of macroinitiator mPEO-S(Boc)-OH. After lactide polymerization, the Boc group could be removed by reaction with TFA/CH_2Cl_2 (1:1) in a quick and efficient way.

The macroinitiator PEO-S(Boc)-OH was synthesized by the coupling of Boc–protected serine to amine-terminated PEO (PEO-NH_2) [45]. Based on a comparison of the ^{1}H NMR spectra for PEO-NH_2 and PEO-S(Boc)-OH (Figure 3-9), the disappearance of the triplet peak (δ = 3.2 ppm) corresponding to the protons of the methylene group adjacent to the terminal amine group of PEO-NH_2 confirmed complete conversion to PEO-S(Boc)-OH. The singlet peak (δ = 1.4 ppm) in the PEO-S(Boc)-OH spectrum corresponds to the methyl group in the Boc protecting group, which also be considered as evidence of successful coupling of Boc–protected serine to amine-terminated PEO (PEO-NH_2).

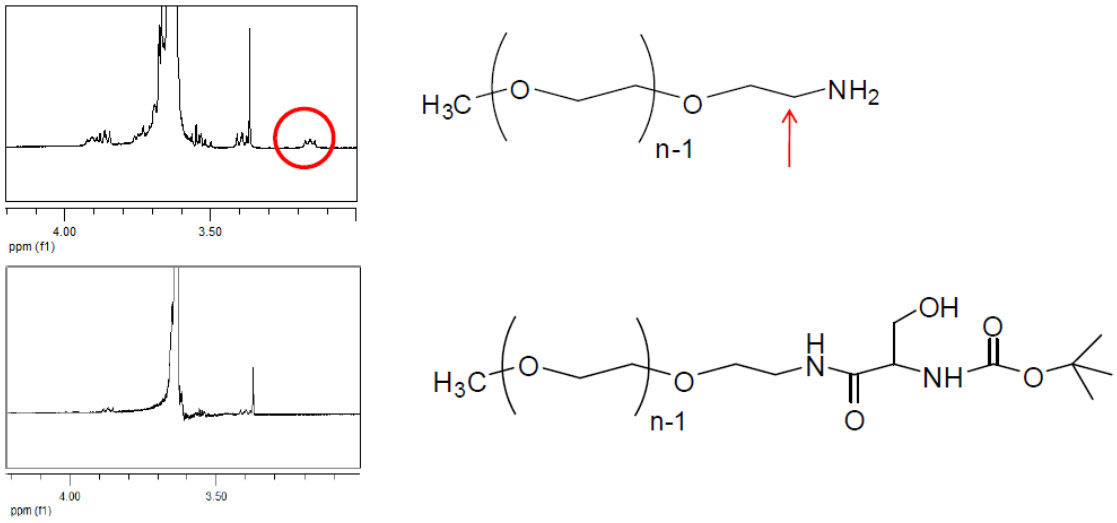

Figure 3- 9 Comparison between 1H NMR spectra of mPEO-amine (top) and mPEO-S(Boc)-OH (bottom) from δ 3.0-4.0 ppm.

3.3.2 Synthesis of diblock copolymer PEO-S(Boc)-PLA

The serine hydroxyl group of PEO-S(Boc)-OH was used to initiate the ring opening polymerization (ROP) of lactide with an appropriate activating agent such as tin 2-ethylhexanoate [25]or DBU [27, 28] to afford the diblock copolymer PEO-S(Boc)-PLA. Tin 2-ethylhexanoate required a relatively high reaction temperature (110 ℃) while DBU could catalyze the polymerization at room temperature. However, an extra precipitation in diethyl ether was needed in DBU polymerizations to remove the benzoic acid used to terminate the polymerization. Regardless of the polymerization method used, the molecular weight of the PLA block could be controlled by the ratio of lactide to macroinitiator PEO-S(Boc)-OH. Peaks in the PEO-S(Boc)-PLA ^{1}H NMR spectrum at δ 1.6-1.8 ppm (-C<u>H</u>$_3$) and δ 5.2-5.0 ppm (-C<u>H</u>-) result from polymerized *D,L*-lactide

Table 3- 1mPEO-S(Boc)-PLA prepared by tin octoate catalyzed polymerization.[a]

Sample	Lactide/MI	$M_{n,\ theory}$ [b] (kg/mol)	$M_{n,NMR}$ [c] (kg/mol)	$M_{n,GPC}$ [d] (kg/mol)	M_w/M_n [d]
PEO5k-PLA1	45	11.2	10.6	5.7	1.15
PEO5k-PLA2	70	13.8	13.6	7.2	1.14
PEO5k-PLA3	90	16.6	16.1	8.5	1.16
PEO5k-PLA4	105	19.0	19.3	10.0	1.16

[a] PEO5k-S(Boc)-OH macroinitiator (MI), [MI] = 4.8 mM, $[Sn(Oct)_2]/[MI]=1.5$. Polymerizations were carried out in toluene at 110 ℃ for 2 h.

[b] $M_{n,\ theory}$ was estimated by ^{1}H NMR of crude polymer sample. The conversion was calculated based on the integration ratio of H peak corresponded to methyl group in monomer and polymer and the $M_{n,\ theory}$ was calculated based on the conversion and monomer feed ratio.

[c] $M_{n,NMR}$ was estimated by ^{1}H NMR of purified polymer sample. The $M_{n,NMR}$ was calculated based on the integration ratio of H peak corresponded to methylene group in PEO and H peak corresponded to methyl group in PLA.

[d] $M_{n,GPC}$ and M_w/M_n were obtained from GPC vs polystyrene standards.

Table 3- 2 PEO-S(Boc)-PLA prepared by DBU catalyzed solution polymerization. [a]

Sample	Lactide/MI	$M_{n,\ theory}$ [b] (kg/mol)	$M_{n,NMR}$ [b] (kg/mol)	$M_{n,GPC}$ [c] (kg/mol)	M_w/M_n [c]
PEO2k-PLA1	5	3.1	3.1	3.2	1.06
PEO2k-PLA2	10	3.8	3.7	3.9	1.08
PEO2k-PLA3	15	4.4	4.5	4.5	1.06
PEO5k-PLA5	45	11.3	11.1	5.6	1.18
PEO5k-PLA6	75	15.1	14.6	7.8	1.17
PEO5k-PLA7	100	19.3	18.5	9.5	1.20

[a] PEO2k-S(Boc)-OH or PEO5k-S(Boc)-OH macroinitiator (MI), DBU loading 1 mol%-relative to lactide with PEO2k MI or 5 mol%-relative to lactide with PEO5k MI. [MI] = 10.8 mM with PEO2k MI; [MI] = 4.8 mM with PEO5k MI. Polymerizations were carried out in THF at room temperature for 2 h.

[b] $M_{n,\ theory}$ was estimated by ^{1}H NMR of crude polymer sample. The conversion was calculated based on the integration ratio of H peak corresponded to methyl group in monomer and polymer and the $M_{n,\ theory}$ was calculated based on the conversion and monomer feed ratio.

[c] $M_{n,NMR}$ was estimated by ^{1}H NMR of purified polymer sample. The $M_{n,NMR}$ was calculated based on the integration ratio of H peak corresponded to methylene group in PEO and H peak corresponded to methyl group in PLA.

[d] $M_{n,GPC}$ and M_w/M_n were obtained from GPC vs polystyrene standards

When the higher molecular weight macroinitiator PEO5k-S(Boc)-OH was used to initiate the ring-opening polymerization of *D,L*-lactide with either $Sn(Oct)_2$ or DBU, high conversions were obtained with monomer feed ratios from 45 to 105 relative to macroinitiator (Tables 3.1 and 3.2). The GPC chromatograms for macroinitiator PEO5k-S(Boc)-OH and diblock copolymer PEO5k-S(Boc)-PLA showed narrow molecular weight distributions and clear shifts when THF was used as GPC eluent (Figure 3.10). When the low molecular weight macroinitiator PEO2k-S(Boc)-OH was used to initiate the ring-opening polymerization of *D,L*-lactide with DBU (Table 3.2), high conversions and narrow molecular weight distributions were obtained with monomer feed ratios from 5 to 15 relative to macroinitiator.

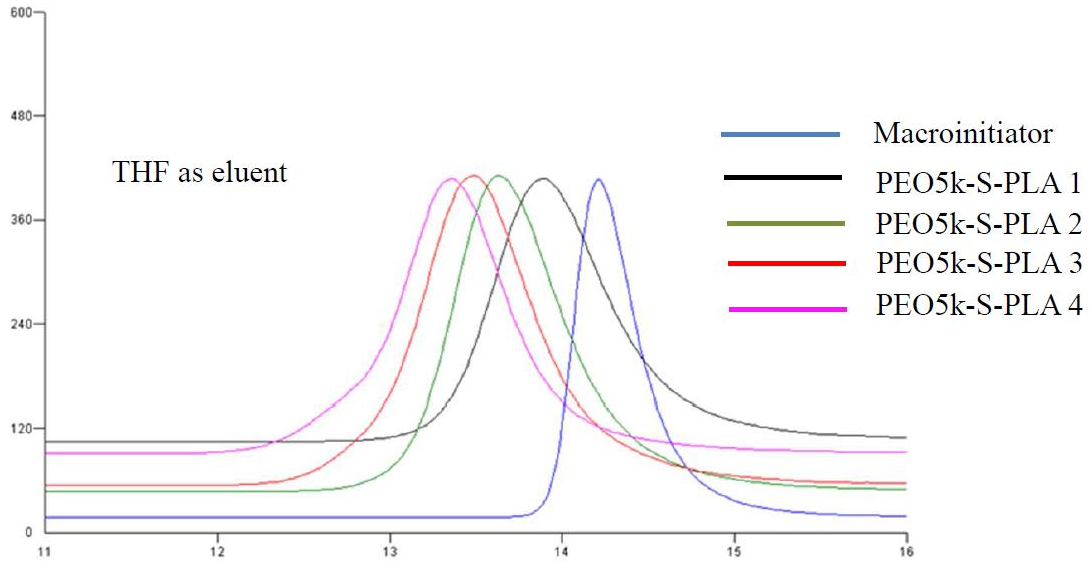

Figure 3- 10 GPC chromatogram of macroinitiator PEO5k-S(Boc)-OH and PEO5k-S-PLA with THF as eluent.

3.3.3 Size Characterization of diblock copolymer PEO-S(Boc)-PLA

The morphologies of PEO-S(Boc)-PLA amphiphilic diblock copolymers PEO5k-S-PLA 5 (M_n 11.1k, DPI 1.18, f(EO)=0.45), PEO5k-S-PLA 6 (M_n 14.6k, DPI 1.17, f(EO)=0.34), PEO5k-S-PLA 7 (M_n 18.5k, DPI 1.20, f(EO)=0.27) in dilute aqueous solution with different concentrations were studied by SAXS (Figure 3-11, Table 3-3) and DLS (Table 3-3).

As we discussed in Chapter 2.2, the Guinier approximation is a model-independent approximation to estimate the radius of gyration R_g in low-q regime [53, 54]. Typical SAXS data (Figure 3-11a) and a Guinier presentation for the SAXS data (Figure 3-11b, fitted by the solid lines) of PEO5k-S-PLA 5(M_n 11.1k, DPI 1.18, f(EO)=0.45) in aqueous solution (concentration 1 mg/mL) are shown. The slope of the Guinier plot of SAXS data was used to estimate the radius of gyration (R_g) of the copolymer micelles. The calculated R_g values for micelles formed by PEO5k-S-PLA5, PEO5k-S-PLA6 and PEO5k-S-PLA7 were 99.3 ± 0.7 Å, 129.9 ± 2.3 Å and 94.3 ± 0.8 Å respectively at a concentration of 1 mg/mL in water. With the increase of solution concentration from 1 mg/mL to 10 mg/mL, the micelle R_g values for each diblock polymer were almost unchanged.

In the DLS measurements, the hydrodynamic radius (R_H) of the micelles formed by the three diblock copolymer samples PEO5k-S-PLA5, PEO5k-S-PLA6 and PEO5k-S-PLA7 were 277.2 ±5.3 Å, 327.5 ±17.0 Å and 235.2 ±5.4 Å respectively at a concentration of 1 mg/mL in water.

For spherical micelles, the theoretical ratio of radius of gyration R_g to hydrodynamic radius R_h is around 0.78[53, 54]. In our system, the ratio of R_g to R_h varied from 0.36 to

0.40, which is lower than expected. A possible reason for this is the limitations of Guinier approximation. The Guinier approximation is valid only in the low-*q* regime ($R_gQ \leq 1$) and the assumption that $\mathrm{Ln}I(Q) \sim -R_g^2Q^2/3$ is only good for spherical structures. When we processed the SAXS data, the proper selection of Q range for analysis was important to obtain the radius of gyration R_g. Also we assumed that all the micelles to be spherical structures in order to use the $\mathrm{Ln}I(Q) \sim -R_g^2Q^2/3$ relationship. If the formed micelles were not well-defined spherical structures, the calculated radius of gyration R_g may not reflect the real radius of gyration R_g of the micelles.

The radii determined through both SAXS and DLS measurements in aqueous solution (0.1-1 wt% polymer) suggested that the size of assemblies for copolymers PEO-S(Boc)-PLA 5 and PEO-S(Boc)-PLA 6 increased with increasing molecular weight of the PLA block. However, the observed assembly size decreased for diblock copolymer PEO-S(Boc)-PLA 7, which has the highest molecular weight PLA block. These observations indicated the possible morphology change from spherical micelles to other morphologies.

Table 3- 3 SAXS and DLS results for radius of gyration Rg and hydrodynamic radius Rh

Sample	M_n	f(EO)	Concentration (mg/ml)	SAXS R_g (Å)	DLS R_H (Å)
PEO5k-PLA5 (EO_{122}-LA_{84})	11.1k	0.45	1	99.3 ±0.7	277.2 ±5.3
			5	100.8 ±0.8	
			10	101.0 ±0.7	
PEO5k-PLA6 (EO_{122}-LA_{134})	14.6k	0.34	1	129.9 ±2.3	327.5 ±17.0
			5	129.9 ±2.3	
			10	128.4 ±2.2	
PEO5k-PLA7 (EO_{122}-LA_{192})	18.5k	0.27	1	94.3 ±0.8	235.2 ±5.4
			5	94.6 ±0.8	

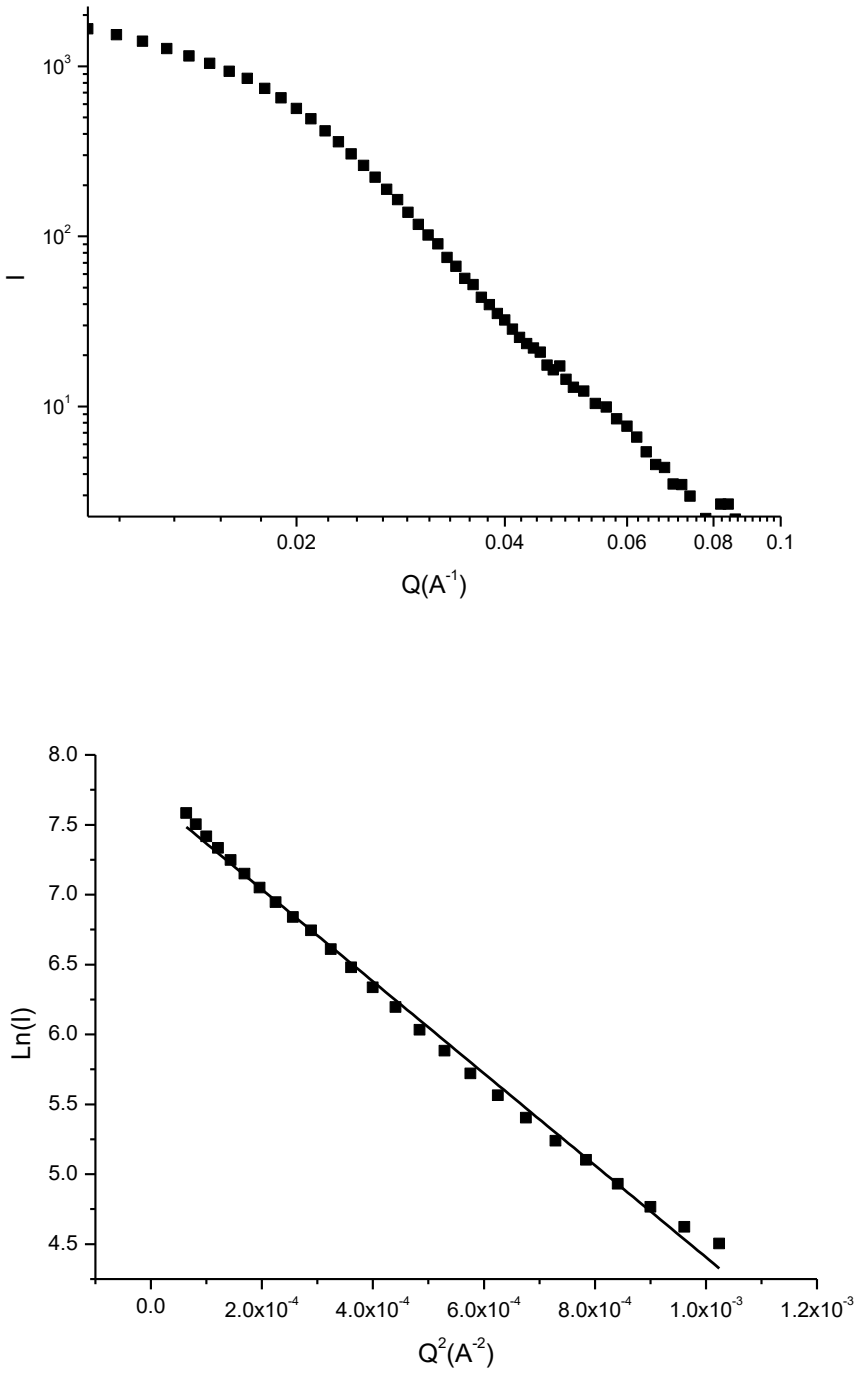

Figure 3- 11 a) The SAXS data and b) Guinier presentation for the SAXS data (fitted by the solid lines) of PEO5k-S-PLA 5 in aqueous solution at 1 mg/mL.

3.3.4 Synthesis of triblock copolymer PEO-S(CK_n)-PLA

A critical step in the synthesis of the star copolymer is the selective deprotection of the amine group at the block junction of PEO-S(Boc)-PLA without degradation of the PLA block. Initially, as described above, a Cbz-protected serine was used at the block junction. After lactide polymerization, attempted cleavage of the Cbz group with HBr/ HOAc led to an undesirable amount of hydrolysis of the PLA block as evidenced by NMR. The Boc-protected serine residue was chosen for further experiments as it has been reported to be selectively removable by treatment with TFA/CH_2Cl_2(1:1) at room temperature [55]. After exposing PEO-S(Boc)-PLA samples to 1:1 TFA/CH_2Cl_2, selective removal of the Boc group without degradation of the PLA block was observed. ^{1}H NMR spectra of the deprotected polymers show disappearance of the peak corresponding to the Boc methyl groups with little change in the integration ratio between PLA peaks and PEO peaks.

The free amine group was then treated with *N*-succinimidyl 3-(2-pyridyldithio)propionate (SPDP)[51] to afford the active disulfide intermediate PEO-S(NH-PDP)-PLA. In the ^{1}H NMR spectrum of PEO-S(NH-PDP)-PLA, the peaks at δ 8.6, 7.6, and 7.0 ppm were attributed to the aromatic pyridyl protons and the peaks at δ 2.8 and 3.2 ppm were attributed to the protons in the two methylene groups in the PDP segment. The extent of conversion of the central amine group to 2-pyridyl disulfide units in PEO-S(NH-PDP)-PLA was estimated by UV spectroscopy after the addition of excess dithiothreitol [51]. The degree of conjugation of PDP was quantified by measuring the UV absorption of 2-pyridinethiol (at 376.25 nm; 5.61×10^3 $M^{-1}cm^{-1}$ in THF, as measured from standard solutions – Figure A) cleaved from the purified PEO-S(NH-PDP)-PLA copolymers. The conversions, back-calculated from the amount of 2-mercaptopyridine

present in the sample solutions for UV measurements, were usually around 90% for PEO2k and 60% for PEO5k.

The target tri-arm star copolymer PEO-S(CK_n)-PLA was obtained by the direct reaction of PEO-S(NH-PDP)-PLA diblock copolymer with HS-CK_n in DMF. ^{1}H NMR spectra of the resulting PEO-S(CK_n)-PLA star copolymers showed the appearance of peaks from δ 4.6-4.8 ppm and δ 3.2-3.4 ppm that can be attributed to backbone methine protons and α-amino methylene protons in the polylysine block. The residual 2-pyridyl disulfide content in PEO-S(CK_n)-PLA was estimated by UV spectroscopy after adding excess dithiothreitol. The conversions were usually above 90% for PEO2k and 60% for PEO5k.

3.3.5 Synthesis of key compounds

Preparation of N-Succinimidyl 3-(2-pyridyldithio)propionate (SPDP)[51, 52]

N-Succinimidyl 3-(2-pyridyldithio)propionate (SPDP) is a heterobifunctional crosslinker which was used to allow disulfide bonding to the polymer [41, 56]. SPDP was synthesized by a literature procedure [51, 52] and confirmed by ^{1}H NMR spectroscopy (Figure 3-12). The three peaks in the range from 8.4 to 7.2 ppm with an integration ratio of 1:2:1 correspond to the four aromatic protons of SPDP. The multiplet at 3.12 ppm corresponds to the four protons of the methylene groups between the disulfide bond and the ester carbonyl group. The singlet at 2.8 ppm represents the four protons of methylene groups in the succinimidyl ring.

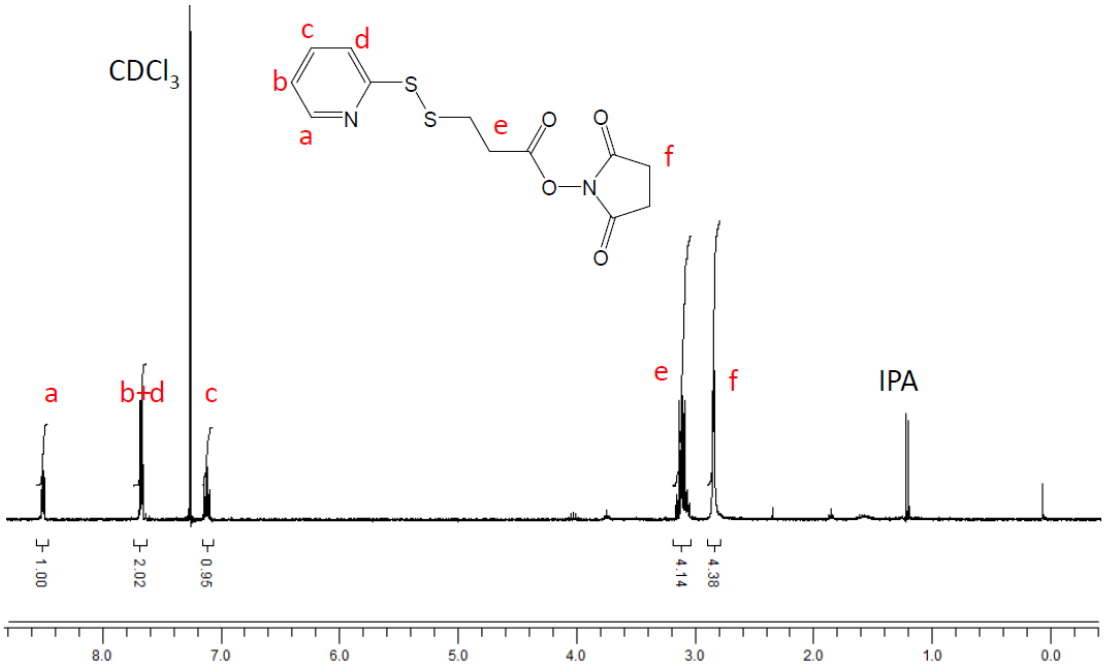

Figure 3- 12 ^{1}H NMR spectrum of SPDP in $CDCl_3$

Preparation of CK_n oligomer

CK_n oligomers with n = 1-6 were synthesized by peptide synthesis [57, 58]. CK_n oligomer synthesis started with the Trt protected cysteine and lysine chain growth was achieved by the repeated addition of Fmoc-Lys(Boc)-OH and deprotection of Fmoc group. The terminal lysine unit was added by addition of Boc-Lys(Boc)-OH, followed by deprotection of all the Trt and Boc groups by reaction with TFA and HBr/HOAc under N_2 flow. The successful synthesis of oligomers CK, CKK and CKKK was confirmed by ^{1}H NMR spectroscopy.

In the NMR spectra of CKK (Figure 3-13), there are three peaks in the range from 4.5 to 3.9 ppm with an integration ratio of 1:1:1 corresponding to backbone methine protons (a, Figure 3-13), overlapping multiplets at 2.8 ppm with an integration around 6

corresponding to methylene protons adjacent to the thiol and amine groups (b, Figure 3-13), and three multiplets from 2.0 to 1.4 ppm with an integration around 12 corresponding to the aliphatic protons of the lysine chain (c, Figure 3-13).

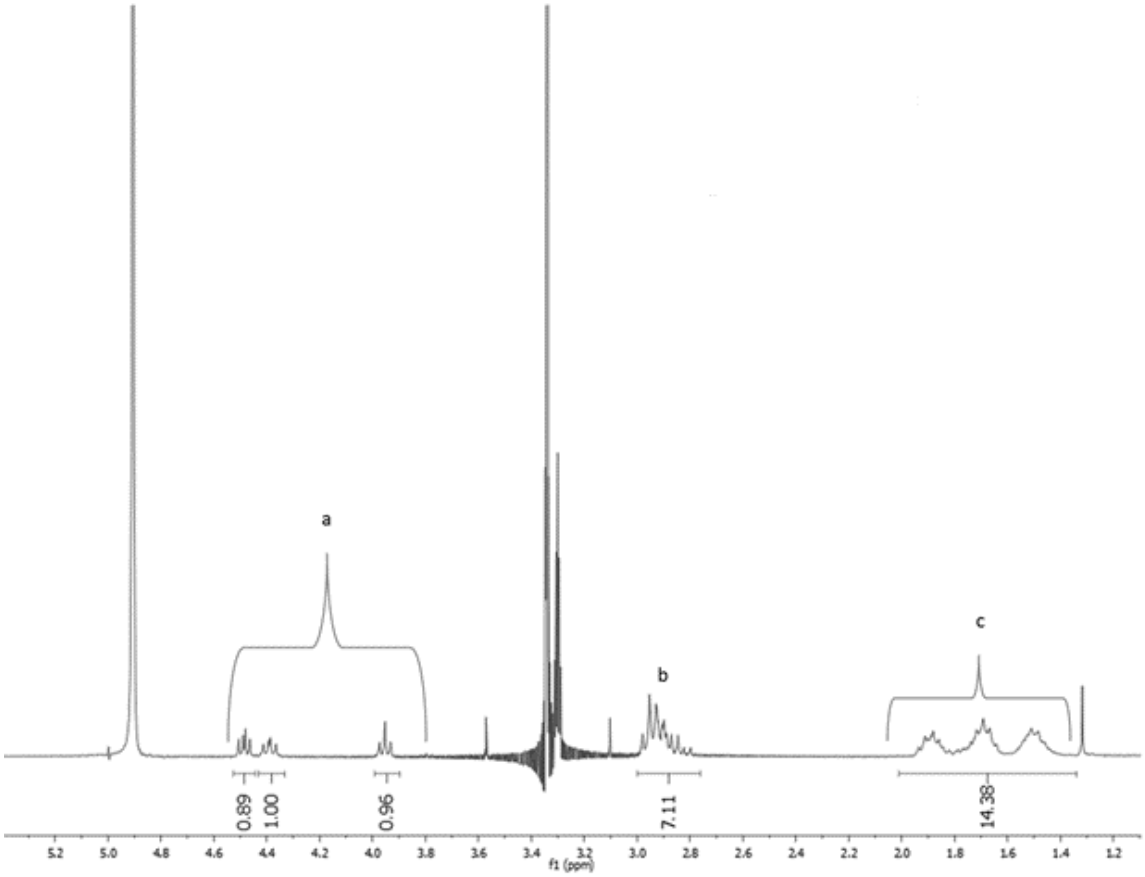

Figure 3- 13 ^{1}H NMR spectrum of CKK in $CDCl_3$

In the NMR spectra of CKKK (Figure 3-14), there were three peaks in the range from 4.5 ppm to 3.9 ppm with integration ratio of 1:2:1 corresponding to backbone methine protons (a, Figure 3-14), overlapping multiplets at 2.8 ppm with an integration around 8 corresponding to methylene protons adjacent to the thiol and amine groups (b, Figure 3-

14), and three multiplets from 2.0 ppm to 1.4 ppm with an integration around 18 corresponding to the aliphatic protons of the lysine chain (c, Figure 3-14).

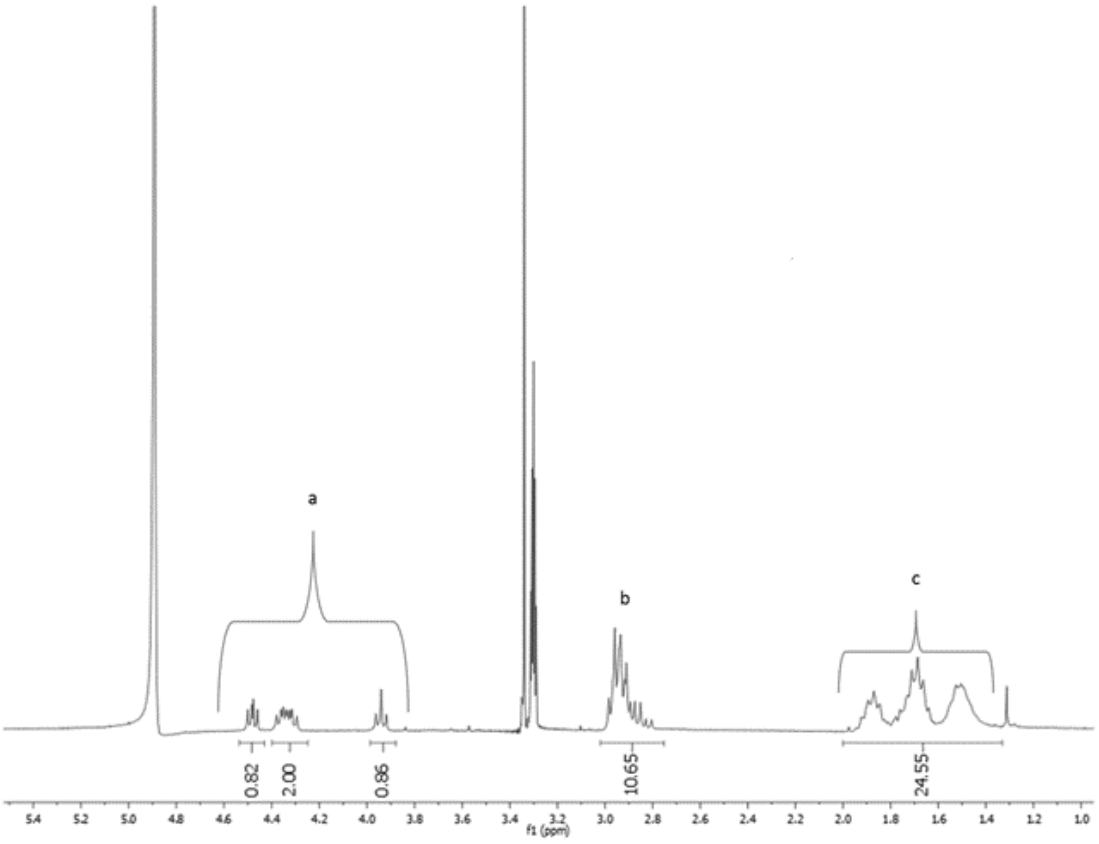

Figure 3- 14 ^{1}H NMR spectrum of CKK in $CDCl_3$

CK_n oligomers with n>10 were synthesized by ring opening polymerization [39, 40]. The polylysine block with one cysteine residue at the C-terminus ($HS\text{-}CK_n$) was synthesized in two steps. First, NH_2-Cys(Trt)-H was used to initiate ring-opening polymerization of Z-lysine-*N*-carboxyanhydride to afford the Trt-cysteine-ended poly(Z)lysine. Based on the integration of aromatic protons (δ 7.2 ppm) and methylene

protons adjacent to the benzene ring (δ= 5.0 ppm) in ^{1}H NMR spectra of the resulting polymers, the conversion of Z-lysine-*N*-carboxyanhydride could be estimated, typically ranging from 85-90 %. The overall yield of the polymers was about 70% after purification. The GPC of unprotected polylysine (Figure 3-15) also provided evidence for the polymerization of Z-lysine-*N*-carboxyanhydride though poor solubility of the polymer in the solvent systems examined (THF, THF:water 90/10 v/v) limited the intensity of the GPC signal.

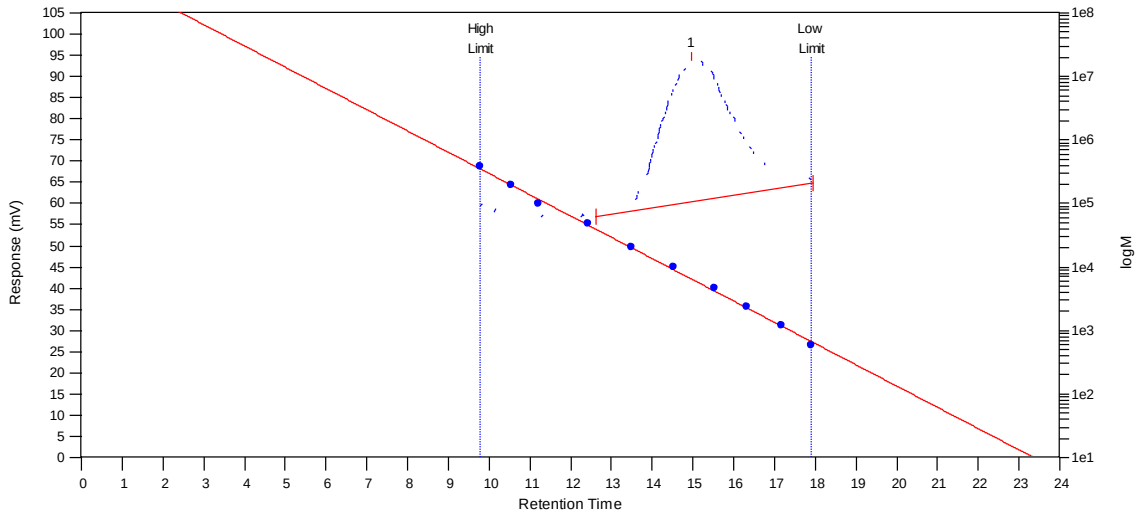

Figure 3- 15 GPC chromatography of Trt-cysteine-terminated poly(Z)lysine (HS-CK$_n$, n=40) with THF/water (90/10 v/v) as eluent.

In a subsequent step, the Trt and Cbz protecting groups were removed by treating the polymer sequentially with TFA and HBr/HOAc under N2 flow. The disappearance of the aromatic peaks and the benzylic methylene peaks in the 1H NMR spectra of the deprotected polymer indicated the successful removal of all the protecting groups.

References (Chapter 3)

1. Forster, S. and M. Antonietti, *Amphiphilic block copolymers in structure-controlled nanomaterial hybrids.* Advanced Materials, 1998. **10**(3): p. 195-+.

2. Discher, D.E. and A. Eisenberg, *Polymer vesicles.* Science, 2002. **297**(5583): p. 967-973.

3. Blanazs, A., S.P. Armes, and A.J. Ryan, *Self-assembled block copolymer aggregates: From micelles to vesicles and their biological applications.* Macromolecular Rapid Communications, 2009. **30**(4-5): p. 267-277.

4. Riess, G., *Micellization of block copolymers.* Progress in Polymer Science, 2003. **28**(7): p. 1107-1170.

5. Israelachvili, J. and H. Wennerström, *Role of hydration and water structure in biological and colloidal interactions.* 1996.

6. Feng, A.C. and J.Y. Yuan, *Smart nanocontainers: Progress on novel stimuli-responsive polymer vesicles.* Macromolecular Rapid Communications, 2014. **35**(8): p. 767-779.

7. Rosler, A., G.W.M. Vandermeulen, and H.A. Klok, *Advanced drug delivery devices via self-assembly of amphiphilic block copolymers.* Advanced Drug Delivery Reviews, 2012. **64**: p. 270-279.

8. Luo, D. and W.M. Saltzman, *Synthetic DNA delivery systems.* Nature Biotechnology, 2000. **18**(1): p. 33-37.

9. Gansbacher, B. and E. European Society Gene Therapy, *Report of a second serious adverse event in a clinical trial of gene therapy for x-linked severe combined immune deficiency (x-scid) - position of the european society of gene therapy (esgt).* Journal of Gene Medicine, 2003. **5**(3): p. 261-262.

10. Dang, J.M. and K.W. Leong, *Natural polymers for gene delivery and tissue engineering.* Advanced Drug Delivery Reviews, 2006. **58**(4): p. 487-499.

11. Pack, D.W., et al., *Design and development of polymers for gene delivery.* Nature Reviews Drug Discovery, 2005. **4**(7): p. 581-593.

12. Neu, M., D. Fischer, and T. Kissel, *Recent advances in rational gene transfer vector design based on poly(ethylene imine) and its derivatives.* Journal of Gene Medicine, 2005. **7**(8): p. 992-1009.

13. Putnam, D., *Polymers for gene delivery across length scales.* Nature Materials, 2006. **5**(6): p. 439-451.

14. Morgan, D.M., V.L. Larvin, and J.D. Pearson, *Biochemical characterisation of polycation-induced cytotoxicity to human vascular endothelial cells.* Journal of Cell Science, 1989. **94**(3): p. 553-559.

15. Fischer, D., et al., *In vitro cytotoxicity testing of polycations: Influence of polymer structure on cell viability and hemolysis.* Biomaterials, 2003. **24**(7): p. 1121-1131.

16. Jeon, S.I., et al., *Protein surface interactions in the presence of polyethylene oxide .1. Simplified theory.* Journal of Colloid and Interface Science, 1991. **142**(1): p. 149-158.

17. Li, X., et al., *Self-assembled polymeric micellar nanoparticles as nanocarriers for poorly soluble anticancer drug ethaselen.* Nanoscale Research Letters, 2009. **4**(12): p. 1502-1511.

18. Mishra, S., et al., *Poly(alkylene oxide) copolymers for nucleic acid delivery.* Accounts of Chemical Research, 2012. **45**(7): p. 1057-1066.

19. Gombotz, W.R. and D.K. Pettit, *Biodegradable polymers for protein and peptide drug-delivery.* Bioconjugate Chemistry, 1995. **6**(4): p. 332-351.

20. Kumar, J.P.J.a.N., *Self assembly of amphiphilic (peg)3-pla copolymer as polymersomes: Preparation, characterization, and their evaluation as drug carrier.* Biomacromolecules, 2010. **11**(4): p. 1027-1035.

21. Zou, W., et al., *Preparation and characterization of cationic pla-peg nanoparticles for delivery of plasmid DNA.* Nanoscale Research Letters, 2009. **4**(9): p. 982-992.

22. Xiong, L.Z. and Z.Q. He, *Synthesis and application for porous scaffold materials of mono-methoxy polyethylene glycol/polylactide diblock copolymer.* Journal of Macromolecular Science Part B-Physics, 2011. **50**(6): p. 1226-1233.

23. Kricheldorf, H.R., I. Kreisersaunders, and C. Boettcher, *Polylactones .31. Sn(ii)octoate-initiated polymerization of l-lactide - a mechanistic study.* Polymer, 1995. **36**(6): p. 1253-1259.

24. Kowalski, A., A. Duda, and S. Penczek, *Kinetics and mechanism of cyclic esters polymerization initiated with tin(ii) octoate, 1 polymerization of epsilon-caprolactone.* Macromolecular Rapid Communications, 1998. **19**(11): p. 567-572.

25. Kricheldorf, H.R., I. Kreiser-Saunders, and A. Stricker, *Polylactones 48. Snoct(2)-initiated polymerizations of lactide: A mechanistic study.* Macromolecules, 2000. **33**(3): p. 702-709.

26. Andrew P. Dove , R.C.P., Bas G. G. Lohmeijer ,Robert M. Waymouth and James L. Hedrick, *Thiourea-based bifunctional organocatalysis: Supramolecular recognition for living polymerization.* J. Am. Chem. Soc, 2005. **127**(40): p. 13798-13799.

27. Bas G. G. Lohmeijer , R.C.P., Frank Leibfarth , John W. Logan, David A. Long , Andrew P. Dove , Fredrik Nederberg , Jeongsoo Choi Charles Wade ,Robert M. Waymouth and James L. Hedrick *Guanidine and amidine organocatalysts for ring-opening polymerization of cyclic esters.* Macromolecules, 2006. **39**(25): p. 8574-8583.

28. Matthew K. Kiesewetter , M.D.S., Nicole Kirn, Ryan L. Weber, James L. Hedrick and Robert M. Waymouth *Cyclic guanidine organic catalysts: What is magic about triazabicyclodecene?* J. Org. Chem., 2009. **74**(24): p. 9490-9496.

29. Marco Frediani, D.S., Alfredo Mariotti, Luca Rosi , Piero Frediani, Laura Rosi, Dominique Matt, Lo ̈c Toupet, *Ring opening polymerization of lactide under solvent-free conditions catalyzed by a chlorotitanium calix[4]arene complex.* Macromolecular Rapid Communications, 2008. **29**(18): p. 1554-1560.

30. Boussif, O., et al., *A versatile vector for gene and oligonucleotide transfer into cells in culture and in-vivo-polyethyleimine.* Proceedings of the National Academy of Sciences of the United States of America, 1995. **92**(16): p. 7297-7301.

31. Akinc, A., et al., *Exploring polyethylenimine-mediated DNA transfection and the proton sponge hypothesis.* Journal of Gene Medicine, 2005. **7**(5): p. 657-663.

32. Zhuojun Dai, T.G., Maria A. Mattebjerg, Chi Wu, Thomas L. Andresen, *Elucidating the interplay between DNA-condensing and free polycations in gene transfection through a mechanistic study of linear and branched pei.* Biomaterials, 2011. **32**(33): p. 8626-8634.

33. Patrick Erbacher, A.C.R., Michel Monsigny, Patrick Midoux, *Putative role of chloroquine in gene transfer into a human hepatoma cell line by DNA/lactosylated polylysine complexes.* Experimental Cell Research, 1996. **225**(1): p. 186-194.

34. Joubert, D., et al., *A note on poly-l-lysine-mediated gene transfer in hela cells.* Drug Delivery, 2003. **10**(3): p. 209-211.

35. Zuzana Kadlecova, Y.R., Mattia Matasci, David Hacker, Lucia Baldi, Florian Maria Wurm, Harm-Anton Klok, *Hyperbranched polylysine: A versatile, biodegradable transfection agent for the production of recombinant proteins by transient gene expression and the transfection of primary cells.* Macromolecular Bioscience, 2012. **12**(6): p. 749-804.

36. Jiehua Zhou, J.W., Nadia Hafdi, Jean-Paul Behr, Patrick Erbacher and Ling Peng, *Pamam dendrimers for efficient sirna delivery and potent gene silencing.* Chemical Communications, 2006(22): p. 2362-2364.

37. Xiao-xuan Liu, P.R., Fan-qi Qu, Shu-quan Zheng, Zi-cai Liang, Martin Gleave , Juan Iovanna, Ling Peng, *Pamam dendrimers mediate sirna delivery to target hsp27 and produce potent antiproliferative effects on prostate cancer cells.* Chem Med Chem, 2009. **4**(8): p. 1302-1310.

38. Xue, Y.N., et al., *Improving gene delivery efficiency of bioreducible poly(amidoamine)s via grafting with dendritic poly(amidoamine)s.* Macromolecular Bioscience, 2010. **10**(4): p. 404-414.

39. Chunhua Fu , X.S., Donghua Liu , Zhijing Chen , Zaijun Lu and Na Zhang *Biodegradable tri-block copolymer poly(lactic acid)-poly(ethylene glycol)-poly(l-lysine)(pla-peg-pll) as a non-viral vector to enhance gene transfection.* Int. J. Mol. Sci., 2011. **12**(2): p. 1371-1388.

40. Xiang, L., et al., *A convenient method for the synthesis of the amphiphilic triblock copolymer poly(l-lactic acid)-block-poly(l-lysine)-block-poly(ethylene glycol) monomethyl ether.* Macromolecular Chemistry and Physics, 2011. **212**(6): p. 563-573.

41. Otto, K.R.W.a.S., *Reversible covalent chemistry in drug delivery.* Current Drug Discovery Technologies, 2005. **2**(3): p. 123-160.

42. Luten, J., et al., *Biodegradable polymers as non-viral carriers for plasmid DNA delivery.* Journal of Controlled Release, 2008. **126**(2): p. 97-110.

43. Kihoon Nam, H.Y.N., Pyung-Hwan Kim, Sung Wan Kim, *Paclitaxel-conjugated peg and arginine-grafted bioreducible poly (disulfide amine) micelles for co-delivery of drug and gene.* Biomaterials, 2012. **33**(32): p. 8122-8130.

44. Cerritelli, S., D. Velluto, and J.A. Hubbell, *Peg-ss-pps: Reduction-sensitive disulfide block copolymer vesicles for intracellular drug delivery.* Biomacromolecules, 2007. **8**(6): p. 1966-1972.

45. Vommina V. Sureshbabu , R.V., Shankar A. Naik ,N. Narendra, *Synthesis of ureido-linked glycosylated amino acids from n α-fmoc-asp/glu-5-oxazolidinones and their application to neoglycopeptide synthesis.* Synthetic Communications, 2008. **38**(21): p. 3640-3654.

46. Karen A. Murphy, J.M.E., Daniel A. Savin, *Synthesis, self-assembly and adsorption of peo-pla block copolymers onto colloidal polystyrene.* Journal of Polymer Science Part B: Polymer Physics, 2008. **46**(3): p. 244-252.

47. Sajiki, H., *Selective-inhibition of benzyl ether hydrogenolysis with pd/c due to the presence of ammonia, pyridine or ammonium acetate.* Tetrahedron Letters, 1995. **36**(20): p. 3465-3468.

48. Wei-Chiang Shenz, H.J.-P.R., and Laura LaManna, *Disulfide spacer between methotrexate and poly(d-lysine). A probe for exploring the reductive process in endocytosis.* J. Biol. Chem, 1985. **260**(20): p. 10905-10908.

49. Cavallaro, G., et al., *Reversibly stable thiopolyplexes for intracellular delivery of genes.* Journal of Controlled Release, 2006. **115**(3): p. 322-334.

50. Navath, R.S., et al., *Dendrimer-drug conjugates for tailored intracellular drug release based on glutathione levels.* Bioconjugate Chemistry, 2008. **19**(12): p. 2446-2455.

51. Jan Carlsson, H.D.a.R.A., *Protein thiolation and reversible protein-protein conjugation. N-succinimidyl 3-(2-pyridyldithio)propionate, a new heterobifunctional reagent.* Biochem J., 1978. **173**(3): p. 723-737.

52. Martin, H., et al., *Nanoscale protein pores modified with pamam dendrimers.* Journal of the American Chemical Society, 2007. **129**(31): p. 9640-9649.

53. Ozcan, Y., et al., *Micellization behavior of tertiary amine-methacrylate-based block copolymers characterized by small-angle x-ray scattering and dynamic light scattering.* Materials Chemistry and Physics, 2013. **138**(2-3): p. 559-564.

54. Chen, S.-H. and T.-L. Lin, *16. Colloidal solutions*, in *Methods in experimental physics*, L.P. David and S. Kurt, Editors. 1987, Academic Press. p. 489-543.

55. Natarajan Srinivasan, A.Y.-G., A. Ganesan, *Rapid deprotection of n-boc amines by tfa combined with freebase generation using basic ion-exchange resins.* Molecular Diversity, 2005. **9**(4): p. 291-293.

56. Saito, G., J.A. Swanson, and K.D. Lee, *Drug delivery strategy utilizing conjugation via reversible disulfide linkages: Role and site of cellular reducing activities.* Advanced Drug Delivery Reviews, 2003. **55**(2): p. 199-215.

57. Bodanszky, M., *Principles of peptide synthesis*, *2nd*. 1993: Springer-Verlag Berlin Heidelberg

58. M. Bodanszky, A.B., *The practice of peptide synthesis*, *2nd*. 1994: Springer-Verlag Berlin Heidelberg.

Chapter 4 Characterization and gene delivery application of complexes of PEO-S(CKn)-PLA and GFP DNA plasmid

4.1 Barriers to gene delivery for non-viral vectors

As discussed in previous chapter, gene therapy has gained great research interest as a potential method for treating genetic diseases such as combined immunodeficiency [1], cystic fibrosis[2], Parkinson's disease [3] or cancer [4]. Gene delivery is a multistep process with barriers in each step (Figure 4.1) [5]. Viral vectors possess natural abilities to overcome cellular barriers and immune defense mechanisms, therefore they demonstrate higher transfection efficiency compared to non-viral vectors. It is of great importance to take these barriers into account to improve current non-viral gene vectors or design new non-viral gene vectors.

At the formulation level, the synthetic non-viral gene vectors need to be cost-efficient; nontoxic and nonimmune-responsive for FDA approval; and convenient to manufacture, store, and transport [5]. At the organism level, serum stability and cell-specific targeting

ability of synthetic nonviral gene vectors are required to achieve high gene transfection efficiency [5-7]. At the cellular level, synthetic nonviral gene vectors need to be provided with functionality to allow them to overcome barriers including cellular uptake, endosomal escape, cytosol transport and nuclear entry [5-7].

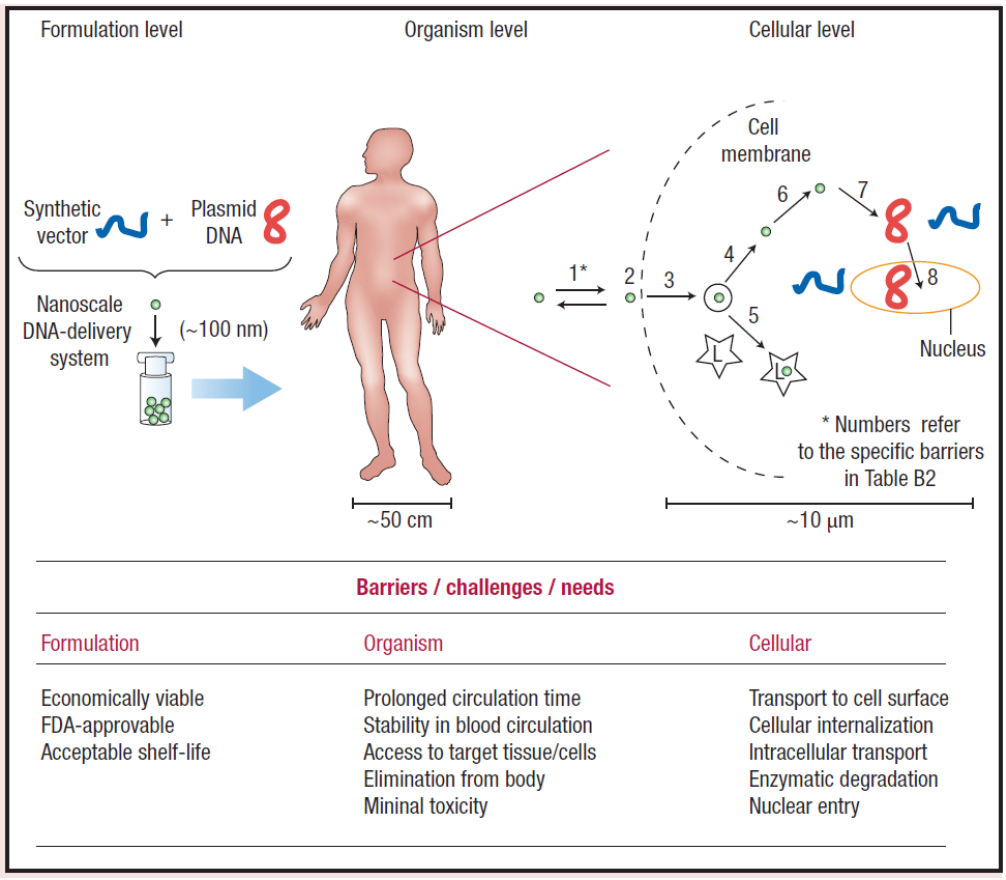

Figure 4- 1 Barriers to gene delivery for non-viral synthetic gene vectors. Numbers 1-8 represent: 1) transport to cell surface, 2) association with cell membrane, 3) cellular uptake, 4) endosomal escape, 5) avoiding transport to lysosome, 6) cytosol transport, 7) dissociation of complexes, 8) nuclear internalization. Reprinted from [5] by permission from Macmillan Publishers Ltd.

4.1.1 Serum stability

Free DNA is not stable in serum due to nuclease degradation[8]. Complexation of polymer and DNA by electrostatic interactions between the positively charged polymer and the negatively charged DNA leads to charge neutralization and DNA condensation. The stability of polymer/DNA complexes depends on the polymer structure and polymer/DNA charge ratio (N/P ratio, the ratio of moles of the primary amine groups of cationic polymers to those of the phosphate groups of DNA) [6]. The surface charges of the polymer/DNA complexes, which are also affected by the N/P ratio, have influence on the stability. Neutral polymer/DNA complexes in serum will quickly aggregate and become ineffective. Positively charged polymer/DNA complexes are usually stable in serum but with the tendency to absorb serum albumin and other negatively charged proteins to form large aggregates which will be cleared by phagocytic cells and the reticuloendothelial system [9, 10] . The polymer/DNA complexes modified with hydrophilic blocks such as polyethylene oxide (PEO) [11, 12] could reduce interactions with plasma proteins and prevent the formation of erythrocyte aggregates which lead to prolonged circulation in the blood.

4.1.2 Cellular Uptake

The cellular uptake of polymer/DNA complexes can be divided into two categories: cationic polymers with or without targeting ligands. The polymer/DNA complexes formed by cationic polymers with targeting ligands such as asialoglycoprotein [13], TAT peptide [14], epidermal growth factor (EGF) [15], and others [16] can be internalized by clathrin-

dependent endocytosis. Therefore, larger complexes with more targeting ligands in the surface have favored cellular uptake. The polymer/DNA complexes formed by cationic polymers without targeting ligands can be internalized via adsorptive pinocytosis [17] with sizes of the complexes affecting on the cellular uptake efficiency [18-20]. The uptake of complexes formed by PLGA copolymer and DNA in Caco-2 cells depended upon the diameter of the complexes as reported by Amidon et al. [18]. The 100 nm diameter PLGA/DNA complexes exhibited 2.5 fold greater cellular uptake on a weight basis than 1 μm diameter complexes and 6 fold greater than 10 μm diameter complexes. Similar results were also obtained by Labhasetwar et al. [19]. The transfection efficiency of smaller-sized PLGA/DNA complexes (diameter = 70 ± 2 nm) was 27-fold higher than that of the larger sized PLGA/DNA complexes (diameter = 202 ± 9 nm) in the COS-7 cell line while 4-fold higher in the HEK-293 cell line. A different type of complex formed by polyethyleneimine nanogels (M-PEIs) and DNA also showed size-dependent properties for gene delivery in cancer cells [20]. In the six samples of complexes with different sizes (38, 75, 87, 121, 132 and 167 nm), the two complexes with size 75 nm and 87 nm had the highest gene transfection efficiency in all four cell lines (A549, Bel7402, BGC-823 and Hela cells).

4.1.3 Endosomal Escape

After cellular uptake, the polymer/DNA complexes have to escape from the endosomal pathway to release DNA into the cytoplasm [6, 8, 21]. In general, the polymer/DNA complexes are first trapped in early endosomes which become acidic (pH 5~6) as they mature into late endosomes due to the action of an ATPase proton-pump

enzyme. If the polymer/DNA complexes cannot escape from endosomes, the complexes will be trafficked into lysosomes (pH 4~5) which contain various degradative enzymes and DNA in the complexes will be degraded. It is very important for polymer/DNA complexes to escape from endosomes into cytoplasm to reach the nucleus.

"Proton-sponge" polymers [22-26] such as polyethyleneimine (PEI) and polyamidoamine (PAMAM) dendrimers, which have abundant secondary and tertiary amines with pKa values between physiological and lysosomal pH, can escape from endosomes through a unique mechanism described by "the proton-sponge hypothesis". The protonation of "Proton-sponge" polymers during endocytic trafficking prevents acidification of endosomes and cause the ATPase to pump more protons into the endosome to reach the desired pH. The accumulation of protons in endosomes requires an influx of counter ions to balance charge which in turn increases ion concentration and leads to osmotic swelling and endosome membrane rupture [6, 8]. Another hypothesis called "the umbrella hypothesis" describes the volumetric expansion of polymers during endosomal acidification. In the formation of polymer/DNA complexes, both polymer and DNA have been condensed into small particles because of electrostatic interactions. After cellular uptake and trafficking into the endosomal pathway, the tertiary amines of the polymers are protonated by the excess of protons in the endosome, which causes electrostatic repulsion between neighboring charged amine groups and results in the extended conformations of terminal polymer branches [21]. Cationic polymers with tertiary amine groups (pH 5-7) and a highly flexible structure capable of volume expansion after protonation can enhance the endosomal escape of complexes because of both the proton-sponge effect and the umbrella effect. Figure 4-2 illustrates the endosomal escape of "Proton-sponge"

polymer/DNA complexes as the results of both the proton-sponge effect and the umbrella effect.

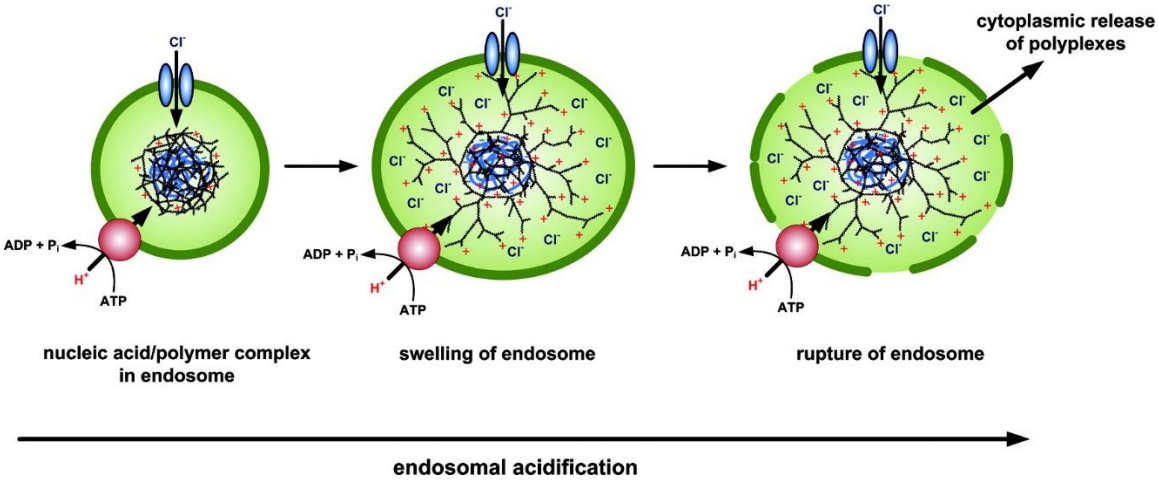

Figure 4- 2 Endosomal escape of "Proton-sponge" polymers/DNA complexes as the results of a) the proton-sponge effect and b) the umbrella effect. Reprinted with permission from [21]. Copyright (2012) American Chemical Society

Other strategies also have been used to enhance the endosomal escape such as treating cells with chloroquine [27-29] during the transfection step. Chloroquine is a well-studied compound which can interfere with the endocytosis process in several ways such as raising the luminal pH of endosomes [30-32], hindering complex delivery to lysosomes [33-35], and reducing intracellular degradation by lysosomal enzymes [36, 37].

4.1.4 Cytoplasmic mobility

After endosomal escape, the polymer/DNA complexes must move through the cytoplasm to the nucleus. Unlike the viral gene vectors which can travel through the cytoplasm by microtubule (MT)-mediated transport [38, 39], synthetic non-viral vectors generally do not undergo MT-mediated transport and need to utilize the directional endosomal pathway, in which endosomes undergo MT-mediated transport toward the nucleus. Even though endosomes could carry the non-viral gene delivery vectors toward the nucleus and release them upon endosomal escape, there are still several disadvantages associated with relying on endosomal transport such as uncontrollable endosomal escape timing and location, lack of MT-mediated transport after endosomal escape, and slow passive diffusion through cytoplasm due to the relatively large size of the complexes[21]. The highly viscous cytoplasm with a high concentration of proteins not only hinders the passive diffusion of relatively large size polymer/DNA complexes but also leads to destabilization of complexes and degradation of DNA [40]. In order to achieve gene delivery to the nucleus by passive diffusion, the sizes of polymer/DNA complexes need to be decreased to increase the passive diffusion speed. Gene vectors with diameters less than 30 nm are able to diffuse in the cytoplasm independently of the MT network [41, 42].

To transport genes from solution to the cell nucleus, synthetic non-viral vectors must overcome several extracellular and intracellular barriers. Inefficiencies for any obstacle will result in an inefficient gene vector. In the following section, tri-arm star copolymers PEO-S(CK_n)-PLA designed and synthesized in Chapter 3 were studied as gene vectors to deliver green fluorescence protein (GFP) DNA to cells. Two triblock copolymers, PEO5k-S(CK_3)-PLA5k and PEO2k-S(CK_{40})-PLA2k, formed complexes with GFP DNA plasmid

at various N/P ratios. For comparison, one diblock copolymer PEO2k-S(CK_{30}) was also used to form complexes with GFP DNA plasmid at various N/P ratios. *In vitro* gene transfection efficiency of these complexes and cytotoxicity of the star triblock copolymers were measured in HeLa cells.

4.2 Experimental

4.2.1 Preparation of triblock copolymer/GFP DNA complexes

Preparation of triblock copolymer/GFP DNA complexes with different N/P ratios (ratio of moles of the primary amine groups of cationic polymers to those of the phosphate groups of DNA), were based on the calculated mass ratio of the tri-arm star copolymer to GFP DNA in each complex [43, 44]. In a typical procedure to prepare PEO2k-S(CK_{40})-PLA2k/GFP DNA complex, GFP DNA plasmid (4700bp) was diluted to 100 ng/μL in deioinized water. Complexes with different N/P ratios were prepared by adding solutions of PEO2k-S(CK_{40})-PLA2k in deionized water solution at various concentrations (42-1250 ng/μL) (Table 4-1) to equal volumes of plasmid solution by pipet and incubating the resulting solution at 37 ℃ for 30 min before characterization by DLS and agarose gel electrophoresis. For the transfection and cytotoxicity tests, DMEM buffer was used instead of deionized water.

Table 4- 1 Calculated mass ratios of polymer to DNA for preparation of PEO2k-S(CK40)-PLA2k/GFP DNA complex with different N/P ratios.

N/P ratio	Mass ratio of polymer to DNA	PEO2k-S(CK_{40})-PLA2k Concentration (ng/μL)	GFP DNA plasmid Concentration (ng/μL)
0.5	0.42	42	100
1	0.83	83	100
2	1.67	167	100
5	4.18	418	100
15	12.5	1250	100

4.2.2 Agarose gel electrophoresis

Agarose gel electrophoresis was performed to check the DNA condensation ability of the triblock copolymer. In a typical procedure for PEO2k-S(CK_{40})-PLA2k/GFP DNA complexes, 10 μl of each PEO2k-S(CK_{40})-PLA2k/GFP DNA complex solution prepared in section 4.2.1 was mixed with 2 μl 6× loading buffer and loaded into a 0.8 wt% Agarose gel containing 0.5 μg/ml ethidium bromide. Electrophoresis was set up in 1× TEA buffer at 95 V and run for 30 min. DNA retardation was analyzed with a UV illuminator.

4.2.3 Transfection

In a typical procedure for gene transfection of MC3T3 cells with PEO5k-S(CK_3)-PLA5k/GFP DNA complexes, 1×10^5 MC3T3 cells were resuspended in 500μl αMEM and then added into each well of a 24-well plate one day prior to transfection. On the day of transfection, 40 μL of a suspension of PEO5k-S(CK_3)-PLA5k/GFP DNA complexes in deionized water was added into each well and mixed with the cells gently. The medium containing the PEO5k-S(CK_3)-PLA5k/GFP DNA complexes was removed after 4 h incubation at 37 ℃ in a humidified atmosphere (95% air, 5% CO_2) and 0.5 ml fresh complete culture medium αMEM (pH 7.4) containing 10% FBS was added. The cells were further incubated at 37 ℃ in a humidified atmosphere (95% air, 5% CO_2) for 48 h. Each transfection condition experiment was carried out in triplicate. The transfection results were observed using a fluorescence microscope.

In a typical procedure for gene transfection of HeLa cells with PEO2k-S(CK_{40})-PLA2k/GFP DNA complexes, 1×10^5 HeLa cells were plated into each well of a 24-well plate one day prior to transfection. On the day of transfection, the medium was removed and 0.5 ml of a DMEM solution containing the PEO2k-S(CK_{40})-PLA2k/GFP DNA complex with or without 100 μM chloroquine was added to each well. The medium with PEO2k-S(CK_{40})-PLA2k/GFP DNA was removed after 4 h incubation at 37 ℃ in a humidified atmosphere (95% air, 5% CO_2) and 0.5 ml fresh complete culture medium (pH 7.4) containing 10% FBS was added. The cells were further incubated at 37 ℃ in a humidified atmosphere (95% air, 5% CO_2) for 48 h. Each transfection condition experiment was carried out in triplicate. The transfection results were observed using a

fluorescence microscope. Gene transfection of PEO2k-S(CK_{30})/GFP DNA complexes in Hela cells was carried out in the same protocol.

4.2.4 Flow Cytometry

After being observed using a fluorescence microscope, the HeLa cells were washed twice and resuspended, and then the analysis of transfection efficiency was performed using a FACS 440 flow cytometer (BD Bioscience, Mountain View, CA, USA). An excitation wavelength of 488 nm was used with fluorescence emission measured at 530 ± 15 nm through fluorescence channel 1 (FL1). A minimum of 10,000 cells per sample were collected and the transfection efficiency was calculated by the ratio of number of collected fluorescence cells to number of total collected cells. Each transfection condition experiment was carried out in triplicate.

4.2.5 Cytotoxicity Assay

The cytotoxicity of polymers against HeLa cells was evaluated using the MTS assay. Before testing, cells in 100 μL of complete DMEM were seeded into 96-well plates at a density of 5000 cells/well. After incubation at 37 ℃ in a humidified atmosphere (95% air, 5% CO_2) for 24 h, 100 μL solutions of polymers in complete DMEM (pH 7.4) at different concentrations were added into the wells separately and the cells were further incubated for 24 h. Nearly 20 μL of MTS solution was added to each well and the cells were allowed to incubate for another 2 h. Cells without addition of MTS were used as blank to calibrate

the microplate reader to zero absorbance. The absorbance of the solution in each well at 490 nm was measured with the microplate reader. Untreated cells were taken as a control with 100% viability. The relative cell viability was calculated as a percentage relative to untreated control cells. Each cytotoxicity condition experiment was performed in triplicate.

4.3 Results and Discussions

4.3.1 Size Characterization by DLS

The sizes of triblock copolymer PEO5k-S(CK_3)-PLA5k assemblies, triblock copolymer PEO2k-S(CK_{40})-PLA2k assemblies, diblock copolymer PEO2k-S(CK_{30}) assemblies, and naked GFP DNA plasmid in deionized water were analyzed by a BIC 90 plus Particle Size Analyzer (Brookhaven Instruments Corp.) at a wavelength of 659.0 nm and a constant angle of 90 °(Figure 4.3).

The measured hydrodynamic radii (R_h) of triblock copolymer PEO5k-S(CK_3)-PLA5k assemblies, triblock copolymer PEO2k-S(CK_{40})-PLA2k assemblies, and diblock copolymer PEO2k-S(CK_{30}) assemblies at a concentration 1 mg/mL in deionized water were 126.7 ± 1.3 nm, 122.2 ± 1.2 nm, and 146.7 ± 3.0 nm, respectively. The electrostatic repulsion of positive charges in polylysine segments prevent the PEO5k-S(CK_n)-PLA5k triblock copolymers and PEO2k-S(CK_{30}) diblock copolymer from forming compact structures. R_h of the naked DNA plasmid with concentration 0.1 mg/mL was 297.2 ± 26.5 nm.

a) PEO5k-S(CK_3)-PLA5k (Mean Eff. Diam. 253.3 ± 2.7 nm, Rh= 126.7 ± 1.3 nm)

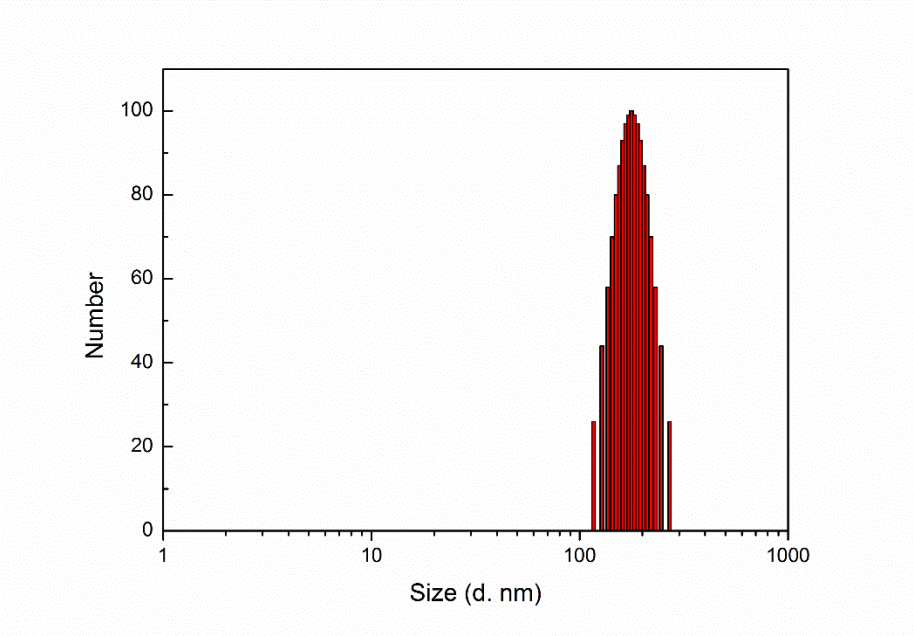

b) PEO2k-S(CK_{40})-PLA2k (Mean Eff. Diam. 244.4 ± 2.4 nm, Rh= 122.2 ± 1.2 nm)

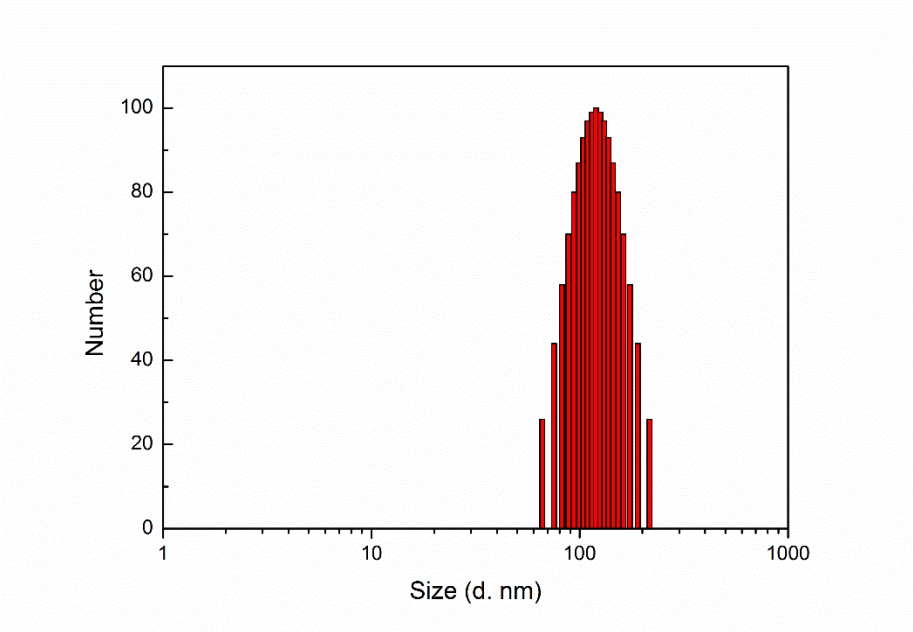

c) PEO2k-S(CK_{30}) (Mean Eff. Diam. 293.4 ± 6.0 nm, Rh= 146.7 ± 3.0 nm)

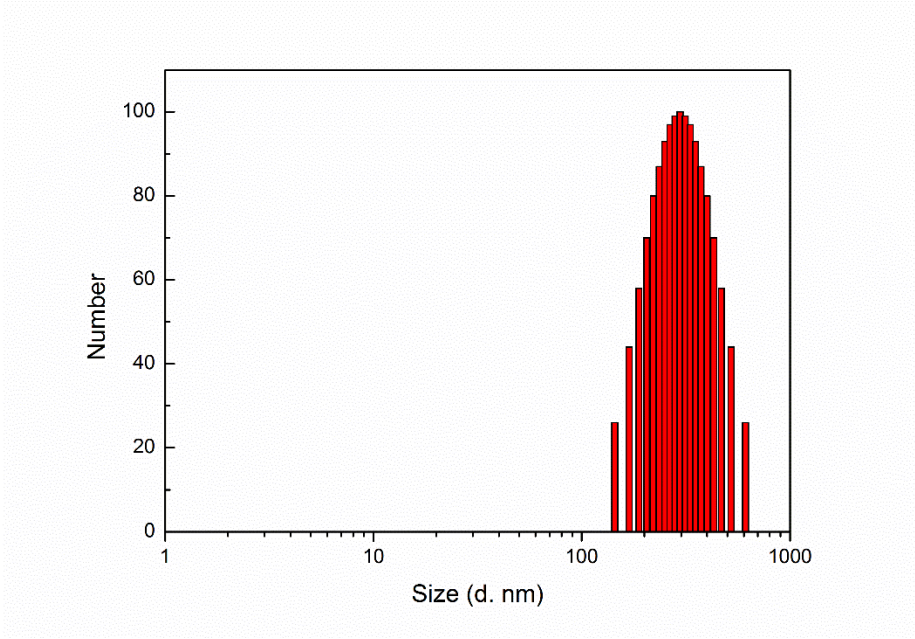

d) Naked DNA plasmid (Mean Eff. Diam. 594.5 ± 52.9 nm, Rh= 297.2 ± 26.5 nm)

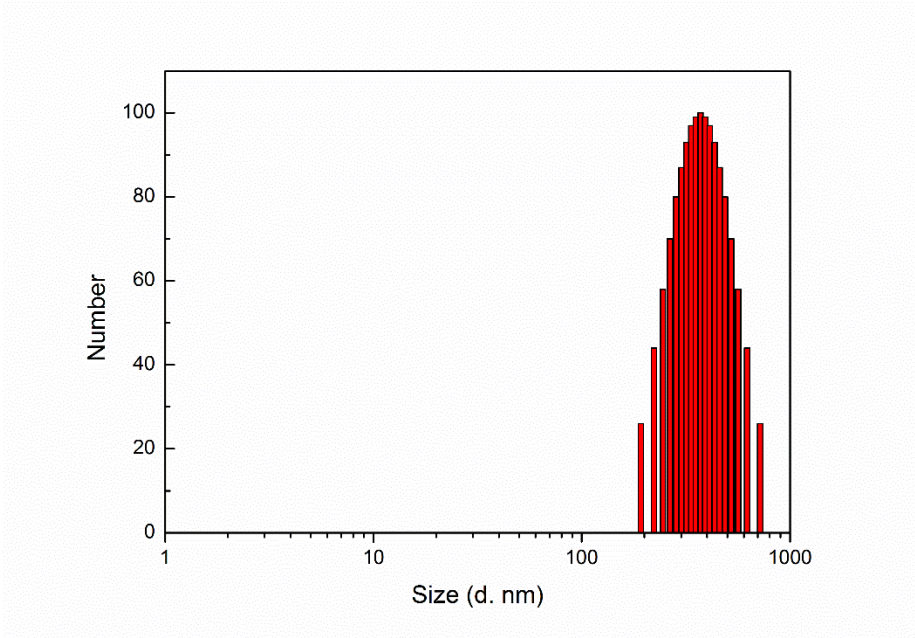

Figure 4- 3 DLS histograms of a) triblock copolymer PEO5k-S(CK3)-PLA5k, b) triblock copolymer PEO2k-S(CK40)-PLA2k, c) diblock copolymer PEO2k-S(CK30), and d) naked GFP DNA plasmid in deionized water.

Complexes with different N/P ratios (from 0.5 to 15) were prepared by adding solutions of PEO2k-S(CK_{40})-PLA2k in deionized water at various concentrations (42 ng/mL to 1250 ng/mL) to equal volumes of plasmid solution (100 ng/mL) and incubating at 37 ℃ for 30 min. The hydrodynamic diameters of PEO2k-S(CK_{40})-PLA2k /GFP DNA complexes were measured by DLS. The triblock copolymer PEO2k-S(CK_{40})-PLA2k could condense GFP DNA plasmids into complexes with R_h from 65 nm to 110 nm (Figure 4-4a) which were appropriate for endocytotic cellular uptake.

The hydrodynamic diameters of PEO2k-S(CK_{30})/GFP DNA complexes of different N/P ratios (from 1 to 20) were also measured by DLS. The diblock copolymer PEO2k-S(CK_{30}) could condense GFP DNA plasmids into complexes with R_h from 47.2 nm to 78.3 nm (Figure 4-4b) which were appropriate for endocytotic cellular uptake.

a) Triblock copolymer PEO2k-S(CK_{40})-PLA2k/GFP DNA complexes

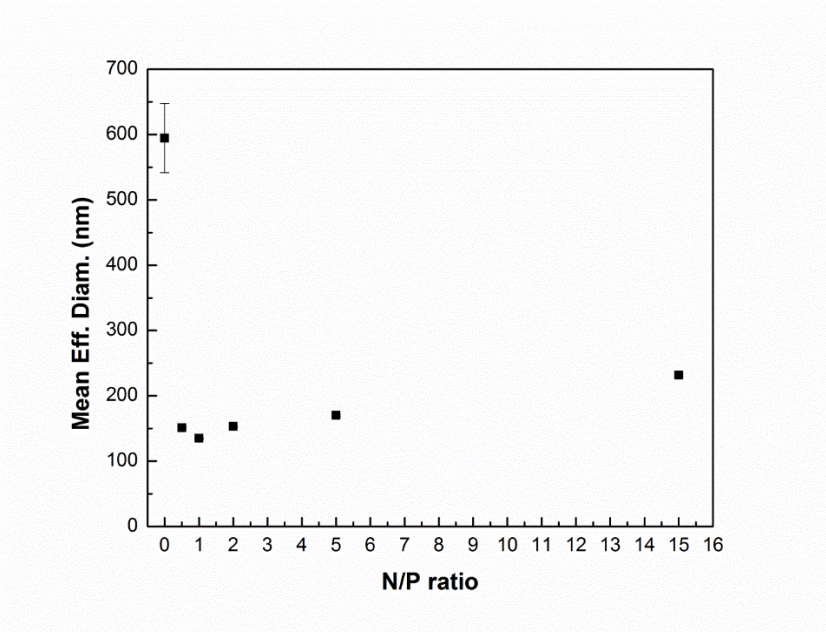

b) Diblock copolymer PEO2k-S(CK_{30})/GFP DNA complexes

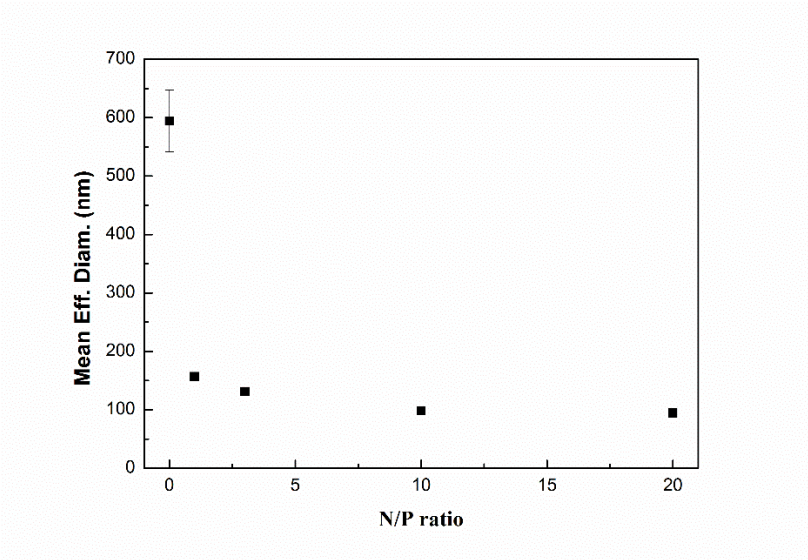

Figure 4- 4 DLS particle size measurements of a) triblock copolymer PEO2k-S(CK40)-PLA2k/GFP DNA complexes b) diblock copolymer PEO2k-S(CK30)/GFP DNA complexes in deionized water at various N/P ratios. N/P = 0 corresponds to the DNA plasmid without any additives. Error bars represent the mean standard deviation (n = 5). Relatively small mean standard deviations (< 2.5 nm) are not visible due to the large Y scale.

4.3.2 Agarose gel electrophoresis

Agarose gel electrophoresis of triblock copolymer PEO2k-S(CK_{40})-PLA2k was performed at various N/P ratios (ranging from 0 to 15) to study the condensation capability of PEO2k-S(CK_{40})-PLA2k with DNA. As shown in Figure 4-5, the naked plasmid DNA migrated toward the positive electrode in two bands. DNA with supercoiled morphology migrated further toward the positive electrode than DNA with open circular morphology. Once the triblock copolymer PEG2k-S(CK_{40})-PLA2k was added (N/P = 0.5), mobility of DNA associated with the copolymer was retarded while free DNA moved to the positive electrode similar to the control DNA. At N/P ratios greater than or equal to 1, the mobility of the plasmid was retarded completely and free DNA bands were not visible.

Agarose gel electrophoresis of diblock copolymer PEO2k-S(CK_{30}) was also performed at various N/P ratios (ranging from 0 to 20) to study the condensation capability of PEO2k-S(CK_{30}) with DNA. As shown in Figure 4-6, the naked plasmid DNA with open circular and supercoiled morphologies migrated at different speeds toward the positive electrode resulting in two visible bands in the gel. Once the diblock copolymer PEO2k-S(CK_{30}) was added, the mobility of DNA was retarded. At N/P ratios greater than or equal to 1, the mobility of the plasmid was retarded completely and free DNA bands were not visible.

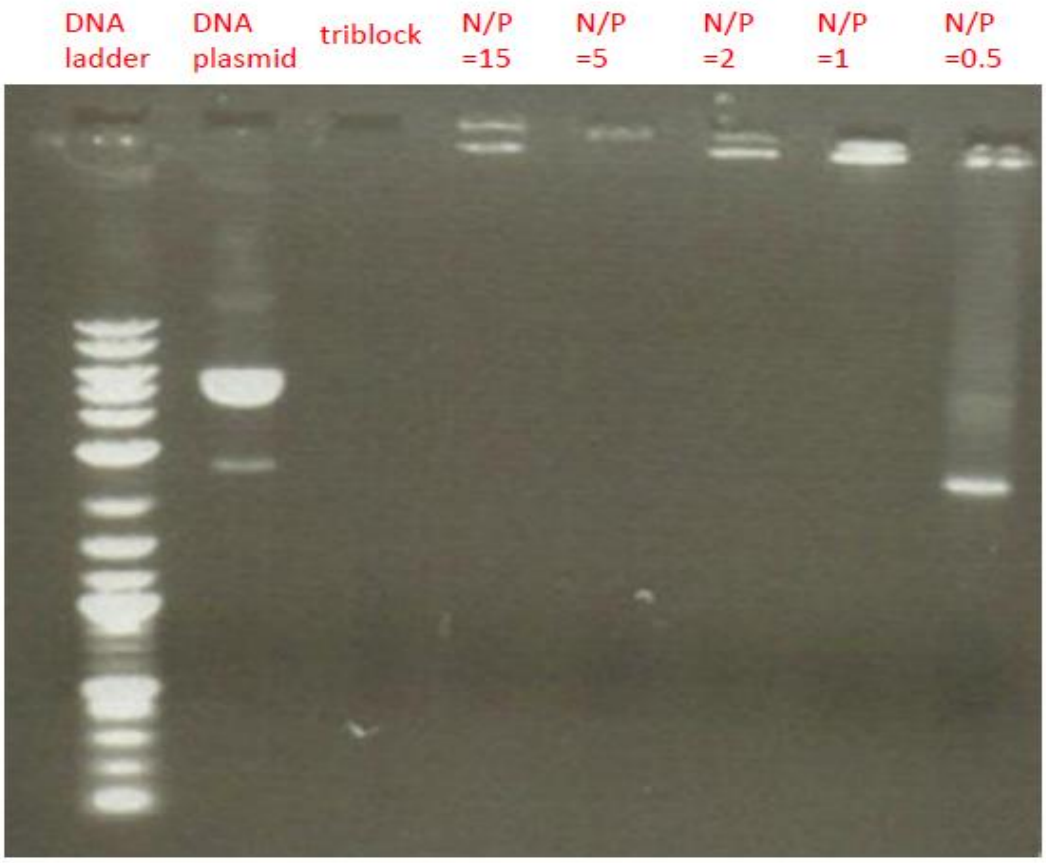

Figure 4- 5 Agarose gel electrophoresis images of triblock copolymer PEO2k-S(CK40)-PLA2k/GFP complexes at various N/P ratios with positive electrode on the bottom. Lane 1: DNA ladder; Lane 2: Naked DNA plasmid; Lane 3: triblock copolymer PEG2k-S(CK40)-PLA2k; Lanes 4-8: PEG2k-S(CK40)-PLA2k/DNA complexes at N/P ratios of 15, 5, 2, 1, and 0.5, respectively.

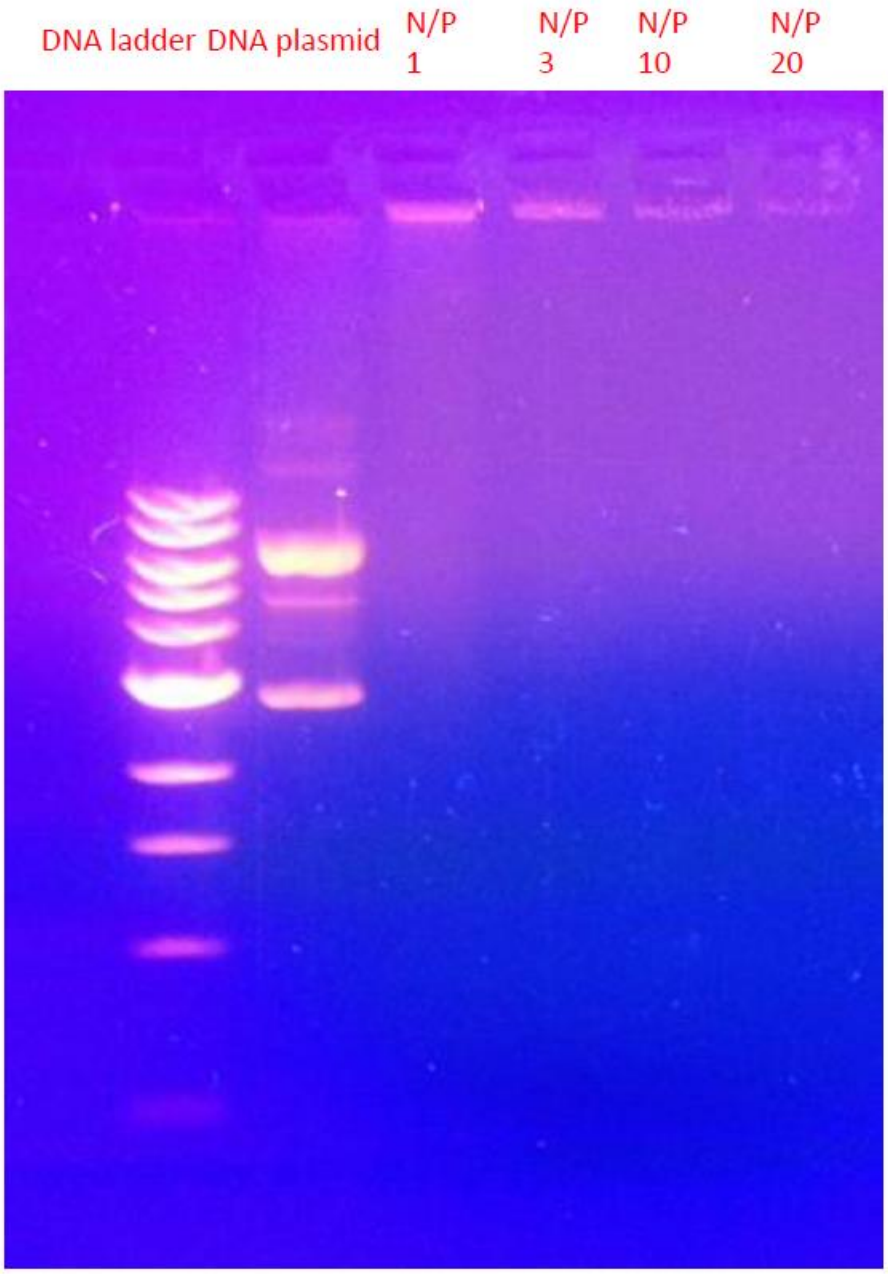

Figure 4- 6 Agarose gel electrophoresis images of diblock copolymer PEO2k-S(CK_{30})/GFP complexes at various N/P ratios with positive electrode on bottom. Lane 1: DNA ladder; Lane 2: Naked DNA plasmid; Lane 3-6: PEG2k-S(CK_{30})/DNA complexes at N/P ratios of 1,3,10, and 20 respectively.

4.3.3 In vitro gene transfection

Gene transfection with triblock copolymer PEO5k-S(CK_3)-PLA5k/GFP DNA complexes was first studied in MC3T3 cells. For comparison, MC3T3 cells were also transfected with lysine oligomer PLL_{40}/GFP DNA complexes under the same transfection conditions. In initial attempts, different transfection conditions were not screened for the different complex systems and a standard gene transfection protocol was adopted for MC3T3 cells. MT3C3 cells transfected by PLL_{40}/GFP complexes and PEO5k-S(CK_3)-PLA5k/GFP complexes at various N/P ratios (N/P ratios 3, 5, 10) were studied and compared as shown in Figure 4-7. Triblock copolymer PEO5k-S(CK_3)-PLA5k/GFP DNA complexes exhibited no enhanced gene transfection efficiency compared to the PLL_{40}/GFP DNA complexes at all the N/P ratios (N/P ratios 3,5,10) examined. One possible reason for the low gene transfection was that the charge of the short lysine oligomer segment CK_3 would be shielded by the relatively long PEO polymer block resulting in inefficient condensation of GFP DNA plasmid. Another possible reason was the extremely high mass ratios between the triblock copolymer PEO5k-S(CK_3)-PLA5k and the GFP DNA plasmid at normal N/P ratios which led to high triblock copolymer PEO5k-S(CK_3)-PLA5k concentrations in the medium and high solution viscosity at the transfection stage.

a) PLL_{40} N/P=3

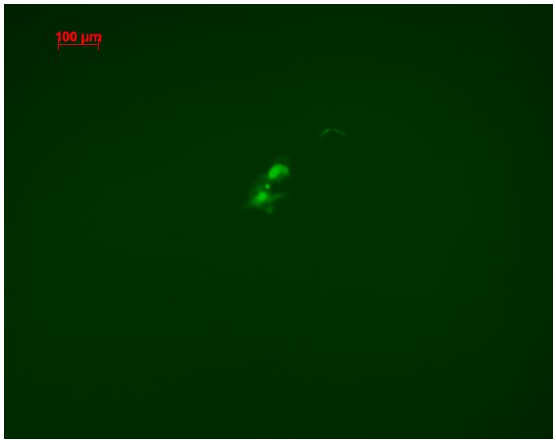

b) PEO5k-S(CK_3)-PLA5k, N/P=3

c) PLL_{40} N/P=5

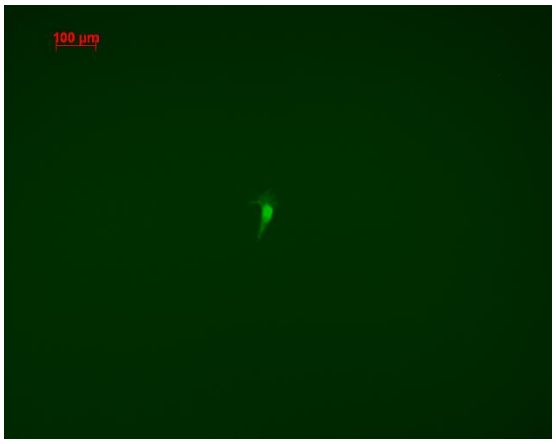

d) PEO5k-S(CK_3)-PLA5k, N/P=5

e) PLL_{40} N/P=10

f) PEO5k-S(CK_3)-PLA5k, N/P=10

Figure 4- 7 Fluorescence images of MT3C3 cells transfected by PLL40/GFP complexes and PEO5k-S(CK3)-PLA5k/GFP complexes at various N/P ratios.

Triblock copolymer PEO2k-S(CK_{40})-PLA2k with a longer CK_{40} lysine oligomer segment and relatively short PEO polymer chain was investigated next for gene transfer efficiency in HeLa cells. Several transfection variables such as N/P ratio, medium pH, addition of chloroquine, and DNA concentration were screened to find the optimal transfection protocol for the triblock copolymer PEO2k-S(CK_{40})-PLA2k/GFP DNA complexes. Flow cytometry data for HeLa cells transfected by PEO2k-S(CK_{40})-PLA2k/GFP complexes in different transfection conditions are summarized in Table 4-2.

Table 4- 2 Flow cytometry data for HeLa cells transfected by PEO2k-S(CK40)-PLA2k/GFP complexes. Each transfection condition was carried out in triplicate.

	1 (%)[a]	**2** (%)[a]	**3** (%)[a]	**Avg** (%)
N/P=3, pH=7.4	0.33	0.42	0.34	0.36 ±0.05[b]
N/P=5, pH=7.4	0.49	0.35	0.44	0.43 ±0.07
N/P=10,pH=7.4	0.30	0.23	0.35	0.29 ±0.06
N/P=5, pH=7.0	0.37	0.57	0.54	0.48 ±0.11
N/P=5, pH=7.2	0.83	0.76	0.75	0.78 ±0.04
N/P=5, pH=7.6	0.32	0.35	0.66	0.44 ±0.19
N/P=5, pH=7.4 with Chloroquine	2.33	1.67	1.24	1.75 ±0.55

a. Gene transfection efficiency for each transfection condition is reported by percentage of the total number of cells counted showing green fluorescence.

b. The error range represent the mean standard deviation (n=3).

The PEO2k-S(CK_{40})-PLA2k/GFP DNA complexes with different N/P ratios had different sizes in deionized water which were measured in Section 4.3.1. The N/P ratio together with other factors such as polymer ionization [45] affect the sizes of PEO2k-S(CK_{40})-PLA2k/GFP DNA complexes in media. The N/P ratios also affect the surface charge density of the polymer/DNA complexes. As discussed in Section 4.1, the nanoparticle size and surface charge have a great effect on cellular uptake and gene transfection. For the PEO2k-S(CK_{40})-PLA2k/GFP DNA complexes with N/P ratios from 3 to 10, the highest gene transfection efficiency 0.43% ± 0.07% was obtained at an N/P ratio of 5, compared to 0.36% ± 0.05% at an N/P ratio of 3, and 0.29% ± 0.06% at an N/P ratio of 10.

In addition to the N/P ratio, the medium pH could also affect the sizes and surface charge densities of the PEO2k-S(CK_{40})-PLA2k/GFP DNA complexes, which in turn could change cellular uptake and gene transfection. In the investigated pH range from 7.0 to 7.6, the gene transfection efficiency showed a peak of 0.78% ± 0.04% at pH 7.2 but otherwise remained around 0.4%.

The important roles of chloroquine in enhancing gene transfection have been discussed in Section 4.1.3. Generally, chloroquine diphosphate can increase endosomal escape of DNA/polymer complexes by raising pH in endosomes and lysosomes, reducing the trafficking of complexes to lysosomes, and protecting complexes from degradation by lysosomal enzymes [27-37]. Addition of 100 μM chloroquine diphosphate to the HeLa cells at the time of transfection resulted an enhancement of gene transfection efficiency from 0.43% ± 0.07% to 1.75% ± 0.55% for PEO2k-S(CK_{40})-PLA2k/GFP DNA complexes with an N/P ratio of 5 in DMEM buffer (pH = 7.4).

The effect of DNA concentration in each well on gene transfection efficiency was also studied. At a constant N/P ratio, the higher GFP DNA concentration would also result in higher triblock copolymer PEO2k-S(CK_{40})-PLA2k concentration and an increased amount of triblock copolymer PEO2k-S(CK_{40})-PLA2k/GFP DNA in each well. Figure 4-8 shows the fluorescence images of HeLa cells transfected by PEO2k-S(CK_{40})-PLA2k/GFP DNA complexes at constant N/P ratio of 5 with different GFP DNA concentrations (4 ng/μL, 10 ng/μL and 16 ng/μL) in DMEM buffer (pH=7.4). The highest transfection efficiency (0.43% ± 0.07%) in these studies was obtained at a GFP DNA concentration of 4 ng/μL. The possible reason for this observation was that the increased amount of polymer/DNA complexes did not enhance the cellular uptake of polymer/DNA complexes but the relatively larger complexes structures formed at high concentration could have hindered the cellular uptake of polymer/DNA complexes.

a) N/P=5, 4 ng/µL

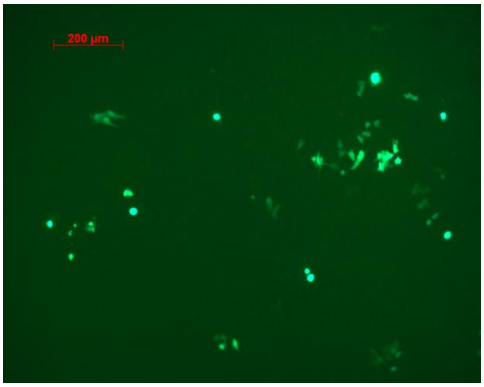

b) N/P=5, 10 ng/µL

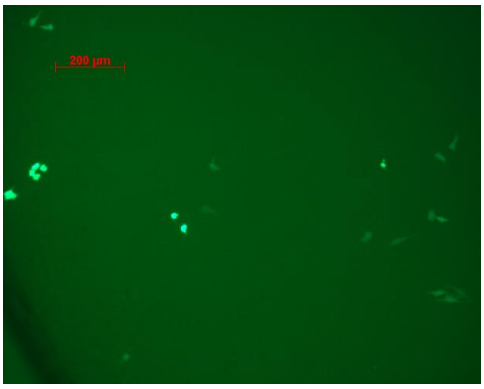

c) N/P=5, 16 ng/µL

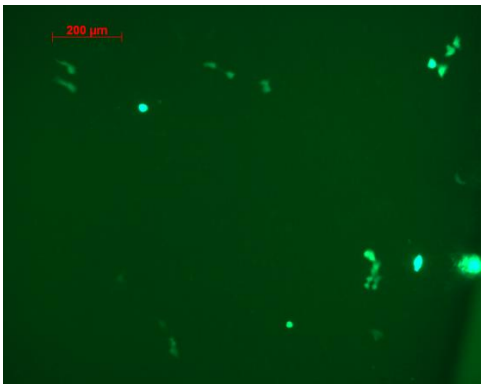

Figure 4- 8 Fluorescence images of HeLa cells transfected by PEO2k-S(CK40)-PLA2k/GFP DNA complexes at constant N/P ratio of 5 in DMEM buffer (pH=7.4) with different GFP DNA concentrations: a) 4 ng/µL, b)10 ng/µL, and c) 16 ng/µL.

For comparison, HeLa cells were also transfected by diblock copolymer PEO2k-S(CK_{30})/GFP DNA complexes and PLL_{40}/GFP complexes under the same transfection conditions. Based upon fluorescence microscopy, triblock copolymer PEO2k-S(CK_{40})-PLA2k/GFP DNA complexes appears to show higher gene transfection activity than PLL_{40}/GFP DNA complexes and diblock copolymer PEO2k-S(CK_{30})/GFP DNA complexes (Figure 4-8a, 4-8c and 4-8e). This increase in transfection efficiency might be explained by enhanced gene protection and transport properties of the star block copolymer PEO2k-S(CK_{40})-PLA2k.

Chloroquine diphosphate, which is known to interfere with the endocytosis process, was added to enhance cell transfection of PLL_{40}/GFP DNA complexes, PEO2k-S(CK_{30})/GFP DNA complexes, and PEO2k-S(CK_{40})-PLA2k/GFP complexes (Figure 4-8b, 4-8d, 4-8f). For all three complex systems, enhancement of transfection efficiency by chloroquine could also be observed. For the PEO2k-S(CK40)-PLA2k/GFP complexes, the fluorescence micrographs (Figure 4-8f) were in good agreement with the chloroquine-enhanced transfection results from the flow cytometry data (Table 4-2).

a) PLL_{40}, N/P=5

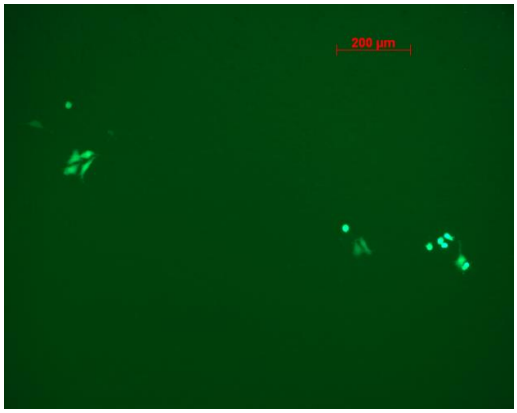

b) PLL_{40}, N/P=5, with chloroquine

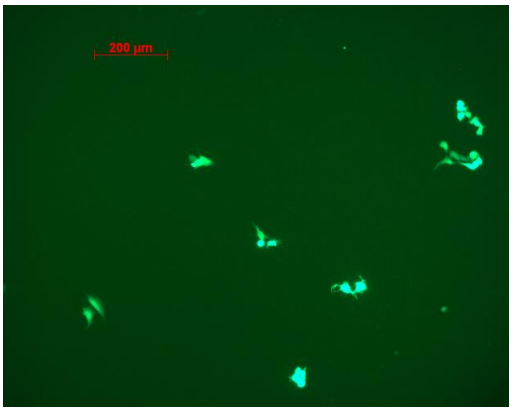

c) PEO2k-S(CK_{30}), N/P=5

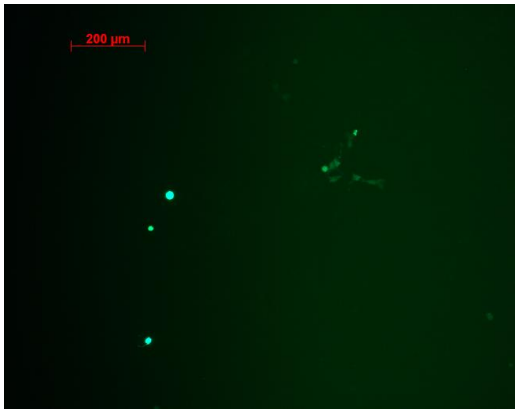

d) PEO2k-S(CK_{30}), N/P=5, with chloroquine

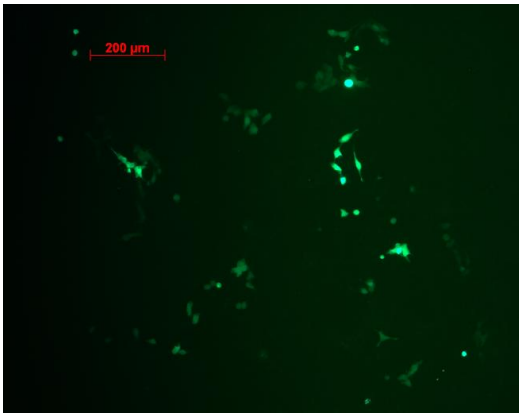

e) PEO2k-S(CK_{40})-PLA2k, N/P=5

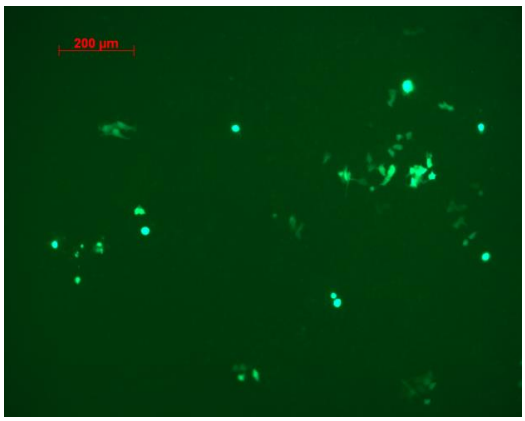

f) PEO2k-S(CK_{40})-PLA2k, N/P=5, chloroquine

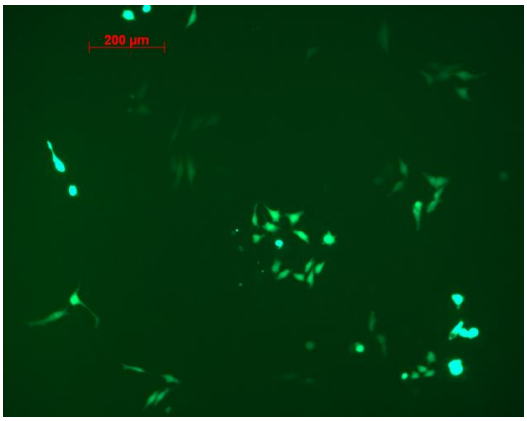

Figure 4- 9 Fluorescence images of HeLa cells transfected by PLL_{40}/GFP DNA complexes, PEO2k-S(CK_{30})/GFP DNA complexes, and PEO2k-S(CK_{40})-PLA2k/GFP complexes at N/P ratio 5 and pH 7.4.

4.3.4 Cytotoxicity

Evaluation of the cytotoxicity of cationic polymers is essential prior to their application in gene and drug delivery systems. The cytotoxicity of PEO2k-S(CK_{40})-PLA2k tri-arm star triblock copolymers was evaluated by the MTS assay in HeLa cell lines at various concentrations, and compared with the corresponding polylysine PLL_{40} and branched polyethyleneimine (PEI, M_w=25000), which is a commonly used transfection platform[22, 26, 46].

Table 4-3. The concentrations of PEO2k-S(CK_{40})-PLA2k triblock copolymers and corresponding polylysine PLL_{40} and branched PEI studied in cytotoxicity.

N/P ratio	Triblock concentration (mg/mL)	Polylysine concentration (mg/mL)	PEI concentration (mg/mL)
3	0.01	0.00518	0.00156
5	0.0167	0.00864	0.0026
10	0.334	0.01728	0.0052
30	0.1	0.0518	0.0156
60	0.2	0.104	0.0312
120	0.4	0.207	0.0624

PEO2k-S(CK_{40})-PLA2k triblock copolymers showed almost no toxicity at all conditions examined while the corresponding polylysine PLL_{40} and branched PEI showed relatively low toxicity at low concentrations (N/P ratios of 3 to 10: 5.18-17.3 μg/mL for polylysine, 1.56-5.2 μg/mL for PEI) but increased toxicity at higher concentrations (N/P

ratios of 30 to 120: 51.8-207 μg/mL for polylysine, 15.6-62.4 μg/mL for PEI) (Figure 4-10).

From the optical micrographs in Figure 4-11, the cells treated with triblock copolymer PEO2k-S(CK_{40})-PLA2k were quite healthy from N/P ratios of 3 to 120. The cells treated with PLL_{40} or PEI were healthy at an N/P ratio of 3, but became less healthy as N/P ratio was increased, and were almost entirely dead at an N/P ratio of 120, demonstrating the much higher cytotoxicity of these systems. The low cytotoxicity of triblock copolymer PEO2k-S(CK_{40})-PLA2k may be explained by the relatively low positive surface charge resulting from a PEO shielding effect [47].

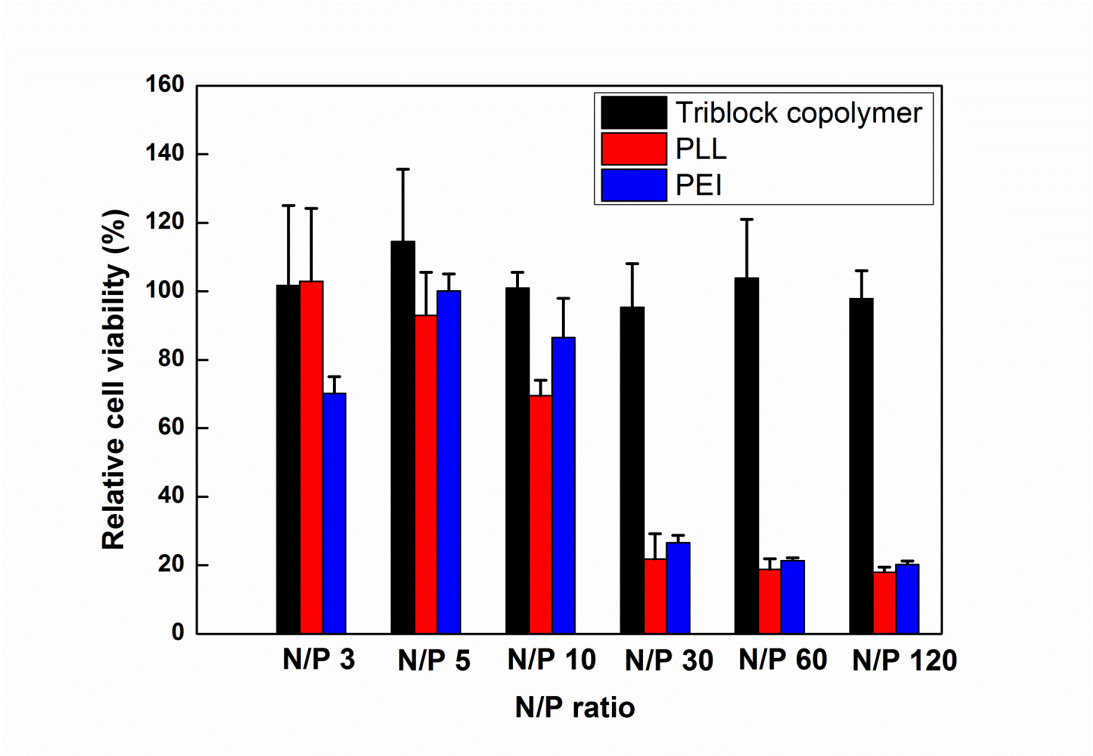

Figure 4- 10 In vitro cytotoxicity of triblock copolymer PEO2k-S(CK40)-PLA2k against HeLa cells using poly(lysine)40 (PLL) and branched polyethyleneimine (PEI, average Mw=25000) as references. Error bars represent the mean standard deviation (n = 3).

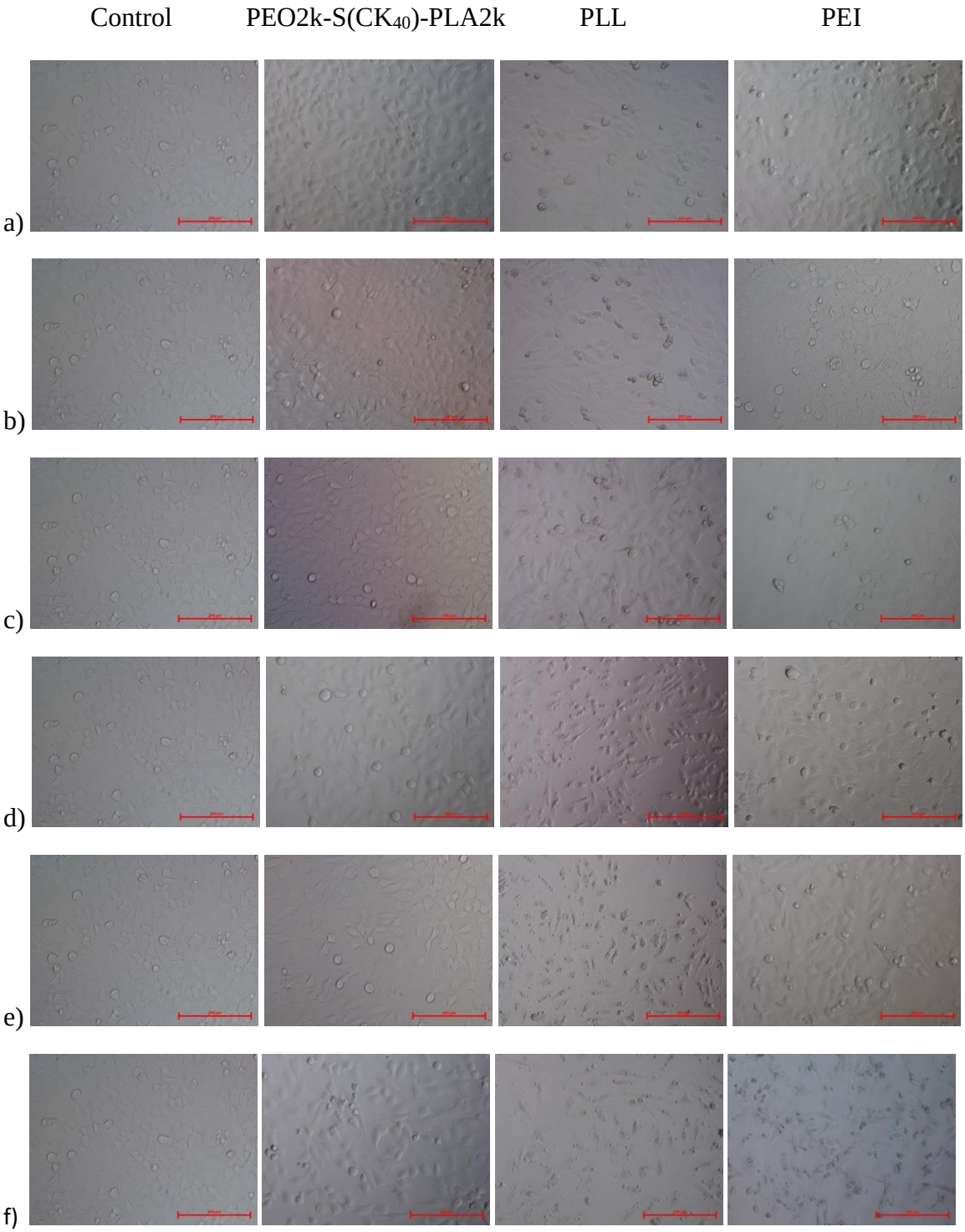

Figure 4- 11 Optical micrographs of cells from cytotoxicity tests of triblock copolymers, PLL and PEI at N/P ratio from 3, 5, 10, 30, 60 to 120 in HeLa cells (Scale bar = 200 µm). a) N/P = 3, b) N/P = 5, c) N/P = 10, d) N/P = 30, e) N/P = 60, f) N/P = 120.

References (Chapter 4)

1. Cavazzana-Calvo, M., et al., *Gene therapy of human severe combined immunodeficiency (scid)-x1 disease.* Science, 2000. **288**(5466): p. 669-672.

2. Boyd.A.C, *Gene and stem cell therapy,* in *Cystic fibrosis 21st century*. 2006, Karger: New York.

3. Kaplitt, M.G., et al., *Safety and tolerability of gene therapy with an adeno-associated virus (aav) borne gad gene for parkinson's disease: An open label, phase i trial.* Lancet, 2007. **369**(9579): p. 2097-2105.

4. Yang, Z.R., et al., *Recent developments in the use of adenoviruses and immunotoxins in cancer gene therapy.* Cancer Gene Therapy, 2007. **14**(7): p. 599-615.

5. Putnam, D., *Polymers for gene delivery across length scales.* Nature Materials, 2006. **5**(6): p. 439-451.

6. Pack, D.W., et al., *Design and development of polymers for gene delivery.* Nature Reviews Drug Discovery, 2005. **4**(7): p. 581-593.

7. Little, S.R. and D.S. Kohane, *Polymers for intracellular delivery of nucleic acids.* Journal of Materials Chemistry, 2008. **18**(8): p. 832-841.

8. Mintzer, M.A. and E.E. Simanek, *Nonviral vectors for gene delivery.* Chemical Reviews, 2009. **109**(2): p. 259-302.

9. Dash, P.R., et al., *Factors affecting blood clearance and in vivo distribution of polyelectrolyte complexes for gene delivery.* Gene Therapy, 1999. **6**(4): p. 643-650.

10. Lai, E. and J.H. van Zanten, *Monitoring DNA/poly-l-lysine polyplex formation with time-resolved multiangle laser light scattering.* Biophysical Journal, 2001. **80**(2): p. 864-873.

11. Toncheva, V., et al., *Novel vectors for gene delivery formed by self-assembly of DNA with poly(l-lysine) grafted with hydrophilic polymers.* Biochimica Et Biophysica Acta-General Subjects, 1998. **1380**(3): p. 354-368.

12. Ogris, M., et al., *Pegylated DNA/transferrin-pei complexes: Reduced interaction with blood components, extended circulation in blood and potential for systemic gene delivery.* Gene Therapy, 1999. **6**(4): p. 595-605.

13. Kim, E.M., et al., *Asialoglycoprotein receptor targeted gene delivery using galactosylated polyethylenimine-graft-poly(ethylene glycol): In vitro and in vivo studies.* Journal of Controlled Release, 2005. **108**(2-3): p. 557-567.

14. Roy, R., D.J. Jerry, and S. Thayumanavan, *Virus-inspired approach to nonviral gene delivery vehicles.* Biomacromolecules, 2009. **10**(8): p. 2189-2193.

15. Xu, J. and M. Amiji, *Therapeutic gene delivery and transfection in human pancreatic cancer cells using epidermal growth factor receptor-targeted gelatin nanoparticles.* Jove-Journal of Visualized Experiments, 2012(59): p. 10.

16. M. Molas, A.G.G.-V., A. Vidal-Alabro, M. Miguel-Turu, J. Bermudez, R. Bartrons and J. C. Perales, *Receptor-mediated gene transfer vectors: Progress towards genetic pharmaceuticals.* Current Gene Therapy, 2003. **3**(5): p. 468-485.

17. Mislick, K.A. and J.D. Baldeschwieler, *Evidence for the role of proteoglycans in cation-mediated gene transfer.* Proceedings of the National Academy of Sciences of the United States of America, 1996. **93**(22): p. 12349-12354.

18. Desai, M.P., et al., *The mechanism of uptake of biodegradable microparticles in caco-2 cells is size dependent.* Pharmaceutical Research, 1997. **14**(11): p. 1568-1573.

19. Prabha, S., et al., *Size-dependency of nanoparticle-mediated gene transfection: Studies with fractionated nanoparticles.* International Journal of Pharmaceutics, 2002. **244**(1-2): p. 105-115.

20. Xu, D.M., et al., *Size-dependent properties of m-peis nanogels for gene delivery in cancer cells.* International Journal of Pharmaceutics, 2007. **338**(1-2): p. 291-296.

21. Szoka, J.N.a.F.C., *Nucleic acid delivery: The missing pieces of the puzzle?* Accounts of chemical research, 2012. **45**(7): p. 1153-1162.

22. Boussif, O., et al., *A versatile vector for gene and oligonucleotide transfer into cells in culture and in-vivo-polyethyleimine.* Proceedings of the National Academy of Sciences of the United States of America, 1995. **92**(16): p. 7297-7301.

23. Behr, J.P., *The proton sponge: A trick to enter cells the viruses did not exploit.* Chimia, 1997. **51**(1-2): p. 34-36.

24. Haensler, J. and F.C. Szoka, *Polyamidoamine cascade polymers mediate efficient transfection of cells in culture.* Bioconjugate Chemistry, 1993. **4**(5): p. 372-379.

25. Tang, M.X., C.T. Redemann, and F.C. Szoka, *In vitro gene delivery by degraded polyamidoamine dendrimers.* Bioconjugate Chemistry, 1996. **7**(6): p. 703-714.

26. Akinc, A., et al., *Exploring polyethylenimine-mediated DNA transfection and the proton sponge hypothesis.* Journal of Gene Medicine, 2005. **7**(5): p. 657-663.

27. Mazahir T. Hasan, R.S., and T. Y. Chang, *High-efficiency stable gene transfection using chloroquine-treated chinese hamster ovary cells.* Somatic Cell and Molecular Genetics, 1991. **17**(5): p. 513-517.

28. Patrick Erbacher, A.C.R., Michel Monsigny, Patrick Midoux, *Putative role of chloroquine in gene transfer into a human hepatoma cell line by DNA/lactosylated polylysine complexes.* Experimental Cell Research, 1996. **225**(1): p. 186-194.

29. Joubert, D., et al., *A note on poly-l-lysine-mediated gene transfer in hela cells.* Drug Delivery, 2003. **10**(3): p. 209-211.

30. Ohkuma, S. and B. Poole, *Fluorescence probe measurement of intralysosomal ph in living cells and perturbation of ph by various agents.* Proceedings of the National Academy of Sciences of the United States of America, 1978. **75**(7): p. 3327-3331.

31. Ohkuma, S., J. Chudzik, and B. Poole, *The effects of basic substances and acidic ionophores on the digestion of exogenous and endogenous proteins in mouse peritoneal-macrophages.* Journal of Cell Biology, 1986. **102**(3): p. 959-966.

32. Maxfield, F.R., *Weak bases and ionophores rapidly and reversibly raise the ph of endocytic vesicles in cultured mouse fibroblasts.* Journal of Cell Biology, 1982. **95**(2): p. 676-681.

33. Strous, G.J., et al., *Effect of lysosomotropic amines on the secretory pathway and on the recycling of the asialoglycoprotein receptor in human hepatoma-cells.* Journal of Cell Biology, 1985. **101**(2): p. 531-539.

34. Hedin, U. and J. Thyberg, *Receptor-mediated endocytosis of immunoglobulin-coated colloidal gold particles in cultured mouse peritoneal-macrophages - chloroquine and monensin inhibit transfer of the ligand from endocytic vesicles to lysosomes.* European Journal of Cell Biology, 1985. **39**(1): p. 130-135.

35. Stenseth, K. and J. Thyberg, *Monensin and chloroquine inhibit transfer to lysosomes of endocytosed macromolecules in cultured mouse peritoneal-macrophages.* European Journal of Cell Biology, 1989. **49**(2): p. 326-333.

36. Wibo, M. and B. Poole, *Protein degradation in cultured-cells .2. Uptake of chloroquine by rat fibroblasts and inhibition of cellular protein degradation and cathepsin-b1*. Journal of Cell Biology, 1974. **63**(2): p. 430-440.

37. Poole, B., S. Ohkuma, and M.J. Warburton, *Accumulation of weakly basic substances in lysosomes and inhibition of intracellular protein degradation.* Acta Biologica Et Medica Germanica, 1977. **36**(11-1): p. 1777-1788.

38. Sodeik, B., M.W. Ebersold, and A. Helenius, *Microtubule-mediated transport of incoming herpes simplex virus 1 capsids to the nucleus.* Journal of Cell Biology, 1997. **136**(5): p. 1007-1021.

39. Leopold, P.L., et al., *Dynein- and microtubule-mediated translocation of adenovirus serotype 5 occurs after endosomal lysis.* Human Gene Therapy, 2000. **11**(1): p. 151-165.

40. Lechardeur, D., et al., *Metabolic instability of plasmid DNA in the cytosol: A potential barrier to gene transfer.* Gene Therapy, 1999. **6**(4): p. 482-497.

41. Babcock, H.P., C. Chen, and X.W. Zhuang, *Using single-particle tracking to study nuclear trafficking of viral genes.* Biophysical Journal, 2004. **87**(4): p. 2749-2758.

42. Lai, S.K., et al., *Privileged delivery of polymer nanoparticles to the perinuclear region of live cells via a non-clathrin, non-degradative pathway.* Biomaterials, 2007. **28**(18): p. 2876-2884.

43. Chunhua Fu , X.S., Donghua Liu , Zhijing Chen , Zaijun Lu and Na Zhang *Biodegradable tri-block copolymer poly(lactic acid)-poly(ethylene glycol)-poly(l-lysine)(pla-peg-pll) as a non-viral vector to enhance gene transfection.* Int. J. Mol. Sci., 2011. **12**(2): p. 1371-1388.

44. Guo, S.T., et al., *Amphiphilic and biodegradable methoxy polyethylene glycol-block-(polycaprolactone-graft-poly(2-(dimethylamino)ethyl methacrylate)) as an effective gene carrier.* Biomaterials, 2011. **32**(3): p. 879-889.

45. Rungsardthong, U., et al., *Effect of polymer ionization on the interaction with DNA in nonviral gene delivery systems.* Biomacromolecules, 2003. **4**(3): p. 683-690.

46. Zhuojun Dai, T.G., Maria A. Mattebjerg, Chi Wu, Thomas L. Andresen, *Elucidating the interplay between DNA-condensing and free polycations in gene transfection through a mechanistic study of linear and branched pei.* Biomaterials, 2011. **32**(33): p. 8626-8634.

47. Lv, H., et al., *Toxicity of cationic lipids and cationic polymers in gene delivery.* Journal of Controlled Release, 2006. **114**(1): p. 100-109.

Chapter 5 Concluding Remarks and Future Challenges

5.1 Concluding remarks

The work summarized in this thesis has centered on the synthesis and characterizations of stimuli-responsive amphiphilic star-shaped triblock copolymers and their biomedical applications for drug/gene delivery.

In chapter 3, redox-responsive amphiphilic star-shaped triblock copolymers PEO-S(CK_n)-PLA have been synthesized. The ring opening polymerization (ROP) of lactide using either $Sn(Oct)_2$ or DBU as a catalyst was used to synthesize PEO-S(Boc)-PLA diblock copolymers with well-controlled molecular weights and narrow molecular weight distributions. The morphologies of PEO-S(Boc)-PLA diblock copolymers in dilute aqueous solution were studied by SAXS and DLS. The radii determined through both SAXS and DLS measurements suggest that the PEO-S(Boc)-PLA diblock copolymers examined assemble into micelles in the dilute regime in aqueous solution (0.1-1 wt% polymer). The cationic oligo- or polylysine segment was synthesized by peptide synthesis or ROP of Z-lysine-N-carboxyanhydride. The cationic oligo/polylysine segments were coupled to the diblock copolymer PEO-S(NH_2)-PLA through a thiol-disulfide

exchange reaction with SPDP as the linkage agent. The extent of conjugated cationic segment CK_n was quantified by measuring UV absorption of 2-mercaptopyridine (present in crude product mixtures. PEO-S(CK_n)-PLA triblock copolymers with different block ratios were successfully synthesized. Two specific triblock copolymers, PEO5k-S(CK_3)-PLA5k and PEO2k-S(CK_{40})-PLA2k, were selected for gene delivery studies in Chapter 4.

In Chapter 4, the PEO5k-S(CK_3)-PLA5k and PEO2k-S(CK_{40})-PLA2k triblock copolymers were used to form complexes with GFP DNA plasmid. The hydrodynamic diameters of triblock copolymer PEO2k-S(CK_{40})-PLA2k and PEO2k-S(CK_{40})-PLA2k/GFP DNA complexes were measured by DLS. The triblock copolymer PEO2k-S(CK_{40})-PLA2k could condense GFP plasmids into complexes with diameters appropriate for endocytotic cellular uptake (from 130 nm to 220 nm) at different N/P ratios. The DNA condensation ability of PEO2k-S(CK_{40})-PLA2k triblock copolymers was also confirmed by agarose gel electrophoresis of PEO2k-S(CK_{40})-PLA2k/GFP DNA complexes at different N/P ratios. GFP DNA migration was completely retarded at N/P ratios above 1. The *in vitro* gene transfection of PEO5k-S(CK_3)-PLA5k/GFP DNA complexes in MT3C3 cells exhibited low activity at all the N/P ratios examined. The possible explanation was the strong shielding effect of relatively long PEO blocks with relatively short lysine oligomers.

In vitro gene transfection studies of PEO2k-S(CK_{40})-PLA2k/GFP DNA complexes in HeLa cells under different transfection conditions were carried out to study the effect of N/P ratio, medium pH, addition of chloroquine, and DNA concentration on transfection efficiency. The gene transfection results for PEO2k-S(CK_{40})-PLA2k/GFP DNA complexes were compared to the gene transfection results for PEO2k-S(CK_{30})/GFP DNA complexes and PLL_{40}/GFP DNA complexes under the same transfection conditions. In the fluorescent micrographs of transfected HeLa cells, enhanced gene transfection activites were observed for PEO2k-S(CK_{40})-PLA2k/GFP DNA

complexes comparing to PEO2k-S(CK_{30})/GFP DNA complexes and PLL_{40}/GFP DNA complexes. The enhancement of gene transfection efficiency might be explained by enhanced gene protection and transport properties of the star block copolymer. The cytotoxicity of PEO2k-S(CK_{40})-PLA2k triblock copolymers was evaluated by the MTS assay in HeLa cells at various concentrations, and compared with the corresponding polylysine PLL_{40} and branched polyethyleneimine (PEI, M_w=25000), which is a commonly used transfection platform. The low cytotoxicity of the triblock copolymer PEO2k-S(CK_{40})-PLA2k may be explained by the relatively low positive surface charge due to PEO shielding effects.

5.2 Future Challenges

Although the amphiphilic cationic star-shaped tri-arm PEO2k-S(CK_{40})-PLA2k triblock copolymer exhibited an enhanced gene transfection efficiency and low cytotoxicity comparing to corresponding polylysine PLL_{40}, it is still far away from clinical gene therapy applications because of the relatively low transfection efficiency compared with commercially available gene vectors.

The amphiphilic character and PEO shielding effect can efficiently enhance serum stability and cellular uptake of the PEO-S(CK_n)-PLA/GFP DNA complexes. After cellular uptake of PEO-S(CK_n)-PLA/GFP DNA complexes and the disulfide cleavage, the linear polylysine CK_n/GFP DNA complexes have to escape from endosomes, be transported through the cytoplasm, and enter the nucleus. Further investigations could be directed towards the enhancement of endosomal escape, cytoplasmic mobility, and nuclear internalization. Changing the structure of polylysine from linear to hyperbranched [1] would be an interesting way to attempt to help the complexes to escape from endosomes and lysosomes because of the hydrogen sponge effect and the umbrella

effect. To enhance cytoplasmic mobility, further studies could either introduce ligands to the polylysine segment with high affinity for motor proteins such as dynein [2, 3] to mediate active transport along MTs or to reduce the size of polylysine/GFP DNA complexes so they are small enough (diameter < 30 nm) to efficiently migrate in the cytoplasm by passive diffusion[4, 5].

References (Chapter 5)

1. Zuzana Kadlecova, Y.R., Mattia Matasci, David Hacker, Lucia Baldi, Florian Maria Wurm, Harm-Anton Klok, *Hyperbranched polylysine: A versatile, biodegradable transfection agent for the production of recombinant proteins by transient gene expression and the transfection of primary cells.* Macromolecular Bioscience, 2012. **12**(6): p. 749-804.

2. Sodeik, B., M.W. Ebersold, and A. Helenius, *Microtubule-mediated transport of incoming herpes simplex virus 1 capsids to the nucleus.* Journal of Cell Biology, 1997. **136**(5): p. 1007-1021.

3. Leopold, P.L., et al., *Dynein- and microtubule-mediated translocation of adenovirus serotype 5 occurs after endosomal lysis.* Human Gene Therapy, 2000. **11**(1): p. 151-165.

4. Babcock, H.P., C. Chen, and X.W. Zhuang, *Using single-particle tracking to study nuclear trafficking of viral genes.* Biophysical Journal, 2004. **87**(4): p. 2749-2758.

5. Lai, S.K., et al., *Privileged delivery of polymer nanoparticles to the perinuclear region of live cells via a non-clathrin, non-degradative pathway.* Biomaterials, 2007. **28**(18): p. 2876-2884.

References

Akinc, A., M. Thomas, A. M. Klibanov and R. Langer (2005). "Exploring Polyethylenimine-Mediated DNA Transfection and the Proton Sponge Hypothesis." Journal of Gene Medicine **7**(5): 657-663.

Andrew P. Dove , R. C. P., Bas G. G. Lohmeijer ,Robert M. Waymouth and James L. Hedrick (2005). "Thiourea-Based Bifunctional Organocatalysis: Supramolecular Recognition for Living Polymerization." J. Am. Chem. Soc **127**(40): 13798-13799.

Arote, R., T.-H. Kim, Y.-K. Kim, S.-K. Hwang, H.-L. Jiang, H.-H. Song, J.-W. Nah, M.-H. Cho and C.-S. Cho (2007). "A Biodegradable Poly(Ester Amine) Based on Polycaprolactone and Polyethylenimine as a Gene Carrier." Biomaterials **28**(4): 735-744.

Babcock, H. P., C. Chen and X. W. Zhuang (2004). "Using Single-Particle Tracking to Study Nuclear Trafficking of Viral Genes." Biophysical Journal **87**(4): 2749-2758.

Bangham, A. D., M. M. Standish and J. C. Watkins (1965). "Diffusion of Univalent Ions across the Lamellae of Swollen Phospholipids." Journal of Molecular Biology **13**(1): 238-IN227.

Bas G. G. Lohmeijer , R. C. P., Frank Leibfarth , John W. Logan, David A. Long , Andrew P. Dove , Fredrik Nederberg , Jeongsoo Choi Charles Wade ,Robert M. Waymouth and James L. Hedrick (2006). "Guanidine and Amidine Organocatalysts for Ring-Opening Polymerization of Cyclic Esters." Macromolecules **39**(25): 8574-8583.

Behr, J. P. (1997). "The Proton Sponge: A Trick to Enter Cells the Viruses Did Not Exploit." Chimia **51**(1-2): 34-36.

Berridge, M. V. and A. S. Tan (1993). "Characterization of the Cellular Reduction of 3-(4,5-Dimethylthiazol-2-Yl)-2,5-Diphenyltetrazolium Bromide (Mtt) - Subcellular-Localization, Substrate Dependence, and Involvement of Mitochondrial Electron-Transport in Mtt Reduction." Archives of Biochemistry and Biophysics **303**(2): 474-482.

Blanazs, A., S. P. Armes and A. J. Ryan (2009). "Self-Assembled Block Copolymer Aggregates: From Micelles to Vesicles and Their Biological Applications." Macromolecular Rapid Communications **30**(4-5): 267-277.

Bodanszky, M. (1993). Principles of Peptide Synthesis, 2nd, Springer-Verlag Berlin Heidelberg

Boussif, O., F. Lezoualch, M. A. Zanta, M. D. Mergny, D. Scherman, B. Demeneix and J. P. Behr (1995). "A Versatile Vector for Gene and Oligonucleotide Transfer into Cells in Culture and in-Vivo-Polyethyleimine." Proceedings of the National Academy of Sciences of the United States of America **92**(16): 7297-7301.

Boyd.A.C (2006). Gene and Stem Cell Therapy. Cystic Fibrosis 21st Century. New York, Karger.

Bruce J. Berne, R. P. (2000). "Dynamic Light Scattering: With Applications to Chemistry, Biology and Physics." Courier Dover Publicatios (2000).

Bruchez, M., M. Moronne, P. Gin, S. Weiss and A. P. Alivisatos (1998). "Semiconductor Nanocrystals as Fluorescent Biological Labels." Science **281**(5385): 2013-2016.

Cavallaro, G., M. Campisi, M. Licciardi, M. Ogris and G. Giammona (2006). "Reversibly Stable Thiopolyplexes for Intracellular Delivery of Genes." Journal of Controlled Release **115**(3): 322-334.

Cavazzana-Calvo, M., S. Hacein-Bey, C. D. Basile, F. Gross, E. Yvon, P. Nusbaum, F. Selz, C. Hue, S. Certain, J. L. Casanova, P. Bousso, F. Le Deist and A. Fischer (2000). "Gene Therapy of Human Severe Combined Immunodeficiency (Scid)-X1 Disease." Science **288**(5466): 669-672.

Cerritelli, S., D. Velluto and J. A. Hubbell (2007). "Peg-Ss-Pps: Reduction-Sensitive Disulfide Block Copolymer Vesicles for Intracellular Drug Delivery." Biomacromolecules **8**(6): 1966-1972.

Chacko, R. T., J. Ventura, J. Zhuang and S. Thayumanavan (2012). "Polymer Nanogels: A Versatile Nanoscopic Drug Delivery Platform." Advanced Drug Delivery Reviews **64**(9): 836-851.

Chan, W. C. W. and S. M. Nie (1998). "Quantum Dot Bioconjugates for Ultrasensitive Nonisotopic Detection." Science **281**(5385): 2016-2018.

Chen, S.-H. and T.-L. Lin (1987). 16. Colloidal Solutions. Methods in Experimental Physics. L. P. David and S. Kurt, Academic Press. **Volume 23, Part B:** 489-543.

Chu, B. (1997). "Laser Light Scattering of Polymer Solutions." Applied Optics **36**(30): 7650-7656.

Chu, B. (2008). "Dynamic Light Scattering." Soft Matter Characterization: 335-372.

Chunhua Fu , X. S., Donghua Liu , Zhijing Chen , Zaijun Lu and Na Zhang (2011). "Biodegradable Tri-Block Copolymer Poly(Lactic Acid)-Poly(Ethylene Glycol)-Poly(L-Lysine)(Pla-Peg-Pll) as a Non-Viral Vector to Enhance Gene Transfection." Int. J. Mol. Sci. **12**(2): 1371-1388.

Committee on Technology, N. S. a. T. C. (2000). National Nanotechnology Initiative: Leading to the Next Industrial Revolution.

Cory, A. H., T. C. Owen, J. A. Barltrop and J. G. Cory (1991). "Use of an Aqueous Soluble Tetrazolium Formazan Assay for Cell-Growth Assays in Culture." Cancer Communications **3**(7): 207-212.

Cui, Y., Q. Q. Wei, H. K. Park and C. M. Lieber (2001). "Nanowire Nanosensors for Highly Sensitive and Selective Detection of Biological and Chemical Species." Science **293**(5533): 1289-1292.

Dang, J. M. and K. W. Leong (2006). "Natural Polymers for Gene Delivery and Tissue Engineering." Advanced Drug Delivery Reviews **58**(4): 487-499.

Dash, P. R., M. L. Read, L. B. Barrett, M. Wolfert and L. W. Seymour (1999). "Factors Affecting Blood Clearance and in Vivo Distribution of Polyelectrolyte Complexes for Gene Delivery." Gene Therapy **6**(4): 643-650.

Davey, H. M. and D. B. Kell (1996). "Flow Cytometry and Cell Sorting of Heterogeneous Microbial Populations: The Importance of Single-Cell Analyses." Microbiological Reviews **60**(4): 641-&.

Davis, M. E., J. E. Zuckerman, C. H. J. Choi, D. Seligson, A. Tolcher, C. A. Alabi, Y. Yen, J. D. Heidel and A. Ribas (2010). "Evidence of Rnai in Humans from Systemically Administered Sirna Via Targeted Nanoparticles." Nature **464**(7291): 1067-U1140.

Desai, M. P., V. Labhasetwar, E. Walter, R. J. Levy and G. L. Amidon (1997). "The Mechanism of Uptake of Biodegradable Microparticles in Caco-2 Cells Is Size Dependent." Pharmaceutical Research **14**(11): 1568-1573.

Discher, D. E. and A. Eisenberg (2002). "Polymer Vesicles." Science **297**(5583): 967-973.

Doan, H., G. M. Chinn and R. R. Jahan-Tigh (2015). "Flow Cytometry Ii: Mass and Imaging Cytometry." Journal of Investigative Dermatology **135**(9): 1-4.

Doane, T. L. and C. Burda (2012). "The Unique Role of Nanoparticles in Nanomedicine: Imaging, Drug Delivery and Therapy." Chemical Society Reviews **41**(7): 2885-2911.

Du, J. Z., Y. Q. Tang, A. L. Lewis and S. P. Armes (2005). "Ph-Sensitive Vesicles Based on a Biocompatible Zwitterionic Diblock Copolymer." Journal of the American Chemical Society **127**(51): 17982-17983.

Farokhzad, O. C. and R. Langer (2006). "Nanomedicine: Developing Smarter Therapeutic and Diagnostic Modalities." Advanced Drug Delivery Reviews **58**(14): 1456-1459.

Feng, A. C. and J. Y. Yuan (2014). "Smart Nanocontainers: Progress on Novel Stimuli-Responsive Polymer Vesicles." Macromolecular Rapid Communications **35**(8): 767-779.

Ferrari, M. (2005). "Cancer Nanotechnology: Opportunities and Challenges." Nat Rev Cancer **5**(3): 161-171.

Fischer, D., Y. X. Li, B. Ahlemeyer, J. Krieglstein and T. Kissel (2003). "In Vitro Cytotoxicity Testing of Polycations: Influence of Polymer Structure on Cell Viability and Hemolysis." Biomaterials **24**(7): 1121-1131.

Fleige, E., M. A. Quadir and R. Haag (2012). "Stimuli-Responsive Polymeric Nanocarriers for the Controlled Transport of Active Compounds: Concepts and Applications." Advanced Drug Delivery Reviews **64**(9): 866-884.

Forster, S. and M. Antonietti (1998). "Amphiphilic Block Copolymers in Structure-Controlled Nanomaterial Hybrids." Advanced Materials **10**(3): 195-+.

Gansbacher, B. and E. European Society Gene Therapy (2003). "Report of a Second Serious Adverse Event in a Clinical Trial of Gene Therapy for X-Linked Severe Combined Immune Deficiency (X-Scid) - Position of the European Society of Gene Therapy (Esgt)." Journal of Gene Medicine **5**(3): 261-262.

Godbey, W. T., K. K. Wu and A. G. Mikos (1999). "Size Matters: Molecular Weight Affects the Efficiency of Poly(Ethylenimine) as a Gene Delivery Vehicle." Journal of Biomedical Materials Research **45**(3): 268-275.

Gombotz, W. R. and D. K. Pettit (1995). "Biodegradable Polymers for Protein and Peptide Drug-Delivery." Bioconjugate Chemistry **6**(4): 332-351.

Gref, R., Y. Minamitake, M. T. Peracchia, V. Trubetskoy, V. Torchilin and R. Langer (1994). "Biodegradable Long-Circulating Polymeric Nanospheres." Science **263**(5153): 1600-1603.

Guo, S. T., Y. Y. Huang, T. Wei, W. D. Zhang, W. W. Wang, D. Lin, X. Zhang, A. Kumar, Q. A. Du, J. F. Xing, L. D. Deng, Z. C. Liang, P. C. Wang, A. J. Dong and X. J. Liang (2011). "Amphiphilic and Biodegradable Methoxy Polyethylene Glycol-Block-(Polycaprolactone-Graft-Poly(2-(Dimethylamino)Ethyl Methacrylate)) as an Effective Gene Carrier." Biomaterials **32**(3): 879-889.

H. Maeda, Y. M. (1989). "Tumouritropic and Lymphotropic Principles of Macromolecular Drugs." Crit. Rev. Ther. Drug Carrier Syst **6**: 193-210.

Haensler, J. and F. C. Szoka (1993). "Polyamidoamine Cascade Polymers Mediate Efficient Transfection of Cells in Culture." Bioconjugate Chemistry **4**(5): 372-379.

Hayashi, H., M. Iijima, K. Kataoka and Y. Nagasaki (2004). "Ph-Sensitive Nanogel Possessing Reactive Peg Tethered Chains on the Surface." Macromolecules **37**(14): 5389-5396.

Hedin, U. and J. Thyberg (1985). "Receptor-Mediated Endocytosis of Immunoglobulin-Coated Colloidal Gold Particles in Cultured Mouse Peritoneal-Macrophages - Chloroquine and Monensin Inhibit Transfer of the Ligand from Endocytic Vesicles to Lysosomes." European Journal of Cell Biology **39**(1): 130-135.

Heidel, J. D., Z. P. Yu, J. Y. C. Liu, S. M. Rele, Y. C. Liang, R. K. Zeidan, D. J. Kornbrust and M. E. Davis (2007). "Administration in Non-Human Primates of Escalating Intravenous Doses of Targeted Nanoparticles Containing Ribonucleotide Reductase Subunit M2 Sirna." Proceedings of the National Academy of Sciences of the United States of America **104**(14): 5715-5721.

Israelachvili, J. and H. Wennerstr öm (1996). "Role of Hydration and Water Structure in Biological and Colloidal Interactions."

Jan Carlsson, H. D. a. R. A. (1978). "Protein Thiolation and Reversible Protein-Protein Conjugation. N-Succinimidyl 3-(2-Pyridyldithio)Propionate, a New Heterobifunctional Reagent." Biochem J. **173**(3): 723-737.

Jeng, U., T. L. Lin, Y. Hu and T. S. Chang (2002). "Study on Aqueous Mixtures of Fullerene-Based Star Lonomers and Sodium Dodecyl Sulfate Using Small Angle Scattering with Contrast Variation." Journal of Physical Chemistry A **106**(51): 12209-12213.

Jeng, U. S., T. L. Lin, C. S. Tsao, C. H. Lee, T. Canteenwala, L. Y. Wang, L. Y. Chiang and C. C. Han (1999). "Study of Aggregates of Fullerene-Based Ionomers in Aqueous Solutions Using Small Angle Neutron and X-Ray Scattering." Journal of Physical Chemistry B **103**(7): 1059-1063.

Jennings, C. D. and K. A. Foon (1997). "Recent Advances in Flow Cytometry: Application to the Diagnosis of Hematologic Malignancy." Blood **90**(8): 2863-2892.

Jeon, S. I., J. H. Lee, J. D. Andrade and P. G. Degennes (1991). "Protein Surface Interactions in the Presence of Polyethylene Oxide .1. Simplified Theory." Journal of Colloid and Interface Science **142**(1): 149-158.

Jiehua Zhou, J. W., Nadia Hafdi, Jean-Paul Behr, Patrick Erbacher and Ling Peng (2006). "Pamam Dendrimers for Efficient Sirna Delivery and Potent Gene Silencing." Chemical Communications(22): 2362-2364.

Joubert, D., J. van Zyl, A. Hawtrey and M. Ariatti (2003). "A Note on Poly-L-Lysine-Mediated Gene Transfer in Hela Cells." Drug Delivery **10**(3): 209-211.

Kaplitt, M. G., A. Feigin, C. Tang, H. L. Fitzsimons, P. Mattis, P. A. Lawlor, R. J. Bland, D. Young, K. Strybing, D. Eidelberg and M. J. During (2007). "Safety and Tolerability of Gene Therapy with an Adeno-Associated Virus (Aav) Borne Gad Gene for Parkinson's Disease: An Open Label, Phase I Trial." Lancet **369**(9579): 2097-2105.

Karen A. Murphy, J. M. E., Daniel A. Savin (2008). "Synthesis, Self-Assembly and Adsorption of Peo-Pla Block Copolymers onto Colloidal Polystyrene." Journal of Polymer Science Part B: Polymer Physics **46**(3): 244-252.

Kihoon Nam, H. Y. N., Pyung-Hwan Kim, Sung Wan Kim (2012). "Paclitaxel-Conjugated Peg and Arginine-Grafted Bioreducible Poly (Disulfide Amine) Micelles for Co-Delivery of Drug and Gene." Biomaterials **33**(32): 8122-8130.

Kikhney, A. G. and D. I. Svergun (2015). "A Practical Guide to Small Angle X-Ray Scattering (Saxs) of Flexible and Intrinsically Disordered Proteins." Febs Letters **589**(19): 2570-2577.

Kim, B. Y. S., J. T. Rutka and W. C. W. Chan (2010). "Current Concepts: Nanomedicine." New England Journal of Medicine **363**(25): 2434-2443.

Kim, E. M., H. J. Jeong, I. K. Park, C. S. Cho, H. B. Moon, D. Y. Yu, H. S. Bom, M. H. Sohn and I. J. Oh (2005). "Asialoglycoprotein Receptor Targeted Gene Delivery Using Galactosylated

Polyethylenimine-Graft-Poly(Ethylene Glycol): In Vitro and in Vivo Studies." Journal of Controlled Release **108**(2-3): 557-567.

Kowalski, A., A. Duda and S. Penczek (1998). "Kinetics and Mechanism of Cyclic Esters Polymerization Initiated with Tin(Ii) Octoate, 1 Polymerization of Epsilon-Caprolactone." Macromolecular Rapid Communications **19**(11): 567-572.

Kricheldorf, H. R., I. Kreiser-Saunders and A. Stricker (2000). "Polylactones 48. Snoct(2)-Initiated Polymerizations of Lactide: A Mechanistic Study." Macromolecules **33**(3): 702-709.

Kricheldorf, H. R., I. Kreisersaunders and C. Boettcher (1995). "Polylactones .31. Sn(Ii)Octoate-Initiated Polymerization of L-Lactide - a Mechanistic Study." Polymer **36**(6): 1253-1259.

Kumar, J. P. J. a. N. (2010). "Self Assembly of Amphiphilic (Peg)3-Pla Copolymer as Polymersomes: Preparation, Characterization, and Their Evaluation as Drug Carrier." Biomacromolecules **11**(4): 1027-1035.

Lai, E. and J. H. van Zanten (2001). "Monitoring DNA/Poly-L-Lysine Polyplex Formation with Time-Resolved Multiangle Laser Light Scattering." Biophysical Journal **80**(2): 864-873.

Lai, S. K., K. Hida, S. T. Man, C. Chen, C. Machamer, T. A. Schroer and J. Hanes (2007). "Privileged Delivery of Polymer Nanoparticles to the Perinuclear Region of Live Cells Via a Non-Clathrin, Non-Degradative Pathway." Biomaterials **28**(18): 2876-2884.

Langer, R. and J. Folkman (1976). "Polymers for the Sustained Release of Proteins and Other Macromolecules." Nature **263**(5580): 797-800.

Lechardeur, D., K. J. Sohn, M. Haardt, P. B. Joshi, M. Monck, R. W. Graham, B. Beatty, J. Squire, H. O'Brodovich and G. L. Lukacs (1999). "Metabolic Instability of Plasmid DNA in the Cytosol: A Potential Barrier to Gene Transfer." Gene Therapy **6**(4): 482-497.

Lee, E. S., H. J. Shin, K. Na and Y. H. Bae (2003). "Poly(L-Histidine)-Peg Block Copolymer Micelles and Ph-Induced Destabilization." Journal of Controlled Release **90**(3): 363-374.

Leopold, P. L., G. Kreitzer, N. Miyazawa, S. Rempel, K. K. Pfister, E. Rodriguez-Boulan and R. G. Crystal (2000). "Dynein- and Microtubule-Mediated Translocation of Adenovirus Serotype 5 Occurs after Endosomal Lysis." Human Gene Therapy **11**(1): 151-165.

Li, X., Z. Yang, K. Yang, Y. Zhou, X. Chen, Y. Zhang, F. Wang, Y. Liu and L. Ren (2009). "Self-Assembled Polymeric Micellar Nanoparticles as Nanocarriers for Poorly Soluble Anticancer Drug Ethaselen." Nanoscale Research Letters **4**(12): 1502-1511.

Liang, D. H., Y. K. Luu, K. S. Kim, B. S. Hsiao, M. Hadjiargyrou and B. Chu (2005). "In Vitro Non-Viral Gene Delivery with Nanofibrous Scaffolds." Nucleic Acids Research **33**(19): 8.

Little, S. R. and D. S. Kohane (2008). "Polymers for Intracellular Delivery of Nucleic Acids." Journal of Materials Chemistry **18**(8): 832-841.

Liu, F. T. and A. Eisenberg (2003). "Preparation and Ph Triggered Inversion of Vesicles from Poly(Acrylic Acid)-Block-Polystyrene-Block-Poly(4-Vinyl Pyridine)." Journal of the American Chemical Society **125**(49): 15059-15064.

Lomas, H., I. Canton, S. MacNeil, J. Du, S. P. Armes, A. J. Ryan, A. L. Lewis and G. Battaglia (2007). "Biomimetic Ph Sensitive Polymersomes for Efficient DNA Encapsulation and Delivery." Advanced Materials **19**(23): 4238-+.

Luo, D. and W. M. Saltzman (2000). "Synthetic DNA Delivery Systems." Nature Biotechnology **18**(1): 33-37.

Luten, J., C. F. van Nostruin, S. C. De Smedt and W. E. Hennink (2008). "Biodegradable Polymers as Non-Viral Carriers for Plasmid DNA Delivery." Journal of Controlled Release **126**(2): 97-110.

Lv, H., S. Zhang, B. Wang, S. Cui and J. Yan (2006). "Toxicity of Cationic Lipids and Cationic Polymers in Gene Delivery." Journal of Controlled Release **114**(1): 100-109.

M. Bodanszky, A. B. (1994). The Practice of Peptide Synthesis, 2nd, Springer-Verlag Berlin Heidelberg.

M. Molas, A. G. G.-V., A. Vidal-Alabro, M. Miguel-Turu, J. Bermudez, R. Bartrons and J. C. Perales (2003). "Receptor-Mediated Gene Transfer Vectors: Progress Towards Genetic Pharmaceuticals." Current Gene Therapy **3**(5): 468-485.

Marco Frediani, D. S., Alfredo Mariotti, Luca Rosi , Piero Frediani, Laura Rosi, Dominique Matt, Lo ̈c Toupet (2008). "Ring Opening Polymerization of Lactide under Solvent-Free Conditions Catalyzed by a Chlorotitanium Calix[4]Arene Complex." Macromolecular Rapid Communications **29**(18): 1554-1560.

Marshall, N. J., C. J. Goodwin and S. J. Holt (1995). "A Critical-Assessment of the Use of Microculture Tetrazolium Assays to Measure Cell-Growth and Function." Growth Regulation **5**(2): 69-84.

Martin, H., H. Kinns, N. Mitchell, Y. Astier, R. Madathil and S. Howorka (2007). "Nanoscale Protein Pores Modified with Pamam Dendrimers." Journal of the American Chemical Society **129**(31): 9640-9649.

Matthew K. Kiesewetter , M. D. S., Nicole Kirn, Ryan L. Weber, James L. Hedrick and Robert M. Waymouth (2009). "Cyclic Guanidine Organic Catalysts: What Is Magic About Triazabicyclodecene?" J. Org. Chem. **74**(24): 9490-9496.

Maxfield, F. R. (1982). "Weak Bases and Ionophores Rapidly and Reversibly Raise the Ph of Endocytic Vesicles in Cultured Mouse Fibroblasts." Journal of Cell Biology **95**(2): 676-681.

Mazahir T. Hasan, R. S., and T. Y. Chang (1991). "High-Efficiency Stable Gene Transfection Using Chloroquine-Treated Chinese Hamster Ovary Cells." Somatic Cell and Molecular Genetics **17**(5): 513-517.

Mintzer, M. A. and E. E. Simanek (2009). "Nonviral Vectors for Gene Delivery." Chemical Reviews **109**(2): 259-302.

Mishra, S., L. Y. Peddada, D. I. Devore and C. M. Roth (2012). "Poly(Alkylene Oxide) Copolymers for Nucleic Acid Delivery." Accounts of Chemical Research **45**(7): 1057-1066.

Mislick, K. A. and J. D. Baldeschwieler (1996). "Evidence for the Role of Proteoglycans in Cation-Mediated Gene Transfer." Proceedings of the National Academy of Sciences of the United States of America **93**(22): 12349-12354.

Morgan, D. M., V. L. Larvin and J. D. Pearson (1989). "Biochemical Characterisation of Polycation-Induced Cytotoxicity to Human Vascular Endothelial Cells." Journal of Cell Science **94**(3): 553-559.

Mosmann, T. (1983). "Rapid Colorimetric Assay for Cellular Growth and Survival - Application to Proliferation and Cyto-Toxicity Assays." Journal of Immunological Methods **65**(1-2): 55-63.

Mukherjee, S., R. N. Ghosh and F. R. Maxfield (1997). "Endocytosis." Physiological Reviews **77**(3): 759-803.

Natarajan Srinivasan, A. Y.-G., A. Ganesan (2005). "Rapid Deprotection of N-Boc Amines by Tfa Combined with Freebase Generation Using Basic Ion-Exchange Resins." Molecular Diversity **9**(4): 291-293.

Navath, R. S., Y. E. Kurtoglu, B. Wang, S. Kannan, R. Romero and R. M. Kannan (2008). "Dendrimer-Drug Conjugates for Tailored Intracellular Drug Release Based on Glutathione Levels." Bioconjugate Chemistry **19**(12): 2446-2455.

Neu, M., D. Fischer and T. Kissel (2005). "Recent Advances in Rational Gene Transfer Vector Design Based on Poly(Ethylene Imine) and Its Derivatives." Journal of Gene Medicine **7**(8): 992-1009.

Ogris, M., S. Brunner, S. Schuller, R. Kircheis and E. Wagner (1999). "Pegylated DNA/Transferrin-Pei Complexes: Reduced Interaction with Blood Components, Extended Circulation in Blood and Potential for Systemic Gene Delivery." Gene Therapy **6**(4): 595-605.

Ohkuma, S., J. Chudzik and B. Poole (1986). "The Effects of Basic Substances and Acidic Ionophores on the Digestion of Exogenous and Endogenous Proteins in Mouse Peritoneal-Macrophages." Journal of Cell Biology **102**(3): 959-966.

Ohkuma, S. and B. Poole (1978). "Fluorescence Probe Measurement of Intralysosomal Ph in Living Cells and Perturbation of Ph by Various Agents." Proceedings of the National Academy of Sciences of the United States of America **75**(7): 3327-3331.

Ohtsuka, N., T. Konno, Y. Miyauchi and H. Maeda (1987). "Anticancer Effects of Arterial Administration of the Anticancer Agent Smancs with Lipiodol on Metastatic Lymph-Nodes." Cancer **59**(9): 1560-1565.

Onaca, O., R. Enea, D. W. Hughes and W. Meier (2009). "Stimuli-Responsive Polymersomes as Nanocarriers for Drug and Gene Delivery." Macromolecular Bioscience **9**(2): 129-139.

Otto, K. R. W. a. S. (2005). "Reversible Covalent Chemistry in Drug Delivery." Current Drug Discovery Technologies **2**(3): 123-160.

Ozcan, Y., S. Ide, U. Jeng, V. Butun, Y. Lai and C. Su (2013). "Micellization Behavior of Tertiary Amine-Methacrylate-Based Block Copolymers Characterized by Small-Angle X-Ray Scattering and Dynamic Light Scattering." Materials Chemistry and Physics **138**(2-3): 559-564.

Pack, D. W., A. S. Hoffman, S. Pun and P. S. Stayton (2005). "Design and Development of Polymers for Gene Delivery." Nature Reviews Drug Discovery **4**(7): 581-593.

Patrick Erbacher, A. C. R., Michel Monsigny, Patrick Midoux (1996). "Putative Role of Chloroquine in Gene Transfer into a Human Hepatoma Cell Line by DNA/Lactosylated Polylysine Complexes." Experimental Cell Research **225**(1): 186-194.

Pecora, R. (2000). "Dynamic Light Scattering Measurement of Nanometer Particles in Liquids." Journal of Nanoparticle Research **2**(2): 123-131.

Pedersen, J. S., C. Svaneborg, K. Almdal, I. W. Hamley and R. N. Young (2003). "A Small-Angle Neutron and X-Ray Contrast Variation Scattering Study of the Structure of Block Copolymer Micelles: Corona Shape and Excluded Volume Interactions." Macromolecules **36**(2): 416-433.

Pedreira, C. E., E. S. Costa, Q. Lecrevisse, J. J. M. van Dongen, A. Orfao and C. EuroFlow (2013). "Overview of Clinical Flow Cytometry Data Analysis: Recent Advances and Future Challenges." Trends in Biotechnology **31**(7): 415-425.

Poole, B., S. Ohkuma and M. J. Warburton (1977). "Accumulation of Weakly Basic Substances in Lysosomes and Inhibition of Intracellular Protein Degradation." Acta Biologica Et Medica Germanica **36**(11-1): 1777-1788.

Pople, J. A., I. W. Hamley, J. P. A. Fairclough, A. J. Ryan, B. U. Komanschek, A. J. Gleeson, G. E. Yu and C. Booth (1997). "Ordered Phases in Aqueous Solutions of Diblock Oxyethylene/Oxybutylene Copolymers Investigated by Simultaneous Small-Angle X-Ray Scattering and Rheology." Macromolecules **30**(19): 5721-5728.

Prabha, S., W. Z. Zhou, J. Panyam and V. Labhasetwar (2002). "Size-Dependency of Nanoparticle-Mediated Gene Transfection: Studies with Fractionated Nanoparticles." International Journal of Pharmaceutics **244**(1-2): 105-115.

Provencher, S. W. (1982). "Contin: A General Purpose Constrained Regularization Program for Inverting Noisy Linear Algebraic and Integral Equations." Computer Physics Communications **27**: 229-242.

Putnam, D. (2006). "Polymers for Gene Delivery across Length Scales." Nature Materials **5**(6): 439-451.

Qin, S. H., Y. Geng, D. E. Discher and S. Yang (2006). "Temperature-Controlled Assembly and Release from Polymer Vesicles of Poly(Ethylene Oxide)-Block-Poly(N-Isopropylacrylamide)." Advanced Materials **18**(21): 2905-+.

Rejman, J., V. Oberle, I. S. Zuhorn and D. Hoekstra (2004). "Size-Dependent Internalization of Particles Via the Pathways of Clathrin-and Caveolae-Mediated Endocytosis." Biochemical Journal **377**: 159-169.

Riess, G. (2003). "Micellization of Block Copolymers." Progress in Polymer Science **28**(7): 1107-1170.

Rosler, A., G. W. M. Vandermeulen and H. A. Klok (2012). "Advanced Drug Delivery Devices Via Self-Assembly of Amphiphilic Block Copolymers." Advanced Drug Delivery Reviews **64**: 270-279.

Roy, R., D. J. Jerry and S. Thayumanavan (2009). "Virus-Inspired Approach to Nonviral Gene Delivery Vehicles." Biomacromolecules **10**(8): 2189-2193.

Rungsardthong, U., T. Ehtezazi, L. Bailey, S. P. Armes, M. C. Garnett and S. Stolnik (2003). "Effect of Polymer Ionization on the Interaction with DNA in Nonviral Gene Delivery Systems." Biomacromolecules **4**(3): 683-690.

Saito, G., J. A. Swanson and K. D. Lee (2003). "Drug Delivery Strategy Utilizing Conjugation Via Reversible Disulfide Linkages: Role and Site of Cellular Reducing Activities." Advanced Drug Delivery Reviews **55**(2): 199-215.

Sajiki, H. (1995). "Selective-Inhibition of Benzyl Ether Hydrogenolysis with Pd/C Due to the Presence of Ammonia, Pyridine or Ammonium Acetate." Tetrahedron Letters **36**(20): 3465-3468.

Schmaljohann, D. (2006). "Thermo- and Ph-Responsive Polymers in Drug Delivery." Advanced Drug Delivery Reviews **58**(15): 1655-1670.

Serwer, P. (1983). "Agarose Gels - Properties and Use for Electrophoresis." Electrophoresis **4**(6): 375-382.

Sethuraman, V. A. and Y. H. Bae (2007). "Tat Peptide-Based Micelle System for Potential Active Targeting of Anti-Cancer Agents to Acidic Solid Tumors." Journal of Controlled Release **118**(2): 216-224.

Sinden, R. R. (1994). DNA Structure and Function, Gulf Professional Publishing.

Sodeik, B., M. W. Ebersold and A. Helenius (1997). "Microtubule-Mediated Transport of Incoming Herpes Simplex Virus 1 Capsids to the Nucleus." Journal of Cell Biology **136**(5): 1007-1021.

Stenseth, K. and J. Thyberg (1989). "Monensin and Chloroquine Inhibit Transfer to Lysosomes of Endocytosed Macromolecules in Cultured Mouse Peritoneal-Macrophages." European Journal of Cell Biology **49**(2): 326-333.

Strous, G. J., A. Dumaine, J. E. Zijderhandbleekemolen, J. W. Slot and A. L. Schwartz (1985). "Effect of Lysosomotropic Amines on the Secretory Pathway and on the Recycling of the Asialoglycoprotein Receptor in Human Hepatoma-Cells." Journal of Cell Biology **101**(2): 531-539.

Sun, P. J., D. H. Zhou and Z. H. Gan (2011). "Novel Reduction-Sensitive Micelles for Triggered Intracellular Drug Release." Journal of Controlled Release **155**(1): 96-103.

Svergun, D. I. and M. H. J. Koch (2003). "Small-Angle Scattering Studies of Biological Macromolecules in Solution." Reports on Progress in Physics **66**(10): 1735-1782.

Szoka, J. N. a. F. C. (2012). "Nucleic Acid Delivery: The Missing Pieces of the Puzzle?" Accounts of chemical research **45**(7): 1153-1162.

Takae, S., K. Miyata, M. Oba, T. Ishii, N. Nishiyama, K. Itaka, Y. Yamasaki, H. Koyama and K. Kataoka (2008). "Peg-Detachable Polyplex Micelles Based on Disulfide-Linked Block Catiomers as Bioresponsive Nonviral Gene Vectors." Journal of the American Chemical Society **130**(18): 6001-6009.

Tang, M. X., C. T. Redemann and F. C. Szoka (1996). "In Vitro Gene Delivery by Degraded Polyamidoamine Dendrimers." Bioconjugate Chemistry **7**(6): 703-714.

Terry L Riss, R. A. M., Andrew L Niles, Helene A Benink, Tracy J Worzella, and Lisa Minor (2013). Cell Viability Assays. Assay Guidance Manual. C. N. Sittampalam GS, Nelson H, et al.

Toncheva, V., M. A. Wolfert, P. R. Dash, D. Oupicky, K. Ulbrich, L. W. Seymour and E. H. Schacht (1998). "Novel Vectors for Gene Delivery Formed by Self-Assembly of DNA with Poly(L-Lysine) Grafted with Hydrophilic Polymers." Biochimica Et Biophysica Acta-General Subjects **1380**(3): 354-368.

Ulbrich, K., T. Etrych, P. Chytil, M. Jelinkova and B. Rihova (2004). "Antibody-Targeted Polymer-Doxorubicin Conjugates with Ph-Controlled Activation." Journal of Drug Targeting **12**(8): 477-489.

Vaupel, P., F. Kallinowski and P. Okunieff (1989). "Blood-Flow, Oxygen and Nutrient Supply, and Metabolic Microenvironment of Human-Tumors - a Review." Cancer Research **49**(23): 6449-6465.

Viovy, J. L. (2000). "Electrophoresis of DNA and Other Polyelectrolytes: Physical Mechanisms." Reviews of Modern Physics **72**(3): 813-872.

Vommina V. Sureshbabu , R. V., Shankar A. Naik ,N. Narendra (2008). "Synthesis of Ureido-Linked Glycosylated Amino Acids from N A-Fmoc-Asp/Glu-5-Oxazolidinones and Their Application to Neoglycopeptide Synthesis." Synthetic Communications **38**(21): 3640-3654.

Wang, Y. C., F. Wang, T. M. Sun and J. Wang (2011). "Redox-Responsive Nanoparticles from the Single Disulfide Bond-Bridged Block Copolymer as Drug Carriers for Overcoming Multidrug Resistance in Cancer Cells." Bioconjugate Chemistry **22**(10): 1939-1945.

Wei-Chiang Shenz, H. J.-P. R., and Laura LaManna (1985). "Disulfide Spacer between Methotrexate and Poly(D-Lysine). A Probe for Exploring the Reductive Process in Endocytosis." J. Biol. Chem **260**(20): 10905-10908.

Wei, H., X. Z. Zhang, C. Cheng, S. X. Cheng and R. X. Zhuo (2007). "Self-Assembled, Thermosensitive Micelles of a Star Block Copolymer Based on Pmma and Pnipaam for Controlled Drug Delivery." Biomaterials **28**(1): 99-107.

Wibo, M. and B. Poole (1974). "Protein Degradation in Cultured-Cells .2. Uptake of Chloroquine by Rat Fibroblasts and Inhibition of Cellular Protein Degradation and Cathepsin-B1." Journal of Cell Biology **63**(2): 430-440.

Xiang, L., L. J. Shen, F. Long, K. Yang, J. B. Fan, Y. J. Li, J. N. Xiang and M. Q. Zhu (2011). "A Convenient Method for the Synthesis of the Amphiphilic Triblock Copolymer Poly(L-Lactic Acid)-Block-Poly(L-Lysine)-Block-Poly(Ethylene Glycol) Monomethyl Ether." Macromolecular Chemistry and Physics **212**(6): 563-573.

Xiao-xuan Liu, P. R., Fan-qi Qu, Shu-quan Zheng, Zi-cai Liang, Martin Gleave , Juan Iovanna, Ling Peng (2009). "Pamam Dendrimers Mediate Sirna Delivery to Target Hsp27 and Produce Potent Antiproliferative Effects on Prostate Cancer Cells." Chem Med Chem **4**(8): 1302-1310.

Xiong, L. Z. and Z. Q. He (2011). "Synthesis and Application for Porous Scaffold Materials of Mono-Methoxy Polyethylene Glycol/Polylactide Diblock Copolymer." Journal of Macromolecular Science Part B-Physics **50**(6): 1226-1233.

Xu, D. M., S. D. Yao, Y. B. Liu, K. L. Sheng, J. Hong, P. J. Gong and L. Dong (2007). "Size-Dependent Properties of M-Peis Nanogels for Gene Delivery in Cancer Cells." International Journal of Pharmaceutics **338**(1-2): 291-296.

Xu, J. and M. Amiji (2012). "Therapeutic Gene Delivery and Transfection in Human Pancreatic Cancer Cells Using Epidermal Growth Factor Receptor-Targeted Gelatin Nanoparticles." Jove-Journal of Visualized Experiments(59): 10.

Xue, Y. N., M. Liu, L. Peng, S. W. Huang and R. X. Zhuo (2010). "Improving Gene Delivery Efficiency of Bioreducible Poly(Amidoamine)S Via Grafting with Dendritic Poly(Amidoamine)S." Macromolecular Bioscience **10**(4): 404-414.

Yang, Y., J. Lee, M. Cho and V. V. Sheares (2006). "Synthesis of Amine-Functionalized Diene-Based Polymers as Novel Gene Delivery Vectors." Macromolecules **39**(25): 8625-8631.

Yang, Z. R., H. F. Wang, J. Zhao, Y. Y. Peng, J. Wang, B. A. Guinn and L. Q. Huang (2007). "Recent Developments in the Use of Adenoviruses and Immunotoxins in Cancer Gene Therapy." Cancer Gene Therapy **14**(7): 599-615.

Yogesh Patil, J. P., , (2009). "Polymeric Nanoparticles for Sirna Delivery and Gene Silencing." International Journal of Pharmaceutics **367**(1-2): 195-203.

Zhuojun Dai, T. G., Maria A. Mattebjerg, Chi Wu, Thomas L. Andresen (2011). "Elucidating the Interplay between DNA-Condensing and Free Polycations in Gene Transfection through a Mechanistic Study of Linear and Branched Pei." Biomaterials **32**(33): 8626-8634.

Zimm, B. H. and S. D. Levene (1992). "Problems and Prospects in the Theory of Gel-Electrophoresis of DNA." Quarterly Reviews of Biophysics **25**(2): 171-204.

Zou, W., C. Liu, Z. Chen and N. Zhang (2009). "Preparation and Characterization of Cationic Pla-Peg Nanoparticles for Delivery of Plasmid DNA." Nanoscale Research Letters **4**(9): 982-992.

Zuzana Kadlecova, Y. R., Mattia Matasci, David Hacker, Lucia Baldi, Florian Maria Wurm, Harm-Anton Klok (2012). "Hyperbranched Polylysine: A Versatile, Biodegradable Transfection

Agent for the Production of Recombinant Proteins by Transient Gene Expression and the Transfection of Primary Cells." Macromolecular Bioscience **12**(6): 749-804.

Appendix 1: Beer's Law slope of pyridine-2-thione

In order to obtain the molar absorptivity of pyridine-2-thione in DMF solution, a set of pyridine-2-thione DMF solutions with various concentrations have been prepared and measured under UV at 376.25 nm (Table A1).

Table A- 1 UV absorbance of different pyridine-2-thione DMF solutions at 376.25 nm

Concentration (mmol/L)	Absorbance
0	0
0.0248	0.185
0.0296	0.203
0.0368	0.236
0.0495	0.343
0.0593	0.380
0.0737	0.445
0.124	0.784
0.148	0.893
0.157	0.927
0.184	1.009

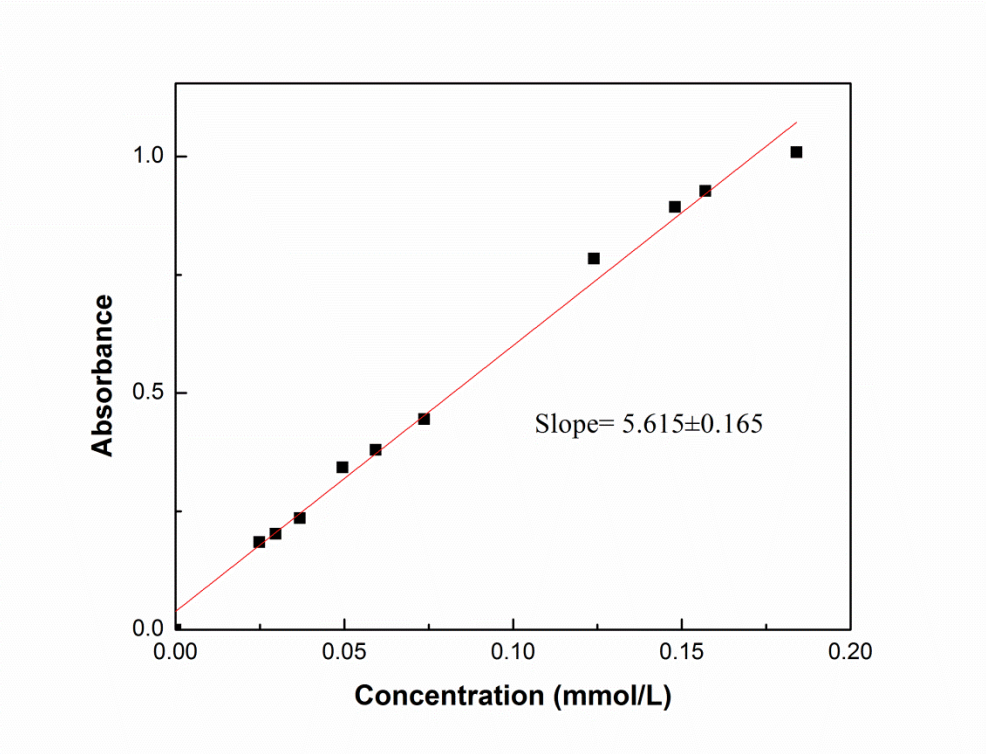

Figure A- 1 Beer's Law slope of pyridine-2-thione in DMF at 376.25 nm.

Appendix 2: Selected NMR spectrum

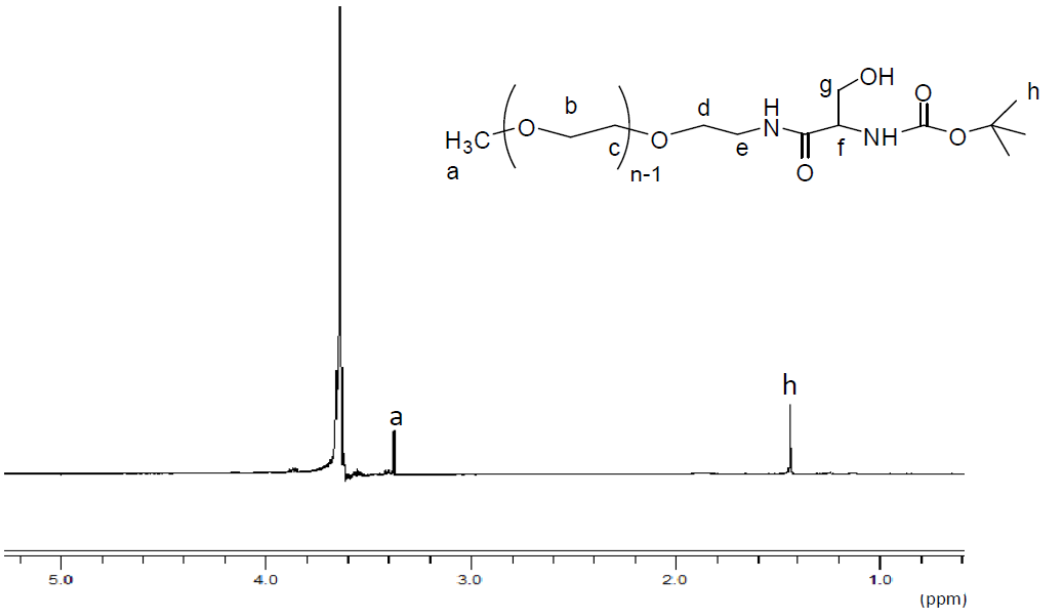

Figure A- 2 1H NMR spectrum of mPEO-S(Boc)-OH in $CDCl_3$

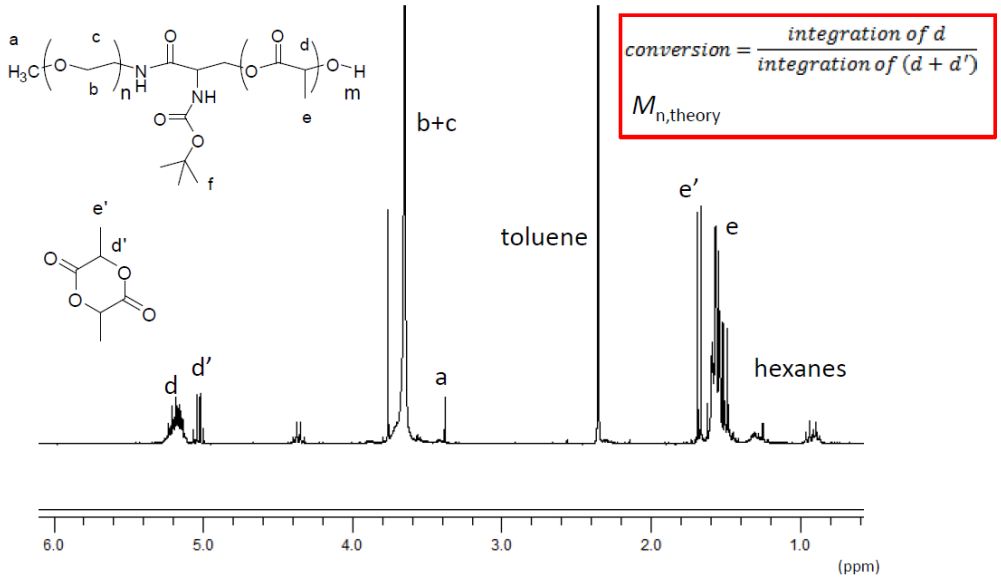

Figure A- 3 1H NMR spectrum of mPEO-S(Boc)-PLA crude product in $CDCl_3$

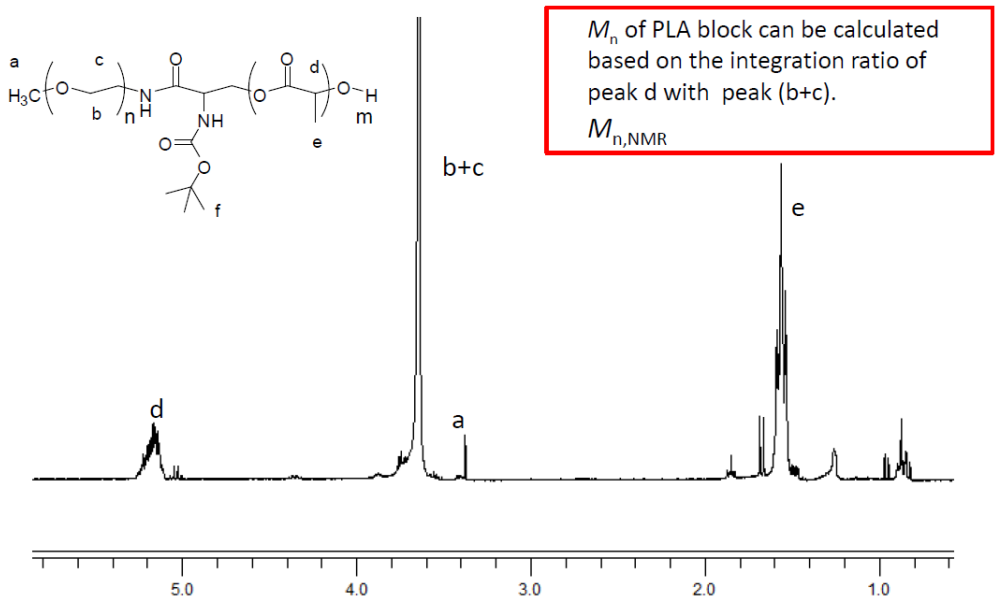

Figure A- 4 1H NMR spectrum of mPEO-S(Boc)-PLA purified product in $CDCl_3$

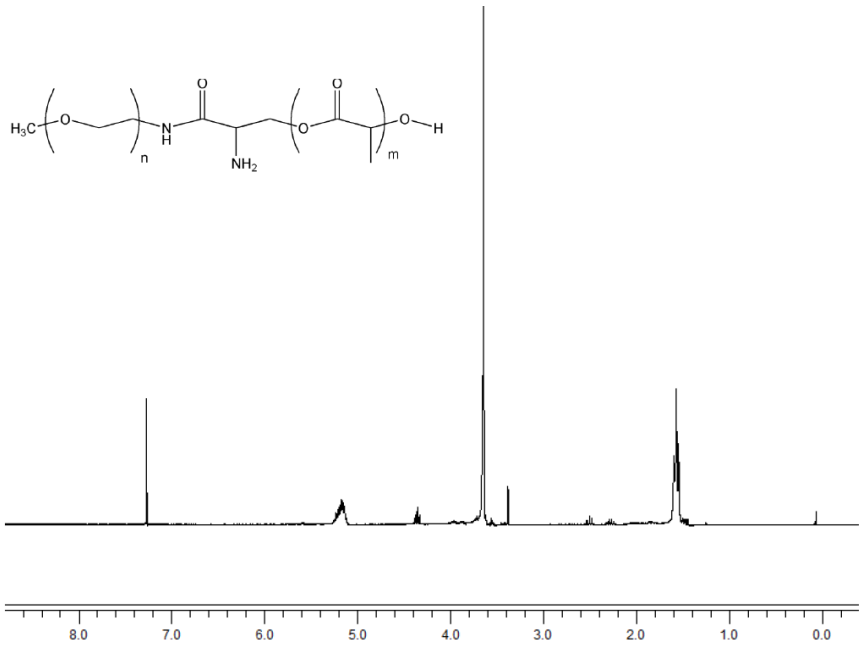

Figure A- 5 1H NMR spectrum of mPEO-S(NH_2)-PLA in $CDCl_3$

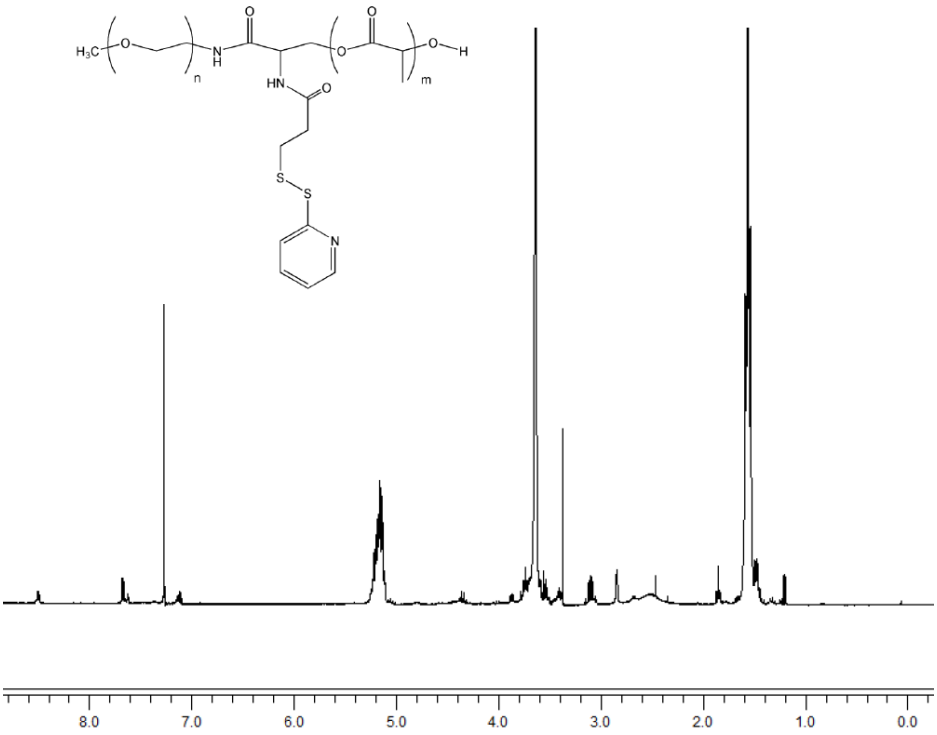

Figure A- 6 1H NMR spectrum of mPEO-S(NH-PDP)-PLA in $CDCl_3$

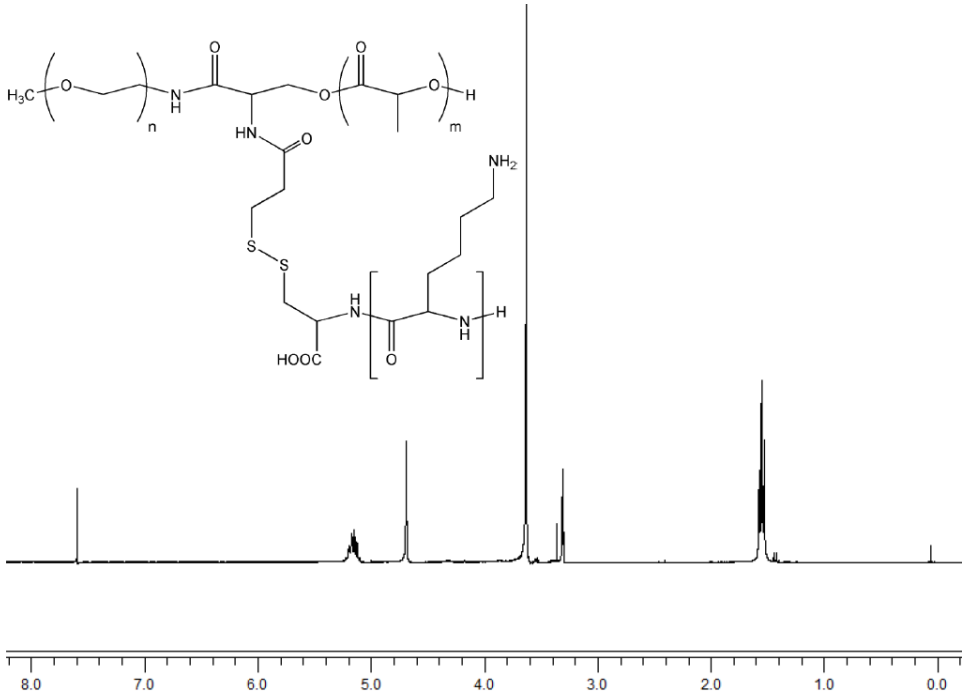

Figure A- 7 1H NMR spectrum of mPEO-S(CK_n)-PLA in $CDCl_3$

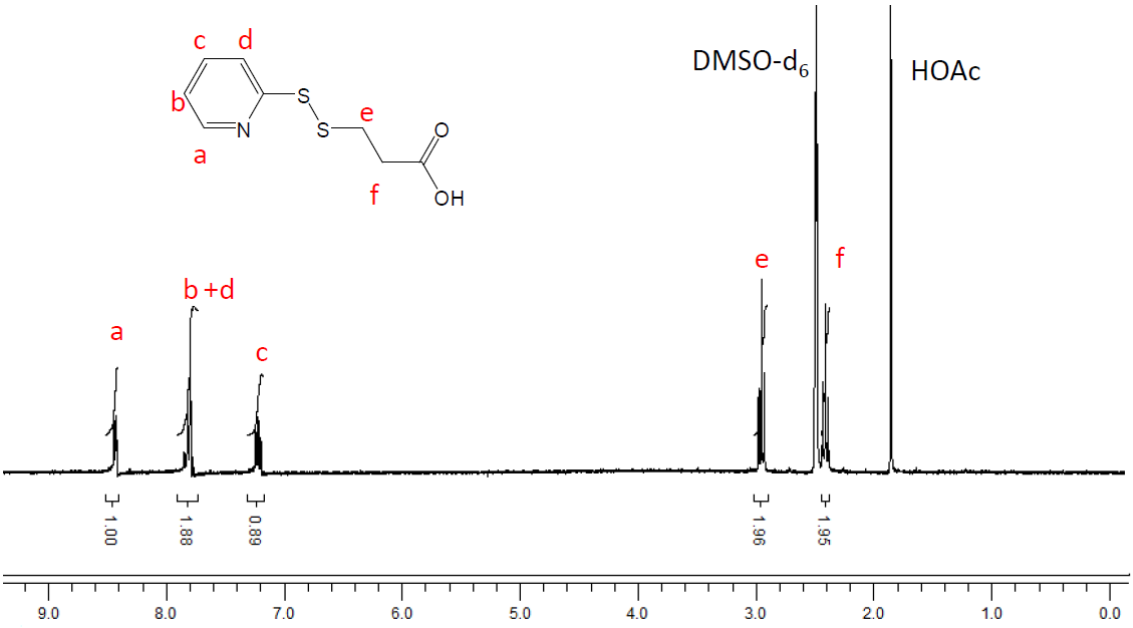

Figure A- 8 1H NMR spectrum of PDP in DMSO-d^6.

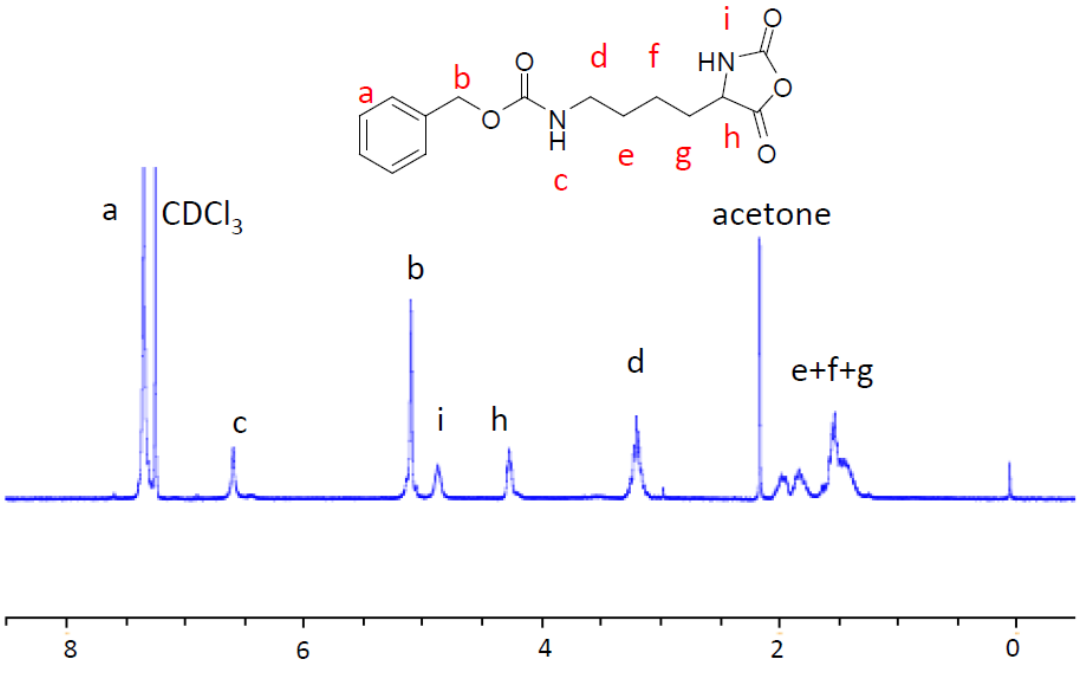

Figure A- 9 1H NMR spectrum of Z-lysine N-anhydride in $CDCl_3$.

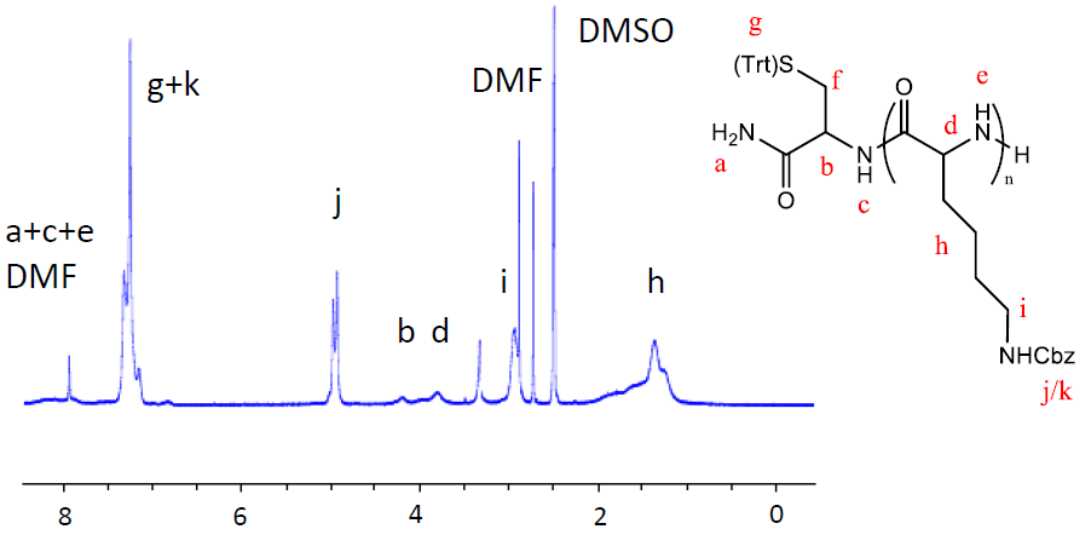

Figure A- 10 1H NMR spectrum of Cys(Trt)-poly(Z)lysine 50 in DMSO-d^6.

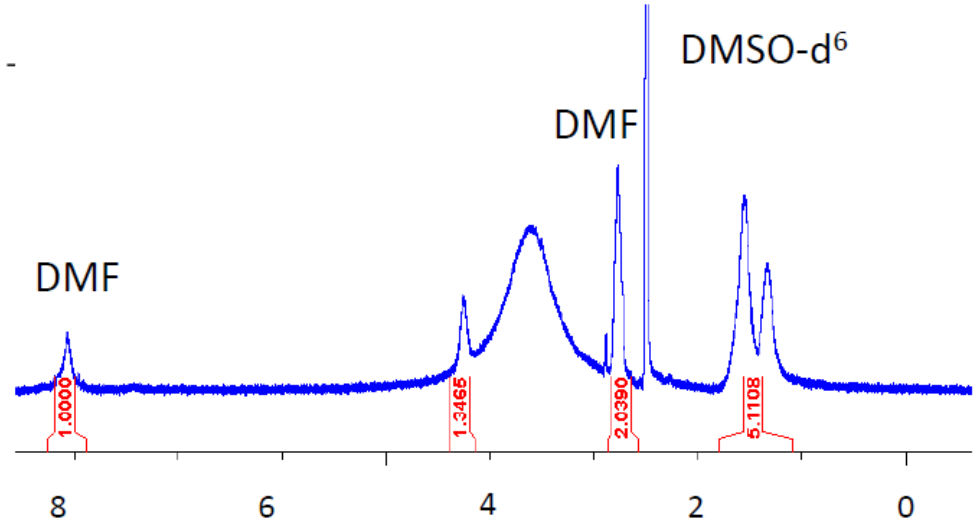

Figure A- 11 1H NMR spectrum of deprotected CK_{50} in DMSO-d^6.